An Investigation of

SOLAR RADIO NOISE

IN RELATION TO

VISIBLE PHENOMENA

A Thesis presented for the degree of

Master of Science of Rhodes University

by

L.M.G. POOLE - B.Sc.Hons (Rhodes).

Department of Physics,
Rhodes University,
Grahamstown.
December 1960.

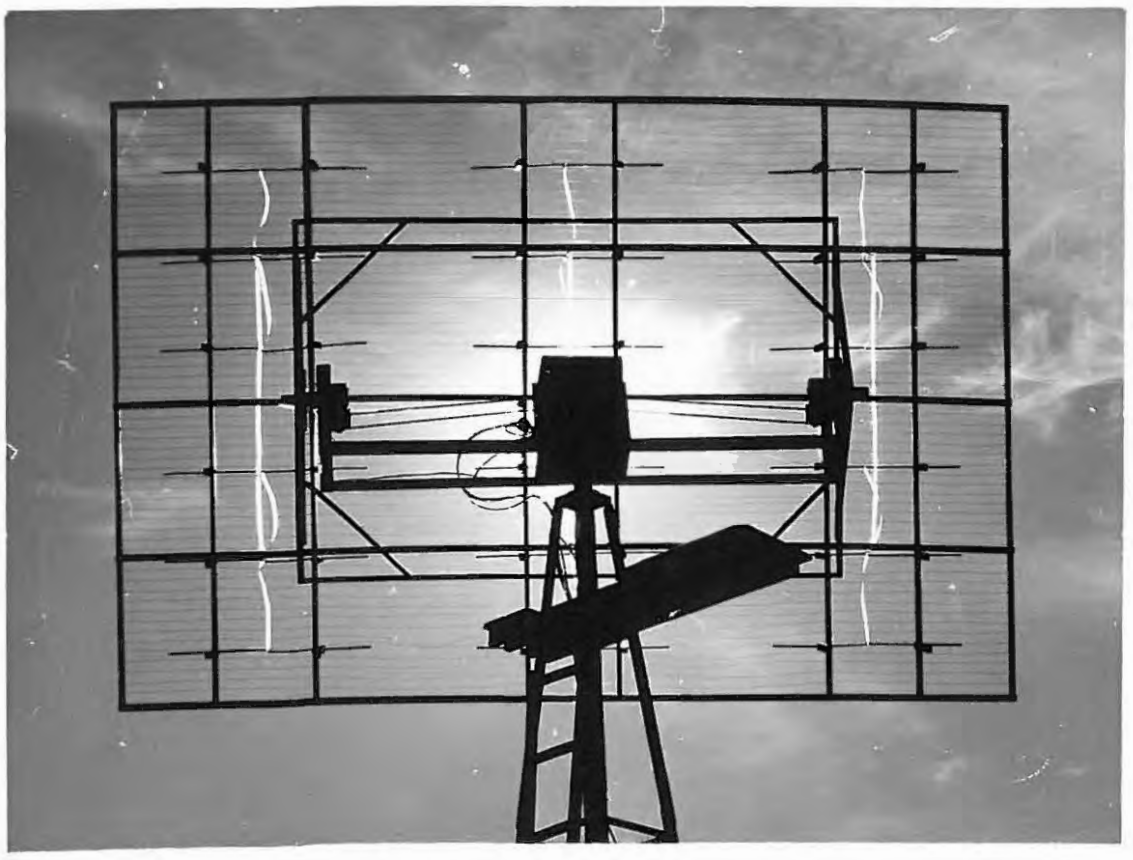

FRONTISPIECE

Frontispiece: The Dipole Array.

CONTENTS.

History of the Project.

At the beginning of 1958 the author and P.A.T. Wild began the construction of a single frequency receiver for the detection of solar radio noise at 300 Mc/s with a view to correlation with visual phenomena. This was at the site of the 125 Mc/s receiver built in 1957 at Rhodes University, which was used by W.L.H. Shuter to whom reference is made in this thesis. It was originally intended that the author should undertake a study of "thermal component" and "enhanced radiation", and Wild a study of "outbursts" and "isolated bursts". (These terms are explained on pages 6 and 8.) During 1959 the author acted as C.S.I.R. Technical Assistant to the project, and in this capacity operated the equipment for a major portion of the time. At the end of 1959 Wild used the records taken up until that time for an investigation of the profiles of noise-storms and isolated bursts. The possibilities provided by this series were limited, and the author resorted to an investigation on a previous series of 125 Mc/s records, together with the 300 Mc/s records, of the relationship between visible and radio events.

The author has described at greater length the construction of those parts of the apparatus with which he was most directly concerned, and the chapter on equipment (Chapter 3) may be considered complementary to P.A.T. Wild's in this respect.

Summary of Content.

The work of previous writers on the origin and propagation of solar radio noise, and particularly the correlation with visual events is reviewed, and then the construction of the author's 300 Mc/s receiver described. With a view to the author's project, absorption of electromagnetic radiation in the solar corona is quantitatively discussed, and a method for determining the intensity without absorption of a radio burst is evolved. The main project involves briefly the discovery of any possible relationship between the magnitude of a visual flare and the corrected intensity of an associated radio burst as measured at 125 Mc/s. It is concluded that no definite relation exists, but from this consideration an approximate shape of the instantaneous frequency profile of outburst elements is obtained. An extension of the theory to isolated bursts enables us to predict both this band-shape, and the velocity of an exciting agency moving radially through the corona.

ACKNOWLEDGEMENTS.

The author wishes to express his sincere thanks to the following:

Dr. E.F. Stack-Forsyth for directing the research, and invaluable help with some of the construction, and for making available for analysis the series of 125 Mc/s records obtained in 1958.

Professor J.A. Gledhill for much helpful criticism and advice, particularly in the drafting of this thesis.

Mr. A.R. Scanlen for aid in the construction of mechanical parts of the apparatus.

Mr. G. Walters for the photographic plates appearing in this thesis, and also for assistance in the construction of apparatus.

Mr. J. West for his contributions towards the engineering of the antenna mounting, and for the use of the ammonia printing machine for the reproduction of diagrams.

Miss K.H.O. Longfield for cutting the wax stencils of the text.

The South African Council for Scientific & Industrial Research for a research grant and bursary in 1958.

CHAPTER ONE.

INTRODUCTION.

A. Description of the Sun and its Atmosphere.

The chief features of the solar sphere which concern radio astronomy may be summarized as follows:

The interior of the sun, consisting mainly of ionized hydrogen in a state of instability and turbulence, is surrounded by the layer which appears as the visible solar disc, emitting a continuous spectrum between the ultra-violet and infra-red regions, known as the photosphere. This may properly be considered to be the innermost of three main layers which form the solar atmosphere. It has a mean radius of about 6.7×10^{10} cm, and is very thin (100 km), with an average temperature of about 6000°K.

The next layer is called the chromosphere, and is separated from the photosphere by a region of transition several hundred km. thick known as the "reversing layer". The chromosphere extends for about 10,000 km., emitting a spectrum which indicates the presence of both ionized and neutral atoms. The free electron density in this region is obtained from the expression for exponential distribution by Cillie & Menzel (1),

$$N = 5.72 \times 10^{11} e^{-7.7 \times 10^{4}(h - 500)} \text{ electrons/cm}^3 \qquad (P1)$$

where h = height above photosphere in km.

The temperature is still comparatively low, being of the order of 10^4 $^{\circ}$K.

Above the chromosphere is the corona, which is by far the largest layer, extending for several million km., or many times the solar radius (usually taken as that of the photosphere), consisting of hot gas in which most atoms are highly ionized. It is rendered visible by the photospheric light scattered by free electrons, and by spectral emission from the ions. Comparatively little is known about the forces and movements of gases in the corona, principally owing to the fact that the relatively low light intensity compared to that of the photosphere has made optical observation of this region difficult. As a result of this, the variation of electron density and kinetic temperature with distance from the sun's centre is given only approximately by the empirical formulae due to Baumbach & Allen, and Smerd & Westfold respectively.

The electron density N is given by Allen's revision of Baumbach's original expression (2), here modified to give the result in terms of the radius to the base of the corona, instead of the photospheric radius as in Allen's version.

$$N = 1.42 \times 10^{8} \rho^{-6} (1 + 1.68 \rho^{-10}) \text{ electrons/cc.} \qquad (P2)$$

where $\rho = \frac{R}{R_o}$ where R = Radius to point in question.

R_o = Radius to base of corona.

This formula is based on observations taken over several years at various stages of the solar cycle, and assumes spherical symmetry.

The electron temperature T is obtained from a modified form of the equation derived by Smerd (3), which incorporated an expression

for the electron temperature due to Alfven (4), and the Baumbach-Allen expression used above

$$T = 1.63 \times 10^6 \; \rho^{-1} \frac{(1 + 0.69\,\rho^{-10})}{(1 + 1.68\,\rho^{-10})} {}^{\circ}K \qquad (P3)$$

where ρ is defined as before. This formula gives a value for T of about 10^6 $^{\circ}K$ over most of the lower corona, and this agrees well with the values obtained from observation.

The electron collision frequency ν at various points in the corona is given by the expression due to Smerd & Westfold (5) in terms of N and T, which can be obtained from equations P2 and P3.

$$\nu = 42NT^{-3/2} \text{ per sec.} \qquad (P4)$$

This is really a simplification of a complex expression which includes a factor taken as constant over most of the corona. This same equation, with a different constant, can be used to find ν in the chromosphere.

The atom-ion-electron composition of the chromosphere and corona is said to form a "plasma", which, under suitable conditions, can undergo oscillations whose frequency in the absence of any magnetic field is proportional to the square-root of the electron density. This important plasma concept is used to explain the origin and propagation of certain radio bursts, and will be discussed more fully later.

B. Solar Events and their relation to Bursts of Radio Noise.

The sun in its normal state is known as the "quiet sun", and

emits radiation over the entire electromagnetic spectrum, the intensity of the radio frequency radiation never dropping below this particular base level.

The visible portions of the sun are, however, subject to sporadic and periodic disturbances or "solar events" of various types; just as the steady "thermal component" of radio noise is subject to sudden variations and irregularities. As one might expect, many of these events have been found to be inter-related, although the results and conclusions of different reporters on this subject are distressingly diverse.

Types of Events.

(a) Visual.

Sunspots. These occur in the photosphere and appear as dark spots which can, if large enough, be seen with the naked eye through a dark filter. These areas owe their dark appearance to the comparatively low temperatures which prevail, about 1000°K below the surroundings. Spots usually appear in clusters having strong magnetic fields associated with them, different spots exhibiting different polarities so that the magnetic flux from some returns through the others. Fields of a few thousand oersteds are characteristic. Although sunspots appear haphazardly in time and space, statistically their incidence is subject to several periodic variations, of which the well-known eleven-year cycle is the most pronounced.

Flares, occur in the chromosphere, and appear as small areas which be-

come suddenly brighter, strongly emitting the H α spectral line, and remain so for a short time, after which they gradually return to normal. The total duration of a flare may be anything between a few minutes and several hours.

Flares vary considerably in size and intensity, and are universally classified in terms of "importance", which has three main divisions 1, 2 and 3; a flare of importance 3 is very large and bright. There are sub-divisions of these groups, designated by + and - signs, ranging from 1- (subflare) to 3+. The method of assigning an importance to any particular flare is not fully understood by the author, to whom it seems to be largely subjective and arbitrary. Ellison (6) (1949), however, mentions that the classification widely used is largely based on flare area, as the short-lived maximum intensities are as a rule difficult to obtain. Flares are thought to emit radiation in the ultra-violet and radio regions, as well as streams of charged particles which travel outwards through the corona at a speed of about 1500 km/sec. Both the electromagnetic and corpuscular emissions cause ionospheric and magnetic disturbances on earth, which are responsible for communication fade-outs and interference. The radio frequency emitted by the flare itself is small, but the particles are thought to give rise to coronal plasma oscillations of the type mentioned in section A. This is one of the mechanisms used to explain the origin of the more intense radio signals which are observed, although the appearance of a flare does not necessarily result in a coincident radio burst. To what extent correlation has been found will be discussed

shortly.

The incidence and position of flares on the solar disc is known to be directly related to sunspot activity. Giovanelli (7) has shown that the frequency of incidence of flares occurring near any spot group is directly dependent on the area and rate of growth of a spot. The strength of the magnetic field has been found not to affect the associated flares.

Filaments or Prominences are huge columns of luminous gaseous matter rising many thousands of km. into the coronal atmosphere, which, after formation can remain stationary for many weeks. These are best observed during eclipses. In contrast to the normal type of prominences are the short-lived "surge prominences" described by Ellison (6), which consist principally of jets of matter which are thrown up from a solar flare, and fall back into the chromosphere.

(b) Radio.

It will be convenient, before examining the relation of radio and other events, and subsequently embarking on a systematic discussion of the growth of solar radio astronomy and its associated theories, to list the various types of radiation under the headings by which they are known today.

(1) Basic Thermal Component. Apart from the sudden rises in flux density of radio waves which we term "bursts", there is at all times the "basic thermal component", which is randomly polarized and has a flux density of the order of 10^{-21} watts/m^2(c/s). This is

the characteristic emission from the "quiet sun", and measurements indicate thermal origin at about 10^4 °K in the chromosphere, or 10^6 °K in the corona for radiation at metre wavelengths (Smerd (8)).

(2) Type I burst. "Storm burst". These bursts are associated with "enhanced radiation" or "noise storms", which are the most common type of high-intensity emission from the sun. A storm, which may last for days, consists of a slowly varying increased background level upon which are superimposed many of these short-lived "storm bursts", which exhibit strong polarization, and have a narrow spectral bandwidth (only a few kc/s). These bursts appear to occur at a fixed frequency during their lifetime, although it seems possible that they may drift very slowly. Some special "drift-storms" have been observed by Wild (67).

(3) Type II bursts. "Outburst". These bursts, particularly intense at metre wavelengths, usually take the form of a fairly sudden increase in flux level which lasts for a few minutes, after which it gradually dies away, sometimes degenerating into a noise storm of the type described in the previous section. These "outbursts" drift slowly toward lower frequencies at the rate of $\frac{1}{4}$ Mc/s per sec, and have a fairly broad bandwidth, which usually exhibits a sharp low-frequency cut-off. Simultaneous emission at harmonic frequencies is a common feature of outbursts, the instantaneous harmonic bandwidth being more symmetrical than that of the fumdamental while the intensity is usually of about the same magnitude. These bursts appear to be randomly polarized, and to be particularly associated with visual flares.

(4) Type III bursts. "Isolated bursts". These are sudden increases in intensity which at any particular frequency appear to fall off exponentially, the lifetime being of the order of seconds. These bursts, which have a very broad bandwidth, drift rapidly to lower frequencies (at 20 Mc/s per sec), the rate of drift decreasing with time until the maximum intensity often appears to become "stopped" at a certain frequency. Harmonic pairs also occur in isolated bursts, which may account for the "double-humped" appearance of some of those bursts observed on one frequency. These double bursts appear as an initial large peak followed closely by a second and usually smaller peak. For a long time it was thought that isolated bursts were also unpolarized, but Komesaroff (9), who has done the most conclusive work to date on the polarization of spectral types I, II and III, has shown that they can exhibit strong elliptical polarization.

(5) Type IV radiation. This is a new spectral type and comprises a general increase of background intensity which can be described as a type I continuum without the superimposed storm bursts. Their incidence is closely associated with flares and cosmic ray emission - Avignon and Pick-Gutmann (1959) (10,11), Kundu and Haddock (1960) (12), McLean (1959) (13). They are thought to be connected with type II bursts which they resemble in that they undergo a slow negative frequency drift.

(6) Type VI radiation. It has been noticed that on many

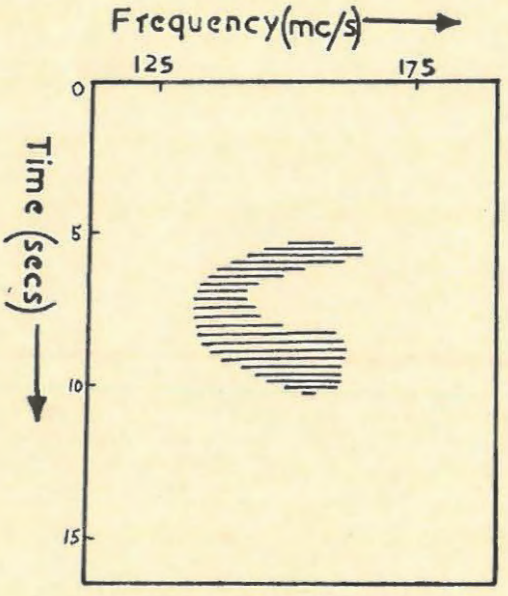

Inverted U-Burst;

Ref. 15.

FIG A

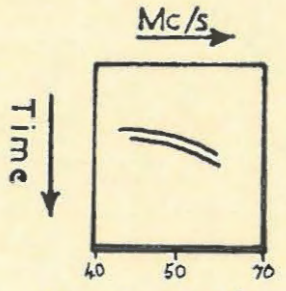

Reverse Pair

Ref. 16.

FIG B

occasions an isolated type III burst is followed by an extremely wide-band continuum (100 Mc/s) which usually occurs below 150 Mc/s, and lasts for a minute or so. This has been designated as type V radiation. There seems to be a definite correlation of the type V-associated isolated bursts with cm. radiation and flares (Neylan (1959) (14)).

(7) Other Rare Spectral Types.

(a) Inverted U Bursts. Maxwell and Swarup (15) have identified this spectral type whose peculiarity is a normal rapid drift to lower frequencies which becomes stopped and then drifts back to higher frequencies, the total lifetime being of the order of seconds. Fig.A. shows the appearance of a typical inverted U burst on a frequency-time record.

(b) Reverse Drift Pairs. Roberts (1958) (16) has reported bursts which contain two elements separated by a few seconds, which drift towards higher frequencies at a rate of a few Mc/s per sec. Fig.B. is drawn from a photographic swept-frequency record of one of these pairs. It is not yet known whether they are polarized.

Both these rare burst types described above appear to be special cases of type III radiation.

Relation between Visual and Radio Events.

As early as 1946 Ryle and Vonberg (17) using a radio interference method (analogous to Michelson's optical interferometer used

to measure stellar diameters) with spaced aerials, measured the angular diameter of solar radio sources on frequencies of 80 and 175 Mc/s, and found them to be of the same order of size as sunspots. The measured intensity of radiation from these sources necessitated the postulation of equivalent temperatures of the order of 10^9 °K at these frequencies. They found that the "larger bursts" were "often accompanied by other evidence of solar activity". Hey, Parsons and Phillips (1948) (18) working on 70 Mc/s found a 50% correlation between outbursts and flares of importance 2 or greater; and 32% correlation with flares of importance 1.

The statistical evidence of Wild and McReady (19) is meagre, but they found that out of 5 large outbursts observed, 3 coincided approximately with the onset of a flare. 30 smaller bursts of this type were found not to correlate with any flare. No other correlation was reported.

Payne-Scott and Little (1952) (20), using a swept lobe interferometer at 97 Mc/s found that the radio frequency source often moved rapidly away from the position of a flare. This supported the idea of an exciting agency moving radially outwards through the corona. (See later)

Dodson, Hedeman and Owren (1953) (21) working on 200 Mc/s did a comprehensive study of flare associated events of all types, and found that the percentage correlations with flares of importance 1, 2 and 3 were 79%, 77% and 50% respectively. Less significance should be attached to the last group, as the number of flares over

the period of observation was only 4 as against 150 of importance 1. These figures together give an overall percentage correlation of 78%.

Dodson, Hedeman and Chamberlain (22) in the same year found distinct association between bursts occurring on radio frequencies and the ejection of high velocity particles at the onset of certain flares.

Menzel (23), working on the terrestrial effects of prominences and particle ejection, also noted the accompaniment of a "major fraction of bright flares" with bursts of radio noise on frequencies of 200 Mc/s and greater. He suggested a magnetohydrodynamic or plasma oscillation mechanism might be responsible for the association of the two phenomena.

Dodson, Hedeman and Covington (1954) (24) working now in the cm. range (2800 Mc/s) found actually a smaller overall percentage correlation (57.3%) with all types of radio events than at 200 Mc/s, but the correlation with bigger flares (importance 2 or more) was much better ($>85\%$). They also observed a number of so-called "sub-flares" (importance <1), only 19.1% of which were associated with radio events.

It was also noted that at this frequency the time of onset of a flare coincided almost exactly with the commencement of the 2800 Mc/s burst, but that the radio event invariably attained a maximum before the flare; and often actually ended at about the time of the flare maximum.

The position of the flare on the solar disc, as well as its size, also appeared to play a part in determining the intensity of the associated radio events that were "gradual rises and falls" as opposed to strictly burstlike events. It was found that in general the bursts tended to show central concentration falling off towards the limb. This appears to be due to the absorption of radiation in the solar atmosphere, which is discussed more fully later.

Far more significant than the above figures for 2800 Mc/s, are the results obtained when the statistics of the number of radio events which are flare associated are considered. It appears that for up to 98.6% of all outstanding 2800 Mc/s events, a flare was either observed, or its existence indicated by other phenomena such as prominences or terrestrial disturbances. There was thus strong evidence to show that there was probably a disturbance at 2800 Mc/s only when a flare or sub-flare was in progress. This conclusion was based on the result of 5 years' observations.

In 1956 Dodson, Hedeman and McMath (25) working on the photometry of flares found in general that 200 Mc/s noise-storm associated flares were large and nebulous or "stringy", rather than the more usual bright, well-defined areas. At the same time they showed that one could not distinguish between flares which causes ionospheric disturbances and those which did not, except that flares smaller than a certain size never produced any measurable effect.

Loughead, Roberts and McCabe (1957) (26) investigating

correlation between isolated (type III) radio bursts and flares found that out of 300 flares observed, 20% had associated bursts. However, 85% of these flares were "microflares" (of importance $<1^-$), and it was found that with larger flares of importance 1 or more, they obtained a 60% correlation. In addition their results indicated that flares with "surges" were more likely to produce bursts. Over 60% of all types of radio events occurred in the lifetime of a flare.

Giovanelli (1958) (27) examined sudden explosive flares known as "flare-puffs" as a cause of isolated bursts. Out of 27 puffs observed, 66% had bursts which coincided to within two minutes. The puff explosions appear to eject two types of corpuscular streams, one with velocities of 100 km/s which appear as flare-associated surges; and another shortly after, with velocities of the order of 1/5 speed of light, which are responsible for radio burst production.

With Roberts, Giovanelli (28) investigated flares as a source of outbursts (type II), and showed that optical disturbances were coincident with at least 13 out of 18 bursts recorded with a radio spectrograph (40-240 Mc/s).

Maxwell and Swarup (1958) (15), discussing a new spectral type, the "inverted U burst" (q.v.), found that 22 out of 28 such bursts recorded had "optical counterparts" to within 5 minutes.

In 1959, Wild, Sheridan and Neylan (29) showed that there was a close association between flares and type III bursts which were accompanied by the new spectral type V. Consideration of the data obtained led them to postulate an important modification of the

accepted outward moving agency model for burst production. (See later in Chapter 2.).

At the end of 1959 Hachenburg and Kruger (30) working on 3.2 and 10 cm., reported the results of 6 months' observations in 1957, when 1396 flares were observed; during which time 395 bursts were recorded, of which 280 coincided with a flare. This gives 20% of flares with associated bursts; while 71% of bursts occurred during a flare. It was further shown that the big flares (> 3) invariably produced an effect in the cm. range, whereas for smaller flares the proportion was considerably smaller. During this period 231 sudden ionospheric disturbances (S.I.D.'s) were also observed, of which 85.7% were associated with flares, and 91% with radio bursts. Of the 1116 flares that definitely had no burst associations, less than 2% could possibly have caused S.I.D.'s. The above results have given the workers good reason to come to the important conclusion that only those flares which give rise to cm. bursts can also cause S.I.D.'s.

Also at about this time Avignon and Pick-Gutmann (10) showed that a new kind of radio burst (type IV) was invariably associated with a flare.

Satellite and balloon experiments as reported by Thompson and Maxwell (1960) (31), and later by Kundu and Haddock (1960) (12), have recently revealed the bombardment of the terrestrial atmosphere by low-energy cosmic rays from the sun, and this has resulted in an investigation into the relationship of these rays to solar bursts and

flares. Large flares (importance 3 or more), are often followed by an outburst of continuum radiation (type IV), which are in turn followed about an hour later by the arrival of 30-300 Mev. protons at the Earth.

The evidence does not indicate that the emission of auroral particles (of velocities of the order of 1000 km/s) is associated with the type of continuum burst described above, but rather with the slow frequency-drift type II burst. There appears to be no relationship between noise-storm (type I), isolated, fast-drift (type III) bursts and solar corpuscular emissions which result in terrestrial disturbances.

Rabben (1960) (32), observed over a period of 200 hours, 136 bursts and 372 flares and found that about 20% of flares coincided with bursts, 88 of the remaining 96 radio events occurring within the lifetime of a flare to within 5 minutes. In addition, several points of interest were noted. He found that the greater the flare, the greater the number of concurrent radio events, but there appeared to be no connection between burst intensity or rate of drift and flare importance. Bigger bursts occurred nearer the onset of a flare than the lesser ones. Burst-producing flares appeared also to favour certain centres of activity, which otherwise exhibited no particular peculiarities.

More recently, however, Edelson, McCullough, Santini and Coates (1960) (33), reported that for simple type I and II bursts a definite trend towards larger peak radio-flux values at 10 cm. accom-

panying larger H α intensities was evident. A remarkable correlation - 99% - of bursts associated with H α flares was reported, whereas, as before, far fewer flares (25%) had coincident bursts. Still no criterion for "burst-flares" is apparent. An outstanding feature of these observations is the simultaneity of the associated events.

SUMMARY. When viewing this work over the last decade in perspective certain common features become apparent, although there may be considerable disagreement between individual sets of results.

Broadly speaking we see that chromospheric flares more than sunspots or prominences are responsible for burst production; larger flares giving closer correlation. In general, too, there is a better correlation at higher radio frequencies. And there is always a higher percentage of bursts with associated flares than vice versa. This indicates that there is probably a certain type of flare which causes a concurrent radio event, but as yet we have not been able to discern an infallibly characteristic feature of these burst-associated flares. (However, see Dodson et al (25), Rabben (32), and Longhead et al (26)).

CHAPTER TWO.

OUTLINE OF PREVIOUS INVESTIGATIONS.

Virtually all the present knowledge we have concerning solar radiation in the radio frequency range has been obtained since World War II, when the development of V.H.F. techniques in connection with radar work facilitated the detection of this type of solar emission.

As early as 1948 Martyn (34) advanced a theory based on classical mechanics to explain the emission of thermal radiation from the sun. He derived theoretically the effective temperatures prevalent in various parts of the solar atmosphere over the radio spectrum, and concluded that a maximum effective temperature of $\pm 10^6$ °K should be associated with radiation of 1 metre wavelength.

Using a more practical approach, Ryle and Vonberg (17) carried out investigations at frequencies of 80 and 175 Mc/s. They found that periods of increased intensity occurred, consistent with temperatures of 10^8 or 10^9 °K. The important discovery that the radio sources are very much smaller than the total solar disc (see earlier) in area implied higher temperatures (10^9 or 10^{10} °K) at the sources. The thermal component appeared to be unpolarized, whereas the more intense emission exhibited strong circular polarization. It appears to the author that these "bursts" were probably what was subsequently termed a "noise-storm", (see type I burst).

Ryle (35) considered the above results theoretically and

suggested that the solar magnetic field and non-uniform rotation of the surface matter could cause a large potential to exist between equator and poles resulting in acceleration of electrons which generate the observed radiation. The magnetic and electric field-strengths are considerably enhanced during sunspot activity, and Ryle considered the implications of this in relation to bursts of polarized radiation.

Williams (1948) (36), using a single frequency receiver at 75 Mc/s detected and studied a number of individual or "isolated" bursts as opposed to the general enhanced radiation observed by Ryle and Vonberg, and found that generally speaking these bursts were characterized by a very rapid rise to maximum intensity followed by a decay portion which appeared in most cases to fall off exponentially. Williams obtained a series of values of "k" in the term e^{-kt} ranging from 0.3 to 1.8 sec^{-1}, giving an average value of 0.7 sec^{-1}. This quantity k is of considerable importance and will henceforth be referred to as the "decay constant".

In the following year Payne-Scott (37) published the results of investigations on four simultaneous frequencies (19, 60, 65 and 85 Mc/s), also concentrating on different aspects of isolated bursts. She found that these bursts, which appeared to be unpolarized, usually arrived in order of decreasing frequency, the average intervals elapsing between the start of a burst on 85 and 60; 65 and 60; and 60 and 19 Mc/s being 0.7; 0.3; and 9.0 secs. respectively. The maximum intensity invariably increased with decreasing frequency,

the average ratio of peak intensities at 60 Mc/s and 85 Mc/s being about 2 : 1 (i.e. the square of the ratio of the respective wavelengths). An examination of the profiles (as measured on a linear intensity-time scale) of about 100 such bursts at these two frequencies revealed that the decay portions fitted well with an exponential curve of the form Ie^{-kt} with an average value of k of 0.6 sec^{-1} (c.f. Williams). Again these isolated bursts all had rapid but finite rise times. The decay constant was also measured on 19 Mc/s and found to be much smaller - viz. about 0.25 sec^{-1}.

Payne-Scott also reported the observation of "double-humped" bursts although these were far less frequent than the normal single-peaked ones. At least one interesting feature of these was that their first peaks appeared to have a higher decay constant (i.e. they decayed more rapidly) than the average single peak burst. The first peak was nearly always larger than the second, the average ratio of intensities being about 4 : 1, and the peaks were separated by a few seconds. Measurements on double-humped bursts by Shuter (38) at 125 Mc/s are in general agreement with the above results.

Typical single and double peak isolated burst intensity-time profiles are given in Fig.C.

Workers on the theoretical side now began attempting to explain the origin of intense radio bursts in terms of "plasma oscillations" as opposed to the previous "thermal" theories. A plasma is said to consist of free positive ions and electrons in equal concentrations, a state of affairs easily realized in electrical discharge

tubes. According to the original theory of Tonks and Langmuir (1929) (39) the electrons in such a system have a natural frequency of oscillation given by

$$f_o = \sqrt{\frac{Ne^2}{\pi m}} \qquad (P5)$$

where N = electron density/cc.

e = electronic charge

m = electronic mass

when suitably excited. The quantity f_o is nowadays loosely termed the "plasma frequency" when discussing the solar corona, which is effectively an extended non-uniform system having "levels" corresponding to different plasma frequencies determined by the value of N at that level as given by Eqn.P2.

Ryle (1949) (40), examined such oscillations as a cause of radio bursts, but was unable to suggest any mechanism whereby they could be excited and maintained, as conditions were very different to those prevailing in discharge tubes where they were first studied. He ruled out the possibility of ionic oscillations (of frequency $= \sqrt{Ne^2/\pi M}$ where M is the ionic mass) as a source of radiation as such oscillations would be of much lower frequency than the plasma frequency, and would thus be in a region of imaginary refractive index in a normal plasma, and be unable to escape.

Westfold (41) showed that even more recent modifications of Appleton's (42) classical theory as used by Ryle (35) were not

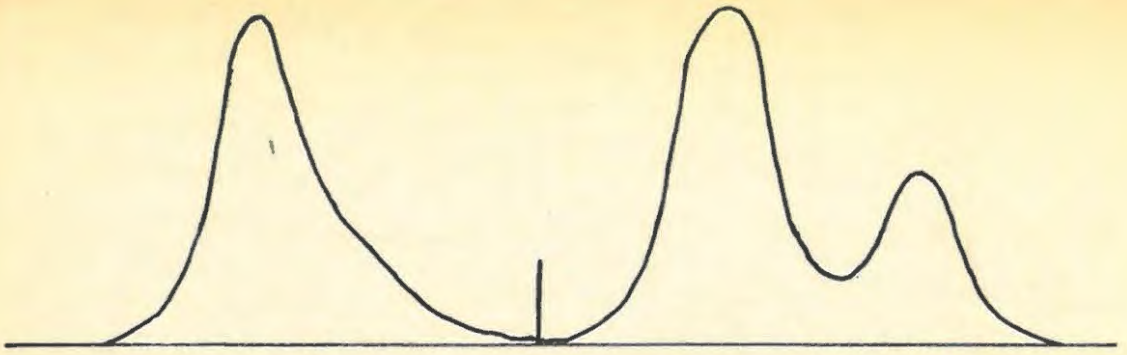

Isolated Burst Profiles

FIG C

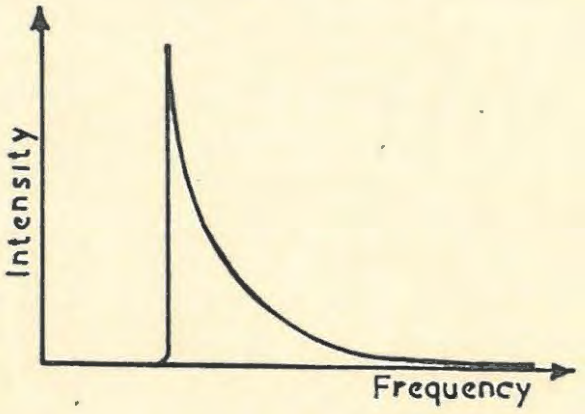

Ref. 43.

FIG D

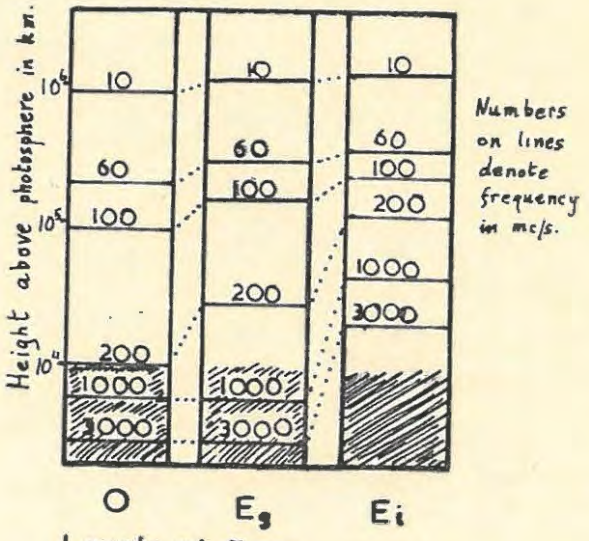

Levels of Zero Refractive Index

FIG E Ref. 3.

justifiable when applied to the solar corona. By considering steady-state plasma oscillations in a magnetic field he concluded that three types are possible, the components exhibiting left-handed, right-handed and linear polarizations. The oscillations would be damped by the electron-ion collisions, the actual value of the damping constant (assuming the damping to be exponential) ranging between $\frac{1}{4}\ \nu$ and $\frac{3}{4}\ \nu$ where ν is the electron collision frequency given by Eqn.P4.

Jaeger and Westfold (43) solved a number of transient problems, considering the effect of a localized disturbance at a particular plasma level f_o. They concluded that the generated radiation would be a maximum at f_o, showing a sharp cut-off below f_o, and a decrease in intensity above f_o according to an inverse square or fourth power law of the frequency. The instantaneous spectral distribution would thus have the appearance shown in Fig. D. At any one frequency, the amplitude of oscillation would probably decay exponentially according to $(\exp - \nu t)$, i.e. with damping constant $= \nu$. (cf. Westfold above).

On this model one would expect to receive both direct and "echo" waves at all frequencies larger than f_o, for a disturbance originating at the f_o plasma level (See discussion on ray trajectories later), the time delays between the two waves being determined by the "excess of equivalent path over distance traversed for a ray proceeding radially outwards" from a point at height ρ (see Eqn.P2) to ∞ , which is given by

$$\int_{\rho}^{\infty} \left(\frac{1}{\mu} - 1 \right) d\rho$$

where μ is the refractive index for radiation of frequency f of the medium where the plasma frequency = f_o, given by

$$\mu = \sqrt{1 - \frac{f_o^2}{f^2}} \qquad (P6)$$

The variable f_o is easily obtainable in terms of using P2 and P5.

These conclusions were tested against the results of Payne-Scott (37), and appeared to show general agreement with regard to decay shapes and time delays, although the writers seem to be confused about the distinction between instantaneous intensity-frequency profiles and intensity maxima at different frequencies at different times.

Bohm and Gross (1949a, b, and 1950) (44, 45, 46) consider the production of plasma oscillations in an unbounded medium, which are set up due to interaction of moving particles in the medium, and grow initially according to a linear approximation, due to a "positive feedback" mechanism, until non-linear effects and damping due to collisions become important, and a steady state is reached. There is a tendency to increased stability as a disturbance moves into regions of decreasing electron density. This would be consistent with the observed greater amplitudes of bursts at lower frequencies. This treatment was extended to include media limited by various types of boundaries that have little practical significance in solar physics.

Smerd (1950) (3, 8) discussed the sun in general as a source of radio frequency radiation, calculating the distribution of temperature and intensity across the disc at coronal and chromospheric frequencies as well as the size of the r.f. disc itself. In considering the effect of a general magnetic field on the origin and escape of radiation he has used the three dimensionless quantities defined in magneto-ionic theory as follows:

$$x = \left(\frac{f_o}{f}\right)^2 ; \quad y = \frac{f_H}{f} ; \quad z = \frac{\nu}{2\pi f} \qquad (P7)$$

where f = frequency of the wave being propagated through the medium

f_o = plasma frequency of medium (from P5)

f_H = electron gyro-frequency, which is defined from classical mechanics as

$$f_H = \frac{eH}{2\pi mc} \qquad (P8)$$

where H = magnetic field in oersteds

m = electronic mass

c = velocity of light in vacuo

ν = electron collision frequency (from P5).

Generally electromagnetic waves are propagated through an ionized medium in the presence of a magnetic field in two modes - the ordinary ray and the extraordinary ray (designated as O ray and E ray respectively). Smerd has shown that for the O ray the refractive index of the medium is zero when x = 1. This is the same

as the case for no magnetic field (See Eqn.P6). For the E ray μ is zero when $x = 1 \pm y$. The case of $x = 1 + y$ is of no practical consequence since radiation generated at this level would definitely be unable to escape. From these conditions he has calculated the heights of these levels of zero refractive index for the O ray and the E ray for the general magnetic field, and also for the intense field obtained near regions of sunspot activity. These are represented diagrammatically in Fig.E, given by O, E_g and E_i respectively. From these considerations it appears that a certain frequency f will not be propagated unless generated in a region where $f_o < f$. At $f = f_o$ the radiation encounters a "stop-band", and is attenuated to an infinite extent. The existence of these zero refractive index levels was thought to account for the echo waves referred to earlier. Radiation actually being generated where $f = f_o$ will be propagated radially outwards. The magnetic field H, and hence the quantities f_H and y were thought by Smerd to be unimportant in the case of the quiet sun; but sunspot fields of 3000-4000 oersted have been thought to be responsible for so-called "synchrotron" radiation. There are, however, objections to this hypothesis which will be examined later when discussing the synchrotron theory of Kruse, Marshall and Platt (60).

Jaeger and Westfold (1950) (47) assuming no solar magnetic field, and a spherically symmetrical corona described by the Baumbach-Allen formula (Eqn.P2), have plotted ray trajectories in the corona for frequencies 60 and 100 Mc/s. An infinite number of such

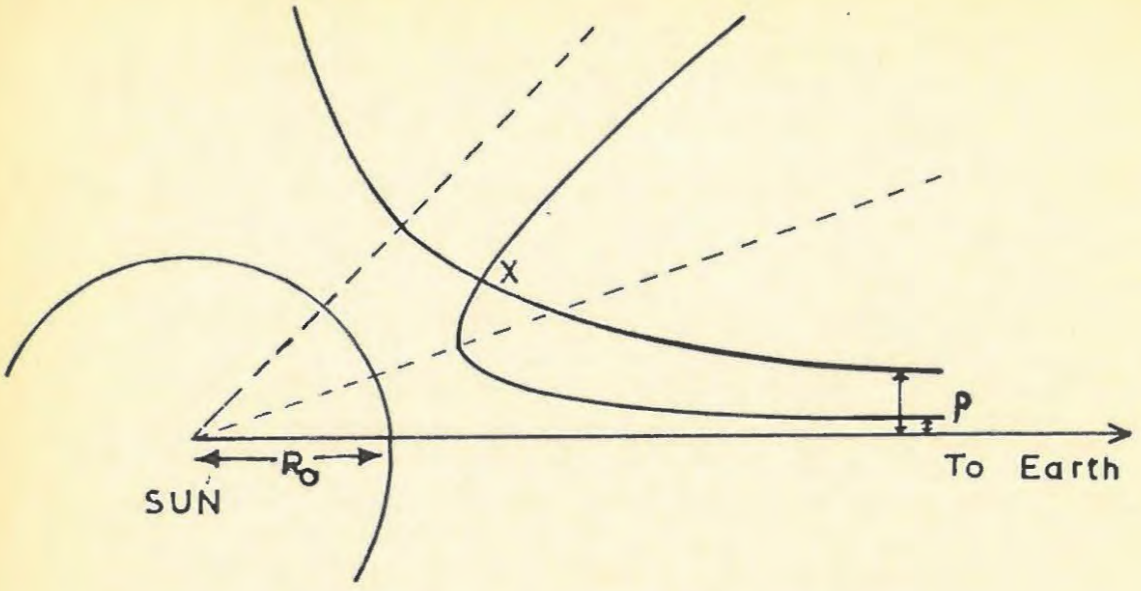

Ray Trajectories in the Solar Corona

FIG F

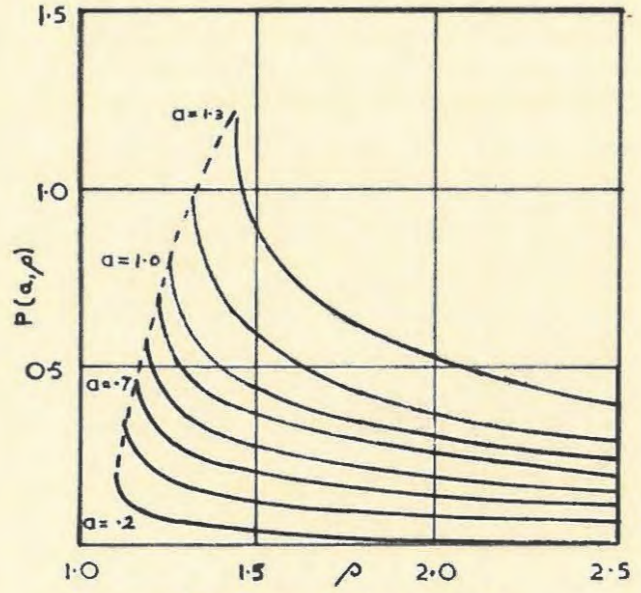

Equivalent Path Integrals

FIG G Ref. 47.

trajectories is possible for each frequency, each depending on the position of its asymtote with respect to a solar radius vector. This is described in terms of a parameter "a" which is defined as

$$a = \frac{p}{R_o} \qquad (P9)$$

where p is the asymtotic distance of any particular trajectory from an axis passing through the centre of the sun,
and R_o = solar radius to base of corona.
Any one trajectory is then characterized by a certain value of "a", and has a point of closest approach (i.e. turning point) about which it is symmetrical. (Fig.F.) It will be seen that a burst originating at point X could escape the solar corona and reach the earth by two possible paths, the time delay between the arrival of the two signals being determined by the extra path travelled by the reflected or echo wave. The observations on double-humped bursts are not altogether what one might expect theoretically from this model. The "harmonic" explanation is now generally favoured. (See later)

The equivalent path over any portion of a trajectory is defined as the distance the wave would have travelled in free space in the time it took to traverse the actual path length and may be determined from the "equivalent path integrals" for various values of "a" calculated by the writers by evaluating the integral

$$P(a,\rho) = \int_{o}^{\frac{1}{\rho}} \frac{d\chi}{\chi} \left\{ \frac{1}{\Delta^{\frac{1}{2}}(a,\chi)} - 1 \right\} \qquad (P10)$$

where $\chi = \frac{1}{\rho}$

where ρ is defined as before, and $\Delta(a,\chi) = \mu^2 - a^2\chi^2$

These curves give the value of the "excess of equivalent path" from any point (defined uniquely in terms of ρ and a) to infinity. A set of equivalent path integral curves is shown in Fig.G.

This is an extension of the treatment by Jaeger and Westfold (1949) (43) where only the case of radial propagation was considered.

Similarly the absorption over a given ray path is found from the absorption integral curves, obtained from the integral

$$\tau(a,\rho) = \int \kappa \quad ds. \qquad (P11)$$

where ds is an element of path, and κ is defined as the "absorption coefficient" given by

$$\kappa = \frac{\nu}{c}\left(\frac{1-\mu^2}{\mu}\right) \qquad (P12)$$

where c = velocity of light in vacuo.
The term τ is usually referred to as the "optical depth". (See Appendix 1).

The author has calculated a full set of ray trajectories and absorption integrals for 125 Mc/s for use with the records taken on this frequency at Rhodes. (See Chapter 4).

Wild and McReady (1950) (19) examined the dynamic spectra of high intensity bursts using a swept-frequency receiver operating between 70 - 130 Mc/s, and tentatively identified the three common

DYNAMIC SPECTRA

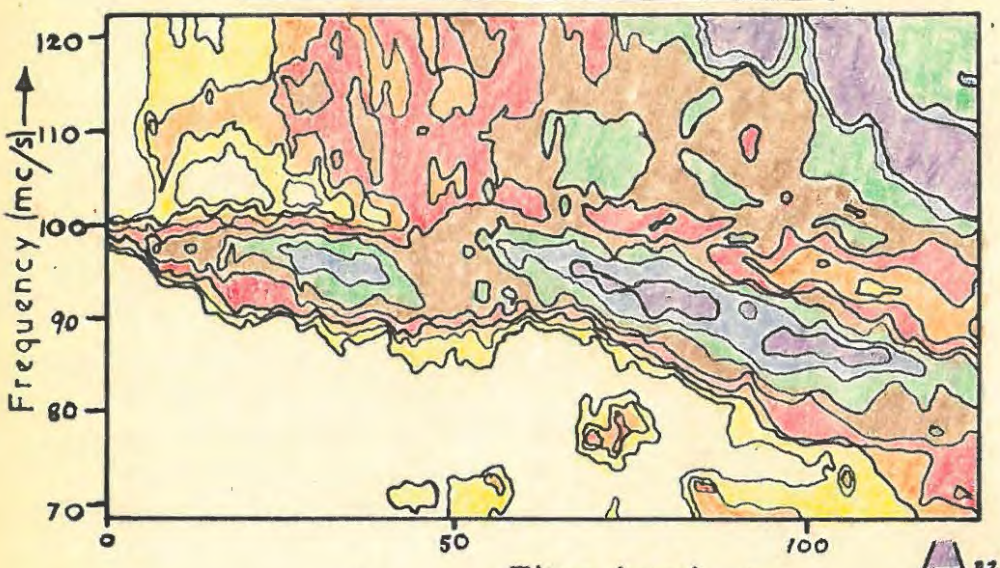

OUTBURST (TYPE III)

FIG H Ref. 48.

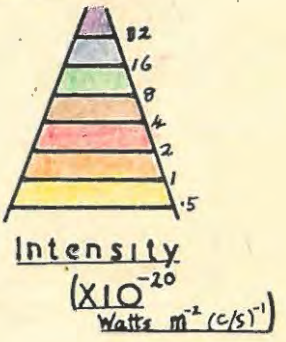

Intensity
($X10^{-20}$ Watts m^{-2} $(c/s)^{-1}$)

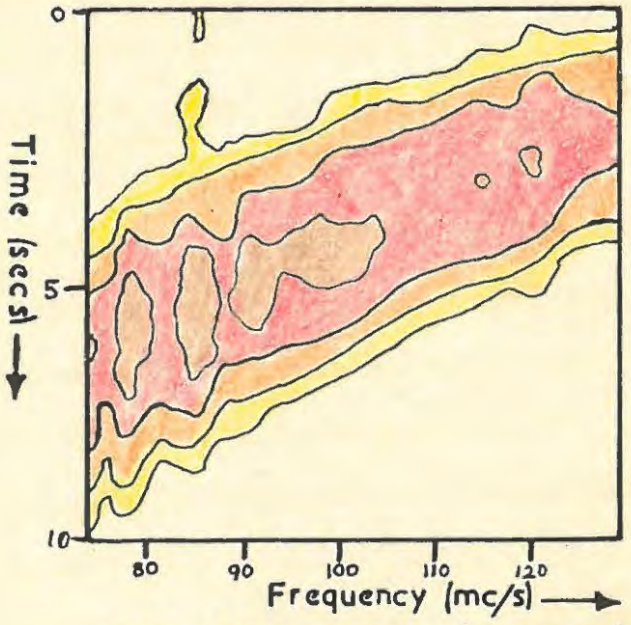

ISOLATED BURST (TYPE III)

FIG I Ref. 49.

spectral classes which are now known as types I, II and III. The receiver swept the band three times a second, each sweep being effectively instantaneous (.07 sec), the output being displayed as an intensity modulated spot sweeping in the "Y-direction" on a cathode-ray screen, being photographed on film moving in the "X-direction", giving in effect a frequency-time diagram upon which variations in solar radio intensity appear as variations in photographic density. This type of record is conveniently represented as a "contour" diagram as shown in Figs. H and I.

Wild (1950 a, b) carried out more extensive observations on (a) Outbursts (48), and (b) Isolated bursts (49) with the above receiver. Outbursts (type II) were generally found to be of more complex a character then the isolated (type III) bursts, and were characterized by a slow but steady drift to lower frequencies (at about $\frac{1}{4}$ Mc/s per sec), the rate of which was independent of frequency. They usually had a life-time of several minutes and exhibited a sharp low-frequency cut-off. A typical outburst is shown in Fig.H. Isolated bursts on the other hand drifted extremely rapidly to lower frequencies (at about 20 Mc/s per sec), the rate of drift being approximately proportional to the frequency. These bursts are very short-lived (a few seconds), but have bandwidths usually greater than 50 Mc/s. Wild termed an intensity contour taken at any particular time a "frequency profile", and one taken at any particular frequency a "time profile". The time profiles taken off Wild's records have very much the same appearance as the

single frequency records of previous workers, and Wild found that the decay constant appeared to increase approximately linearly with frequency. The frequency profiles, as in the case of outbursts, fell off more sharply on the low frequency edge. A typical isolated burst is shown in Fig.I.

The observed behaviour of both burst-types is explained by Wild in terms of the outward passage of various types of corpuscular streams, which initiate plasma oscillations at the various levels. The high correlation between flares and outbursts would seem to suggest that flare associated surge prominences and/or streams of "magnetic storm particles" could be the exciting agencies. The known velocities of both types (of the order of 10^3km/s) would give a frequency drift of the order observed. The rapid drift of isolated bursts is explained in terms of a source travelling at 10^4 - 10^5 km/sec, rather than selective group retardation of waves in the corona, or variations of the wave frequency controlled by the magnetic field. If the decay constant is determined by the amount of damping due to electron collisions, (See refs. 41 and 43) then it is necessary also to postulate an outward motion through the corona. However, the observed decay at any frequency is far more gradual than one would expect from the value of ν at the corresponding level. In addition, the fact that radiation of frequency f_o emanating from the f_o plasma level should only be able to escape radially (See refs. 43 and 3, 8) indicates that we should only be able to receive radiation from very near the centre of the solar disc. This is at var-

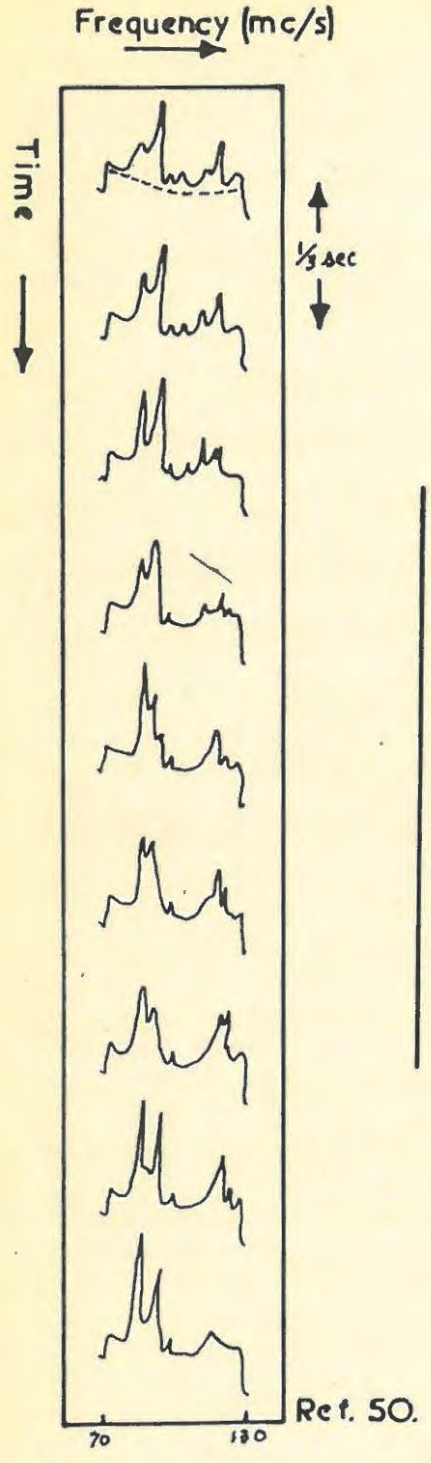

Ref. 50.

FIG J

Refs. 56 & 57

FIG K

iance with the observations of subsequent workers. It is evident that certain refinements of these hypotheses as they stood were still necessary.

In 1951 Wild (50) examined the enhanced radiation or noise-storms comprising type I bursts between 70 and 130 Mc/s, relating the individual behaviour of the background continuum and the bursts themselves. These polarized bursts are very short-lived, appear fixed in frequency, and have narrow bandwidths. The 3-dimensional type of record described above is not suitable for examining this prolonged type of radiation, and the display was modified so as to present the sweeps as a series of successive frequency profiles separated by $\frac{1}{3}$ sec., as shown in Fig.J. He was unable to report anything vitally conclusive in respect of intercorrelation of type I phenomena.

Bailey (1951) (51) developed a theory for the growth of amplified waves in the presence of a magnetic field, and interpreted solar radio bursts due to spot associated sources in terms of this hypothesis. The radiation generated would in general be elliptically polarized, and Bailey explained the apparent random polarization observed in many bursts as being due to the inability of the existing receivers to distinguish between mixtures of differently polarized, and truly unpolarized radiation, although he considered the possibility of random polarization in the absence of a magnetic field.

Twiss (1951) (52) repudiates most of Bailey's conclusions, showing that growing waves could only be generated in a medium bound-

ed by a critically characteristic impedance which would induce resonant reflections. This state of affairs is very unlikely to be realized in the corona near sunspots, and Twiss further indicates that even if amplification on Bailey's model were possible, the radiation would be unable to escape from the region.

Cristiansen et al (1951) (53) examined two remarkable bursts occurring a few days apart, with seven single-frequency receivers working over the comprehensive range 62-9400 Mc/s, and compared the results with other associated phenomena. Both bursts were flare associated, and both had simultaneous radio fade-outs on earth. The polarization, where measured, also behaved similarly in both cases, the sense staying fixed at higher frequencies, but changing at the lower end of the spectrum. However, the first showed a distinct frequency drift; while the second, more prolonged, appeared to occur simultaneously on all frequencies, and to last longer at the lower end. There was in addition, a magnetic storm 35 hrs. after the second burst. It seems that the bursts were of different types; but neither can be explained completely in terms of any accepted theory. Corpuscular velocities of the order of 10^3 km/sec, obtained from the delay of the magnetic storm, would have fitted the drift observations on the first burst well. If magnetic and/or electric fields are deemed to be the causes in case 2, then their application to case 1 does not fit observation. It appears apparent that the explanations must, however, be sought in terms of some synchrotron process, due to powerful magnetic fields which tend to be more variable in the outer regions of

the corona. The incidence of sunspot groups with both the bursts lends substance to this point of view. This case is typical of the many anomalies encountered in this field.

Piddington and Minnett (1951) (54) discuss two models for the thermal emission of radio noise from "hot-spots" above sunspots, which give good qualitative agreement with the values obtained from observation. They conclude that certain slowly varying radiation could have thermal origin in regions at about 10^7 °K, the emission correlating with sunspot area, and varying slowly in intensity owing to the enormous masses of gas involved.

Payne-Scott and Little in an important series of observations on noise-storms (1951) (55), and outbursts (1952) (20), using an interferometer at 97 Mc/s, studied the relative positions of radio sources and associated spots or flares respectively. They found storm radiation to be associated particularly with an individual spot in a group, and showed in general right-handed polarization to be associated with a south-seeking pole, and conversely left-handed with a north pole. The increased discrepancy between apparent source and spot positions on the disc towards the solar limb indicated elevated storm sources up to one photospheric radius above the visible disc. They showed that for the O-ray at least, these heights are probably always above the reflection level and it would thus be propagated. These observations appear also to refute earlier theories which require considerably lower levels of origin (Saha 1947, Bailey 1950).

Outburst sources were observed to travel rapidly away from associated flares, indicating corpuscular source velocities of the usual order (10^3 km/sec.). Polarization was invariably random at the start of an outburst, but often became coherent at a later stage following the same rule for right- or left-handedness as noise-storms, leading the writers to suppose that the two types of radiation were identical at this level. The reason for random polarization in early stages is not immediately obvious, although it appears to the author that magnetic turbulence prevalent in the lower regions, as opposed to the more uniform and static conditions further out, (representing an integrated field over a wider area) might account for this. It is conceivable that polarization might be induced during propagation through an ionized medium in a magnetic field, even if it originates as randomly polarized radiation. (See Wild (1957), later.) This could explain the similar aspects of two types of radio noise which are essentially different.

Wild, Murray and Rowe (1953) (56) and (1954) (57) discuss the occurrence of harmonics in the spectra of outbursts observed with a swept-frequency receiver covering the range 38-240 Mc/s. A burst containing two simultaneous components at harmonic frequencies was called an "Harmonic pair". The dynamic spectrum of a typical burst of this type is reproduced in Fig.K. It was found in general that the maxima were separated by a frequency ratio usually slightly less than the expected 2 : 1, and that the intensities of the fundamental and the harmonic bands were about the same. The writers in-

terpreted these results as being due to an outward moving source, which at any plasma level f_o generates a band of frequencies about f_o and $2f_o$, the fundamental oscillation being of far greater amplitude. According to the conditions for escape of radiation from the corona derived by Smerd (unpublished), the lowest frequency that can be received at the earth from the f_o level for a given source angle θ (known as the critical escape frequency f_c) is given approximately by

$$f_c = f_o \sec \quad 0.87\theta \qquad \text{(P13)}$$

which is a simplification of a complex relationship, but which in a Baumbach-Allen corona is accurate to within a few per cent for frequencies of about 100 Mc/s and for θ between 0^o and 80^o. This "source angle" is defined as the angle between a solar radius passing through the source and the direction of the sun-earth line. This means that for a source in the centre of the disc ($\theta = 0^o$) all the lower half of the generated band will be cut off, and only the top half will be received. This would tend to give the frequency profiles of received radiation the assymetric appearance observed previously; and in the case of $\theta > 0^o$, the cut-off would result in a displacement of the peak towards higher frequencies. For the harmonic band on the other hand, $2f_o$ is well above f_c, the radiation at this frequency suffers practically no attenuation, and the profile is received as generated. On this model then, the greater the source angle, the more the fundamental band is cut-off in any part

of the corona, giving a lower "harmonic ratio". It appears that the 3rd harmonic is not excited as this band would undoubtedly have been detected if it were present. It was also found that in some cases the fundamental exhibited 'band-splitting' which was duplicated in the harmonic. It was thought that this might be some Zeeman effect due to coronal fields.

A plot of height of radiating source in the corona against time obtained from the observed frequency drift rates should be linear if the outward motion is constant, giving a measure of the source velocity. From such a linear plot the writers obtained "derived velocities" of a few hundred km/sec. The difference between these values and those obtained by Payne-Scott and Little (20), and the known velocities of magnetic storm particles can be explained in terms of oversimplification of electron distribution in a Baumbach-Allen corona.

Wild, Roberts and Murray (1954) (58) derived source velocities of about 10^5 km/sec for isolated bursts, and by extrapolating the source positions to correspond in time with the onset of an associated flare they deduced original source positions at the base of the corona. This applied to compound bursts of type II and III combined which indicated a common explosion which ejected fast and slow particles.

The presence of harmonic pairs in type III radiation appears to provide the natural interpretation of double-humped bursts. A time profile on a typical record has similar characteristics to the

profiles obtained on single frequencies by Shuter (38) and the author.

All the above work by Payne-Scott, Little, Wild, Murray, Rowe and Roberts provides incontestable evidence of the importance of moving source models for types II and III burst production.

Smerd (1955) (59) discussed the various results of Wild et al, interpreting the observed harmonic structure in terms of non-linear longitudinal plasma oscillations, and concluded that higher harmonics should be possible.

Kruse, Marshall and Platt (1956) (60) arguing in favour of radiation produced by gyro electrons rotating in a magnetic field (at the gyro-frequency f_H) i.e. a "synchrotron" mechanism, to explain high intensity radiation, particularly harmonics (dismissed by earlier workers), showed that such radiation can, under certain conditions of magnetic field, escape the solar atmosphere in either or both the O and E modes. Assuming an expression due to Schwinger (1949) (61) for the power radiated into the harmonics of the gyro-frequency f_H (Eqn.P8), they calculated the flux densities which might be expected, taking into account the respective absorption of the harmonic bands. The results obtained were only in good agreement with experiment provided a value of electron velocity was used which was (a) greater than that consistent with the absence of a 3rd harmonic, (b) greater than that corresponding to kinetic temperatures of 10^4 ^oK prevailing above the sunspots out of which the non-relativistic electrons were thought to spiral along the magnetic lines of force, (c) less than that consistent with the observed ratios of peak intensities for the

first and second harmonics.

It seems likely that this model might be the correct one for those type III bursts which were found by Komesaroff (9) to exhibit elliptical polarization; which is, in general, to be expected from synchrotron radiation in an inclined magnetic field (Pawsey and Bracewell (1955) (62)). It may be shown subsequently that what has hitherto been known as type III radiation is in reality two distinct types with only superficially similar characteristics.

The author, however, feels that most of the observed features, particularly frequency drift, are more easily explained in terms of plasma oscillations excited at successive levels, rather than being due to gyro-electrons moving into regions of different magnetic intensity, as the solar fields are not predictable (near sunspots particularly) and the bursts would tend to be more inconsistent than is generally observed.

Westfold (1957) (63) in discussing the different order of source velocities for type II and III bursts suggests that acoustic shock waves might be responsible for excitation of oscillations, the high velocities in the latter case being effected by magnetic fields of the order of a few hundred oersted, giving a magnetohydrodynamic component. He considers the model of a stream of particles (auroral or corpuscular) preceded by shock-wavefront, and shows that the results are similar to those obtained by Jaeger and Westfold in their previous theory of transients. (43).

Christiansen, Warburton and Davies (1957) (64) in studying

the distribution of radio brightness across the solar disc at decimeter wavelengths, attributed the slow variations in the background radiation to sources which were associated with long-lived bright areas in the photosphere where coronal temperatures prevailed. Using a 32-element interferometer they found that the sources were in general about 22,000 km above these "plages facularies". From the fact that the intensity of radiation from any individual source was found to fall off almost exactly according to a cosine relationship toward the solar limb, it was assumed that the source took the form of a thin sheet lying parallel to the photosphere. Significant correlation between the emission of X-ray and ultra-violet radiation and these active areas was also found, and it seems very probable that all these phenomena are inter-related, and in fact are manifestations of a single disturbed source emitting thermally over the entire spectrum. The apparent differences in position of radio and visible sources may be in part due to dispersive refraction of the various components by the solar atmosphere. Sunspots, flares and other sporadic events are associated with, and occur during the lifetime of a plage; and can thus still be responsible for the more intense shortlived burst of radio noise.

Swarup and Parthasarathy (1958) (65) carried out similar investigations at a lower frequency, observing more rapid fluctuations in radio brightness than was consistent with purely thermal mechanisms of origin. They also calculated considerably higher temperatures from radio than from optical observations, which they

took as further evidence that the slowly varying component was at least partly non-thermal in origin.

The results of swept-frequency observations by Wild and Sheridan (1958) (66) using an interferometer over the range 40-70 Mc/s indicate that the source size increases with decreasing frequency, suggesting a cone-shaped emitting region in the corona, the diameter increasing with height.

The reverse-drift pairs described by Roberts (1958) (16) have already been mentioned. It is difficult to reconcile the observed characteristics of these bursts with accepted mechanisms for type III burst production, although they are obviously related. The second elements are thought to be echoes of the first which occur high in the corona at the second harmonic of the plasma frequency. The time delays expected are of the right order, but the relative intensities do not always conform. The positive drift-rate is thought to be due to either inward moving sources; or outward moving sources responsible for the usual type III burst encountering irregularities of "hills" of electron density in the corona. Further study of the relationship between these and type III events is desirable before either of these postulates can be definitely favoured.

Komesaroff (1958) (9) in his polarization determinations showed that type I radiation showed the usual strong tendency to circular polarization, but his results for type II were inconclusive. An exhaustive study of type III bursts revealed the signi-

ficant fact that those bursts which exhibited harmonic structure were invariably polarized. This supports the author's contention that there could be a division of type III phenomena into at least two sub-sections. (See discussion on synchrotron radiation a few pages back). Wild (1957) (67) however, attributes polarization of some type III bursts to terrestrial effects (propagation through ionosphere) as these were observed either early in the morning or late in the evening.

Roberts (1959) (68) carried out further extensive investigations on type II radiation, and found that there was a closer association with type III than was previously thought, combinations of the two types being common. There appeared also to be some cause to suppose that this radiation is indistinguishable from the special drifting type I described by Wild (1957) (67). Drift rates and hence derived source velocities were found to be of the same order as hitherto expected. The drift rate was found in fact to vary with frequency approximately according to a relation of the form

$$\frac{df}{dt} = 0.1\left(\frac{f}{50}\right)^{1.5} \qquad (P14)$$

Again harmonic structure was observed to be common, although there was still no evidence of harmonics higher than the second. (See Smerd (1955) (59)). The relationship between position of source on the disc, and harmonic ratio did not altogether support the

theory of Wild, Murray and Rowe (56, 57) but confirmed that in general the ratio was less than 2 : 1. Association with flares was considerably more for very large flares (> 3) but in any case only a small percentage of flares had accompanying bursts. Band slitting of the type noted by Wild et al (1954) (56, 57) is discussed, and various interpretations reviewed. None is entirely satisfactory, although it seems that a magnetic effect of some sort is responsible, rather than mere simultaneous emission at adjacent frequencies due to two different disturbances. The author further supports this attitude by considering two points. Firstly, the relative intensities of the elements would hardly be likely to be similar (as observed) on the latter hypothesis; and secondly, on this theory there could easily be splitting into more than two elements due to a succession of disturbances. As yet no such multiple splitting has been noted.

Shane and Higgins (1959) (69) using an interferometer at 19 Mc/s showed that the radio sources at this frequency were much higher in the corona above the corresponding optical centres than the normal plasma level, and even higher than the 9.5 Mc/s level, if one supposes that the second harmonic was observed. This was attributed to "coronal streamers", presumably emanating from the active regions, of higher electron density than attains in the normal corona. More observations of this kind at higher frequencies would be useful, as these streamers might only affect the homogeneity of electron distribution appreciably at the higher levels.

Wild, Sheridan and Neyland (1959) (29) in a new investigation of type III source velocities, using simultaneous interferometric observations on several frequencies between 40 and 70 Mc/s showed evidence supporting the idea of areas of increased electron density - i.e. streamers. The velocities they measured were far greater than those obtained previously from dynamic spectra records, the average value being about half the velocity of light. The recently observed type V continuum, which is often associated with type III radiation is discussed in the light of these high velocities. The close association between combined type III - V events and flares (See previous chapter) led to the postulation of streams of relativistic electrons spiralling outward along magnetic lines of force from the disturbed centre, giving rise to plasma oscillations resulting in type III radiation in the usual way; while the spiralling electrons themselves emit synchrotron radiation responsible for the type V burst. The fact that the isolated burst precedes the continuum which arrives at a lower frequency suggests to the author that the synchrotron radiation might be unable to escape from the lower corona, so that it is only received when the electrons have been transported further out. The duration of this burst type could be explained in terms of anomalies in the magnetic field which trap the electrons which would otherwise pass out of the solar atmosphere in a few seconds. This idea also supplies an explanation of the inverted U bursts described by Maxwell and Swarup (15). It is thought that electrons following the magnetic field configuration can be

guided back into the sun giving the positive frequency drift limb characteristic of these bursts. The radiation here would then be oscillatory in nature, and not synchrotron as suggested by Shuter (38). Again conclusive polarization determinations could decide this point. The characteristics of this spectral type and its relationship with cm. radiation and chromospheric flares are discussed by Neylan (1959) (14) who supports in general the above hypotheses.

The other new spectral type IV is described by McLean (1959) (13), and the close association with other phenomena has led to the postulation of a common cloud of gas from a flare being responsible for all the events. Although type IV has been described as smooth type I radiation it is apparent that the two are quite independent. A synchrotron origin is suggested - due to electrons in the expanding gas cloud being trapped by "frozen-in" magnetic fields. The comparatively slow corpuscular stream would be responsible for the geomagnetic storms almost invariably observed a few days after a type IV burst. It is clear that on this model the relationship between these and type II bursts is merely the counterpart of the type III - V association discussed above, where the velocities involved here are of a much lower order (non-relativistic), explaining the longer duration, and slower drift-rates of type II - IV events.

The work of various workers in 1960 on the correlation of the new types IV and V radiations with optical observations and incidence of cosmic rays has already been mentioned. (Previous chapter).

Rabben (1960) (32) made some interesting comparisons between type III bursts and associated optical phenomena (q.v.).

Boischot, Lee and Warwick (1960) (70) examined type III radiation in the low frequency range 15 - 38 Mc/s, and found, as might be expected, that the bursts had a longer lifetime, and showed a slower drift than their counterparts at metre wavelengths. They observed also steady continuum noise sources lasting for a few days at these frequencies.

The previous pages represent a short survey of the present knowledge of solar radio astronomy. As will be seen, the last few years have not resulted in much change in the fundamental notions propounded about ten years ago. The plasma theories seem in general, to the author at any rate, to be more tenable than gyro or synchrotron models, as mechanisms of burst production. The author wished to pursue the question of optical correlations further, with particular emphasis on the comparison of the relative intensities of the associated phenomena. For this purpose the 300 Mc/s receiver described in the following chapter was used.

CHAPTER THREE.

THE EQUIPMENT.

The apparatus used for the measurement of solar radio noise at a frequency of 300 Mc/s consisted essentially of:-

(a) Antenna system.

(b) Antenna drive.

(c) 300 Mc/s preamplifier.

(d) 30 Mc/s I.F. amplifier.

(e) D.C. amplifier.

(f) C.R.T. display.

(g) Photographic recording equipment.

(h) Noise diode.

(i) Power supplies and regulators.

The radio frequency signals incident upon the antenna array were amplified by the various stages and eventually obtained as variations of D.C. potential which were used to deflect a spot vertically on the C.R.T. screen. The movement was recorded on film moving continuously in the horizontal direction giving effectively an intensity vs. time graph of the incoming signal.

The equipment for the most part was housed in the radio astronomy "shack" situated at Rhodes University, Grahamstown; geographical coordinates 33°18'39" S, 26°31'08" E. The antenna was mounted on a windmill tower (next to the shack) which also housed the

PLATE I

first preamplifier stage (c). See Plate I.

(a) The Antenna System consisted of an array of 18 half-wave centre-fed dipoles arranged and connected together with 300 ohm plastic twin-feeder tape as shown in Fig.L. The dipoles were held in polystyrene insulators mounted upon a wooden frame backed by a copper wire screen about 9" behind the dipoles. At the final junction, the twin-feeder lines were connected to a simple balun transforming from 100 ohm balanced line (3 x 300 ohm in parallel) to 50 ohm unbalanced coaxial line, which carried the signal to the preamplifier.

Construction and testing of array. The main supporting frame was constructed from light yet strong Phillipine Mahogany beams held rigid by a smaller rectangular angle-iron frame attached to the drive supports. Lengths of copper wire were stretched across the frame parallel to the dipoles, a few inches apart, to provide a ground screen for the "back" of the array. The dipole-holders were short lengths of wood bolted onto the frame so that they projected vertically. The insulators at the end of these struts consisted merely of small blocks of polystyrene with holes drilled through to accommodate the dipoles, which were lengths of tubing about $\frac{3}{8}$" in diameter and a little less than 48 cms. long. (This being the empirical value of the half-wavelength of a 300 Mc/s oscillation on such a line). They were initially polished to remove poorly conducting oxide layer, and coated with a varnish of satisfactory dielectric properties so as to minimise propagation losses.

In the initial construction the dipoles were connected together with parallel transmission lines of heavy gauge copper wire spaced by insulators to give the required characteristic impedance of 300 ohms in air. This, however, was found to be clumsy and difficult to work with, and was later replaced by the far more convenient twin-feeder tape. The preliminary adjustments were made on the ground, using the array supported against the side of a building as a transmitting antenna, and measuring the field-strength at a distance of about 10 wavelengths. With only one "sextuplet" array connected, the spacing between the dipoles and the backing screen was adjusted by moving the holders to give maximum output. This was not found to be critical. Matching stubs for the leads connecting each of the sextuplets to the balun were calculated from standing wave measurements, and attached at the end nearest the respective arrays. Ideally each individual dipole should have been matched to the line, but time did not permit of such a procedure. Each section of the array was tested separately and then together, fine alterations to the stubs being made to give the best horizontal polar diagram that could be measured on the ground using a field-strength meter.

Final adjustments to the matching could not be effected until the array was mounted upon the tower, acting as a receiving antenna, after the testing of the rest of the equipment had been completed. A 5-watt balanced oscillator transmitting through a folded dipole was placed about a mile away from the receiver, and the antenna orientated to give a maximum reading on a meter connected

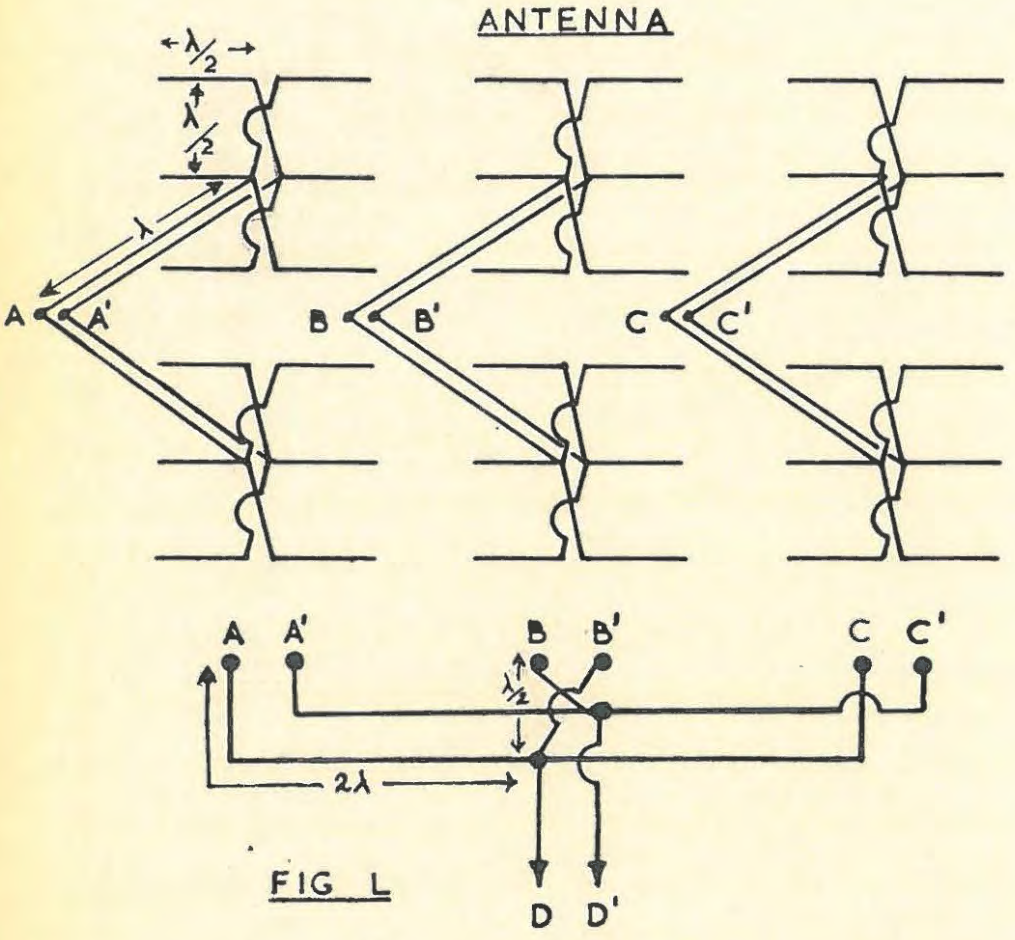

FIG L

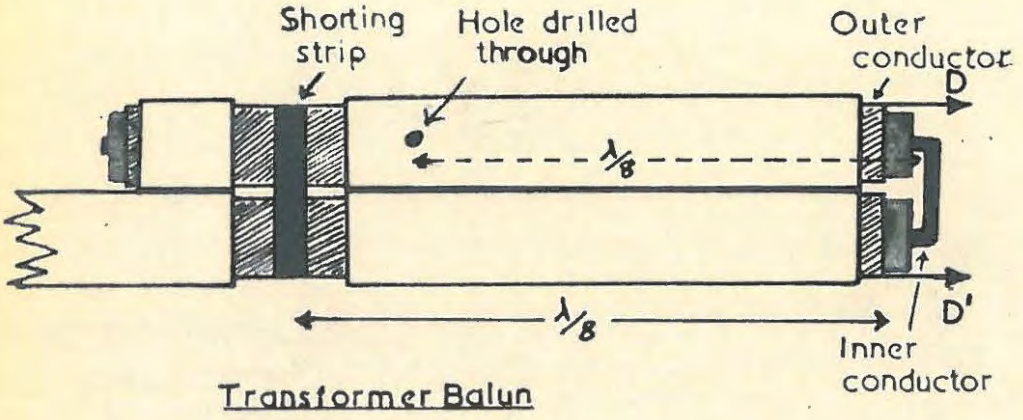

Transformer Balun

FIG M

to the D.C. output. Stub adjustments were made to increase this to an optimum value. Polar diagrams of the antenna pattern were then obtained by (i) sweeping the array about a vertical axis to give the horizontal pattern, and (ii) turning the array to face the oscillator and sweeping about a horizontal axis to give the vertical plot. The gain of the antenna was compared with that of a single dipole, similarly matched to the receiver input, placed just in front of the array.

The balun transformer used was constructed from the design by Roberts (1957) (71), after an original version built by G. L. Verschuur had been found to be unwieldy and unsatisfactory for use with the equipment. The principal features of this balun were its simplicity of design, compactness and broadband characteristics. It consisted essentially of two lengths of 50 ohm coaxial cable placed side by side, the outer conductors forming a balanced transmission line, shorted at one end as shown in Fig.M and connected to the twin-feeder tape at points D and D' while one length of coaxial cable carried on to form the unbalanced conductor. The dimensions were such that the conducting lengths on the shorter arm and on the outer parallel conductors were both $\frac{1}{8}$ wavelength. As wavelength is shorter on the former, it was severed by drilling a hole through at the appropriate place.

It is shown that for a balun of this type, the impedance looking into the longer length of coaxial cable at D' is given by the expression

POLAR DIAGRAMS

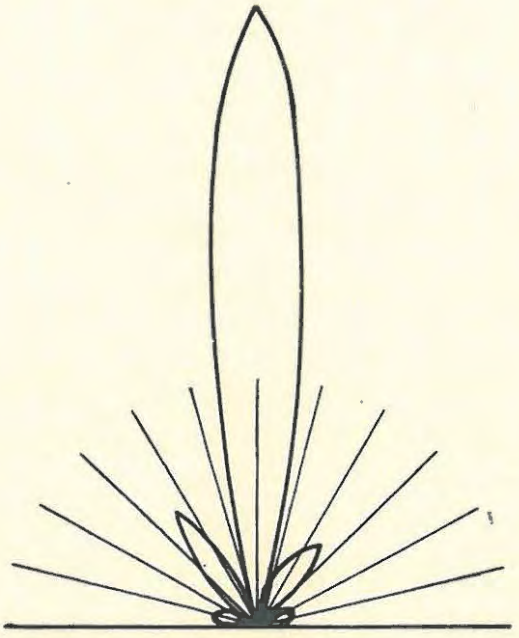

Horizontal Sweep

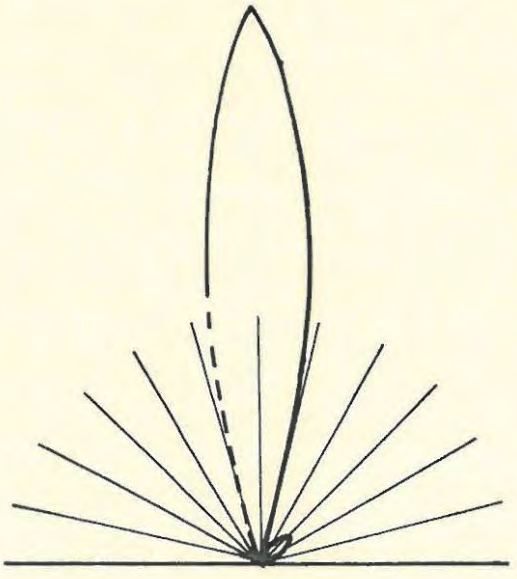

Vertical Sweep

FIG N

$$Z = R \sin^2\theta + j \cot\theta \, (R \sin^2\theta - S) \qquad (P15)$$

where R = characteristic impedance of the transmission line formed by the outers (DD').

S = characteristic impedance of coaxial cable forming the arms of the balun.

θ = electrical lengths of the lines.

The reactance for this is zero for $\cot\theta = 0$ and $\sin^2\theta = S/R$. The roots of $\sin^2\theta = S/R$, θ_1 and θ_2, give values of θ at which a perfect match is obtained, i.e. where $Z = S$; while the solution of $\cot\theta = 0$ ($\theta = \pi/2$) gives the centre of the band.

For our purposes the broadband characteristics were not required, and the balun was constructed to conform with a point of perfect match. The physical spacing between the outer conductors was adjusted to give a 100 ohm impedance to match into the three 300 ohms balanced lines connected in parallel across DD'.

In this case we have S = 50 ohm, R = 100 ohm $\therefore$ $\sin^2\theta = S/R = 50/100$ $\therefore$ $\theta = 45^\circ$ or 135°, i.e. length of coaxial line forming balun = $\frac{1}{8}$ or $\frac{3}{8}$ wavelengths. For convenience the balun was made to conform with the $\frac{1}{8}$ wavelength specification.

Fig.N. shows the vertical and horizontal polar diagrams of the matched array, obtained by plotting D.C. output vs. angular position of the antenna. From this the beamwidth, directive gain and effective area of the antenna were determined.

Beamwidth is measured directly between half power points on

the diagram.

Directive Gain is given by

$$g = \frac{\text{Power absorbed in direction of maximum gain}}{\text{Mean power absorbed over all orientations.}}$$

which, by the theorem of reciprocity, assuming equal power to be fed into the antenna and an isotropic radiator

$$= \frac{\text{Power radiated in direction of maximum gain from antenna}}{\text{Power radiated in any direction from an isotropic radiator.}}$$

As the two polar diagrams are symmetrical, and of comparable beamwidths, we can assume that the diagram is symmetrical about the axis of maximum gain in all directions.

From this the flux density in any particular direction specified by the angle θ (this thus defines a cone), is proportional to

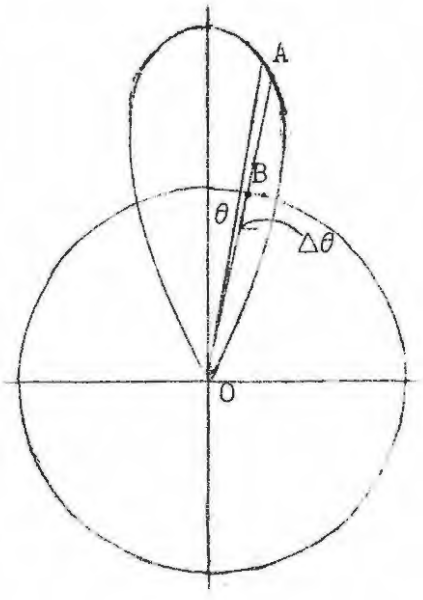

$$\frac{(OA)^2}{120\pi}$$

where 120π is the permittivity of free space. The flux through the annulus formed by the angular increment $\Delta\theta$, on a sphere of radius r, will then be proportional to

$$\frac{(OA)^2}{120\pi} \times (2\pi r \sin\theta)(r\Delta\theta)$$

The total flux in all directions will thus be given by

$$F_a = K \sum \frac{(OA)^2}{120\pi} \times 2\pi r^2 \sin\theta \Delta\theta$$

$$= \frac{K\pi r^2 \Delta\theta}{60\pi} \sum (OA)^2 \sin\theta$$

where K is some constant depending on the units of the diagram.

Similarly for an isotropic radiator (having a spherical polar diagram, radius OB,) the total flux in all directions is given by

$$F_i = \frac{K(OB)^2}{120\pi} \times 4\pi r^2$$

Since we know $F_a = F_i$, we can get an expression for OB

$$OB^2 = \frac{\Delta\theta}{2} \sum (OA)^2 \sin\theta$$

From our definition of directive gain above, we get

$$g = \frac{OA^2_{max}}{OB^2} = \frac{2\,OA^2_{max}}{\Delta\theta \Sigma OA^2 \sin\theta} \qquad (P16)$$

The values of OA corresponding to many different values of θ separated by a small but finite constant angular interval $\Delta\theta$ are measured from the diagram and P16 used to obtain g which may be expressed in decibels from the relation

$$G(db) = 10 \log_{10} g$$

Effective Area (A) is related to the directive gain by the expression

Azimuth Drive

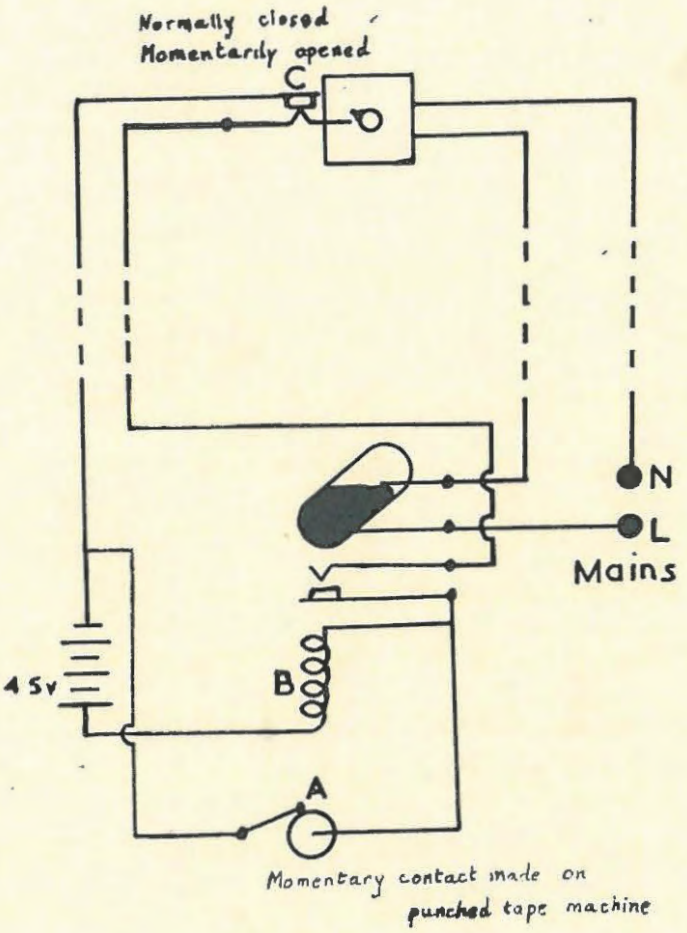

FIG O

RHODES UNIVERSITY LIBRARY

$$A = \frac{g\lambda}{4\pi} \qquad (P17)$$

where λ is the operative wavelength.

From the above considerations we obtain the antanna parameters as follows:-

Average beamwidth	17^{o}
g	71
G	18.5 db
A	5.65 sq.m.

(b) The Antenna Drive. The whole dipole array is fixed to an alt-azimuth mounting which can be rotated independently about a vertical axis (controlled by the azimuth drive), and about a horizontal axis (controlled by the altitude drive). Both drives are activated by a momentary contact from the "time-tape machine", and each turns the antenna through a certain fixed angle before switching itself off. The frequency of activation depends on the "time-tapes" which are lengths of 35 mm film punched at precalculated intervals and passed over a brass drum at a constant speed determined by a synchronous fractional h.p. motor. A spring loaded contact rests upon the moving film, and makes an almost instantaneous contact with the drum through a punched hole, initiating a cycle of the drive. Plate II shows this "time-tape machine" with tapes for both the antenna drives.

Azimuth Drive. The circuitry for this is shown in Fig.0. When contact is made at A, the relay B causes the mercury switch to close, and the drive motor to operate. The holding circuit will keep

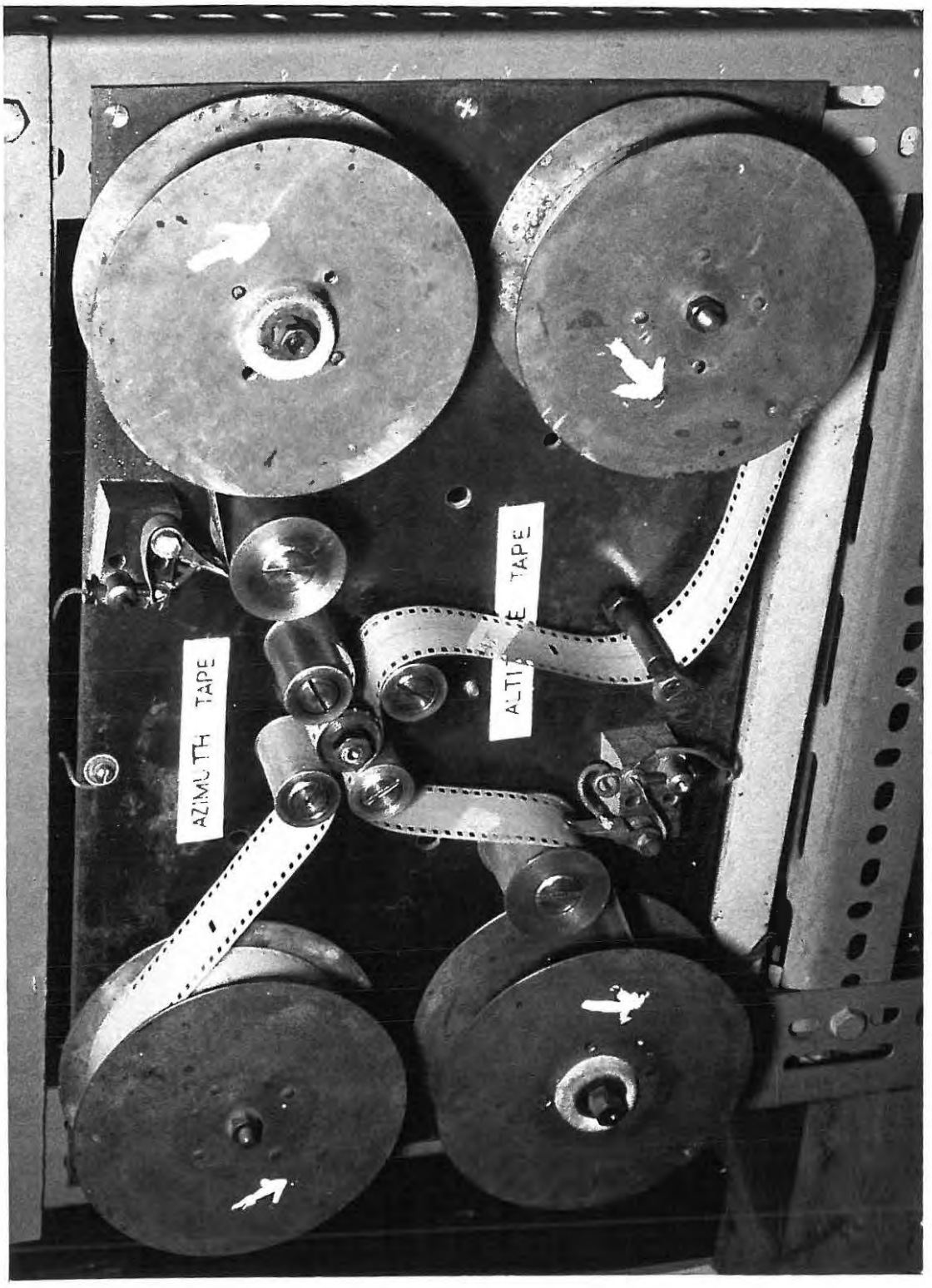

PLATE II

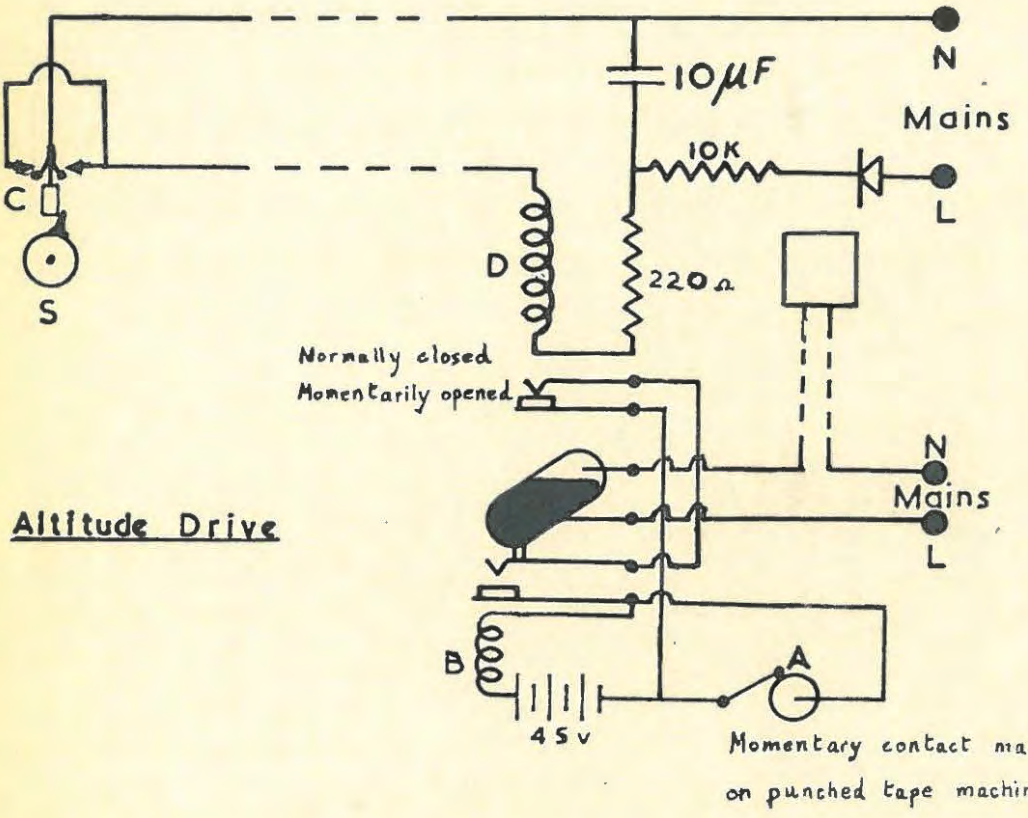

Altitude Drive

FIG P

the relay closed after contact at A has been broken by the passage of the time-tape. The motor operates through a gear ratio 150 : 1, and the slow shaft executes one revolution before momentarily breaking contact at C, causing the relay to be released, stopping the motor, ready for the next activation. A reciprocating arm on the slow shaft turns a 19 toothed ratchet wheel through 1 tooth during the cycle. This wheel acts directly through a further 150 : 1 gear onto the vertical azimuth drive shaft. Thus at every contact on the time-machine the antenna is moved through a horizontal angle given by $\frac{360^{\circ}}{150 \times 19} = .126^{\circ}$.

Altitude Drive. Fig.P. shows this drive circuitry. Momentary contact at A closes relay B which holds itself and sets motor running as before. The drive is connected to the antenna supports directly through two 150 : 1 gears in series, the intermediate shaft S rotating once per contact. The contact C can in this case be initially either open or closed. If C is open, the 10μF condenser is charged from the rectifier circuit. When contact is made after the shaft S has completed one revolution, the condenser is discharged rapidly through relay D, causing the points to open momentarily releasing relay B, stopping the motor as before. If C is initially held closed by the cam on shaft S, the condenser remains unchanged, but the time of revolution of S enables it to attain a full charge so that when C is once again closed by the cam the relay D is activated just as before. After the cycle, C is either open or closed

depending on the position of the cam when S comes to rest. Each activation in this case causes the antenna to be rotated in the vertical plane through an angle given by $\frac{360^{\circ}}{150} = 2.4^{\circ}$.

From the concurrent operation of these two drives at times determined by the time-tape spacings, the antenna can be made to follow the solar celestial path over a day to within a few degrees, which are easily accommodated by the beamwidth. Errors are principally due to the fact that the time tapes have to be changed at intervals during the year, and ideally any tape will only be accurate for one day in the middle of the period over which it is used. It was found sufficiently accurate to change the tapes every 6 weeks.

Calculation of Time Tapes.

From astronomical formulae given by Godfray (1894) (72), the sun's azimuth A, is given by two relationships:

$$(1) \quad \cot A = \frac{\tan \delta \cos \phi - \sin \phi \cos h}{\sin h} \qquad (P18)$$

$$\text{and} \quad (2) \quad \cos A = \frac{\sin \delta - \cos \alpha \sin \phi}{\sin \alpha \cos \phi} \qquad (P19)$$

where A = azimuth of sun measured from South.

h = "Hour angle" of sun

= 15t where t = number of hours after midnight.

ϕ = latitude of observation (= $33^{\circ}19'$).

δ = declination, which is taken as positive in summer, and negative in winter.

α = zenith distance of the sun = 90° - Altitude.

The first (P18) gives the variation of azimuth with time

for any part of the year specified by δ . Thus by plotting values of A against h for various values of δ , a set of curves is obtained, from which a series of azimuth time tapes can be made, time being easily translated into distance along the tape. In this case the times corresponding to 5° intervals on the azimuth axis were read off, and the corresponding tape spacings divided into 40 equal parts, thus effectively dividing the time-tape into $\frac{1}{8}^{\circ}$ intervals. Over the daily running period of about 8 hours this is not significantly different from the $.126^{\circ}$ intervals calculated from the azimuth drive gearing.

Using P19, a set of A vs Altitude curves can be drawn in the same way. With this and the above graph, curves of Altitude vs Time for various δ are plotted, which are used for the altitude time-tapes. Here the times corresponding to the exact 2.4° intervals given by one cycle of the altitude drive were read off, determining the positions of the punch holes as before.

(c) 300 Mc/s Preamplifier consisted of one 300 Mc/s amplification stage, local oscillator and mixer, and 3 stages of I.F. amplification. (30 Mc/s). Because of high propagation losses at 300 Mc/s the pre-amplifier was mounted in a special housing on the windmill tower, the I.F. signal being carried across to the shack along a thin coaxial line.

The construction of a satisfactory preamplifier occasioned much trouble and it was principally this which held up operation of the equipment.

Mk.I consisted of one R.F. cascode stage, first detector and 3 I.F. stages stagger-tuned around 30 Mc/s (See I.F. amp. later). It was found, however, that inherent capacitances prevented the tuned circuit from resonating above about 220 Mc/s.

Mk.II employed a tuned line anode load for the 300 Mc/s stage, with a crystal mixer. The oscillator frequency was controlled by a crystal ground to a frequency of 9.165 Mc/s which was doubled, trebled twice, and doubled again to give 330 Mc/s. The I.F. stages were essentially the same as in Mk.I. The R.F. section appeared to work satisfactorily, and was consequently used as the basis for later models. The oscillator signal was, however, very weak and for this reason the oscillator had to be abandoned.

Mk.III In this version, R.F., mixer, and oscillator tuning were all effected by means of plungers in cylindrical coaxial lines. Insecure contacts with the plungers led to instability.

Mk.IV may be considered to be the prototype of the final successful amplifier, and consisted of an R.F. stage and mixer stage taken from the discarded Mk.II version, built onto a wooden frame which also contained the remains of the Mk.III whose local oscillator and I.F. stages were used. This was an inherently unsatisfactory arrangement, and was unreliable.

Mk.V shown in Plate III incorporated all the features of the Mk.IV built onto one solid brass chassis; except that the plunger oscillator was replaced by a 165 Mc/s oscillator and doubler circuit with tuned line plate load. This amplifier proved to be satisfactory,

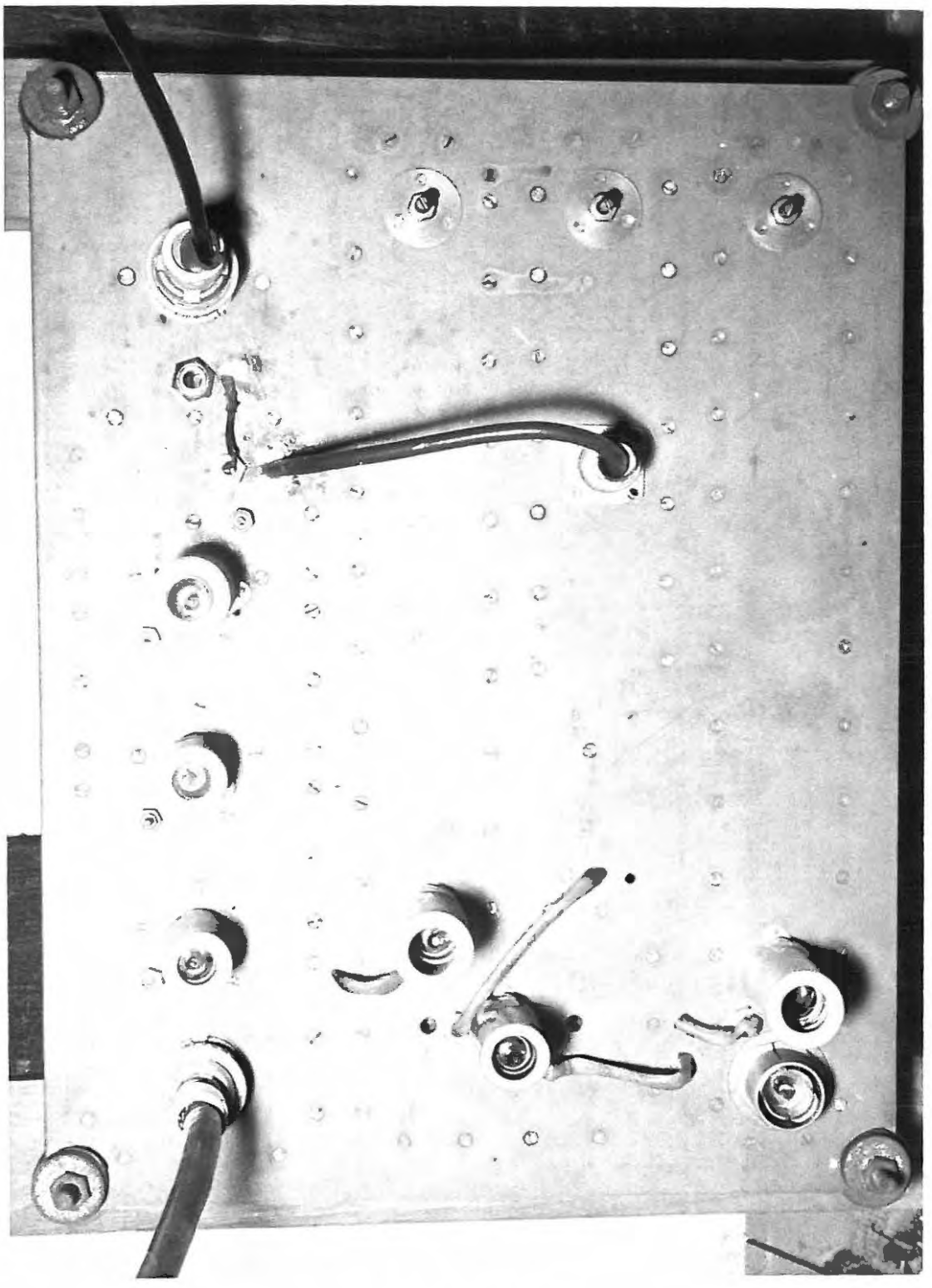

PLATE III

and was installed permanently on the windmill tower.

Fig.Q. gives the circuit diagram of the amplifier, the output of the final I.F. stage being transformer matched into 90 ohm coaxial cable which carried the signal to the I.F. amplifier proper (next section). The final amplifier had a gain of 40 db. and a bandwidth of 1 Mc/s.

(d) 30 mc/s I.F. Amplifier. The design of the original flat-staggered triple was based on the curves given by Volley & Wallman (73). A staggered triple consists of 3 stages, one tuning at the required frequency, and the other two at predetermined frequencies on either side of this central frequency. When correctly balanced these should give a broad, flat-topped resultant response curve. This high bandwidth is necessary to allow for fluctuations in the local oscillator frequency, which might cause the input to the I.F. to shift appreciably from 30 Mc/s. The triple for the preamplifier was designed along similar lines, so that both had to be taken into account in determining the resultant bandwidth and gain.

Theory gives us the following relationship for m flat staggered triples:

$$G_t B_t = \frac{1}{1.06\sqrt{m}} \times \frac{g_m}{2\pi C} \qquad \text{(P20)}$$

where G_t = total gain.
B_t = resultant bandwidth.
g_m = transconductance of the tubes used.
C = total interstage capacity.

LEGEND

R1	56K	V1	6J6
R2 R5 R9 R13 R17	470	V2 V3	6AJ4
R3 R4	100	V4	ECC81
R6 R7 R11 R15	180	V5 V6	EF92
R10 R12 R14 R16	2.2K	C4	500 pf ceramic
		C6	470 pf stand-off
R8a	220K	C7 C8	3000 pf ceramic
b	270K	C14 C15 C16	copper disc trimmers
L1 L2	4 turns on a ¼" former (slug tuned)	C1 C2 C3 C5 C9 C10 C11 C12 C13	470 pf feed-through
L3	3 turns wound around L2		

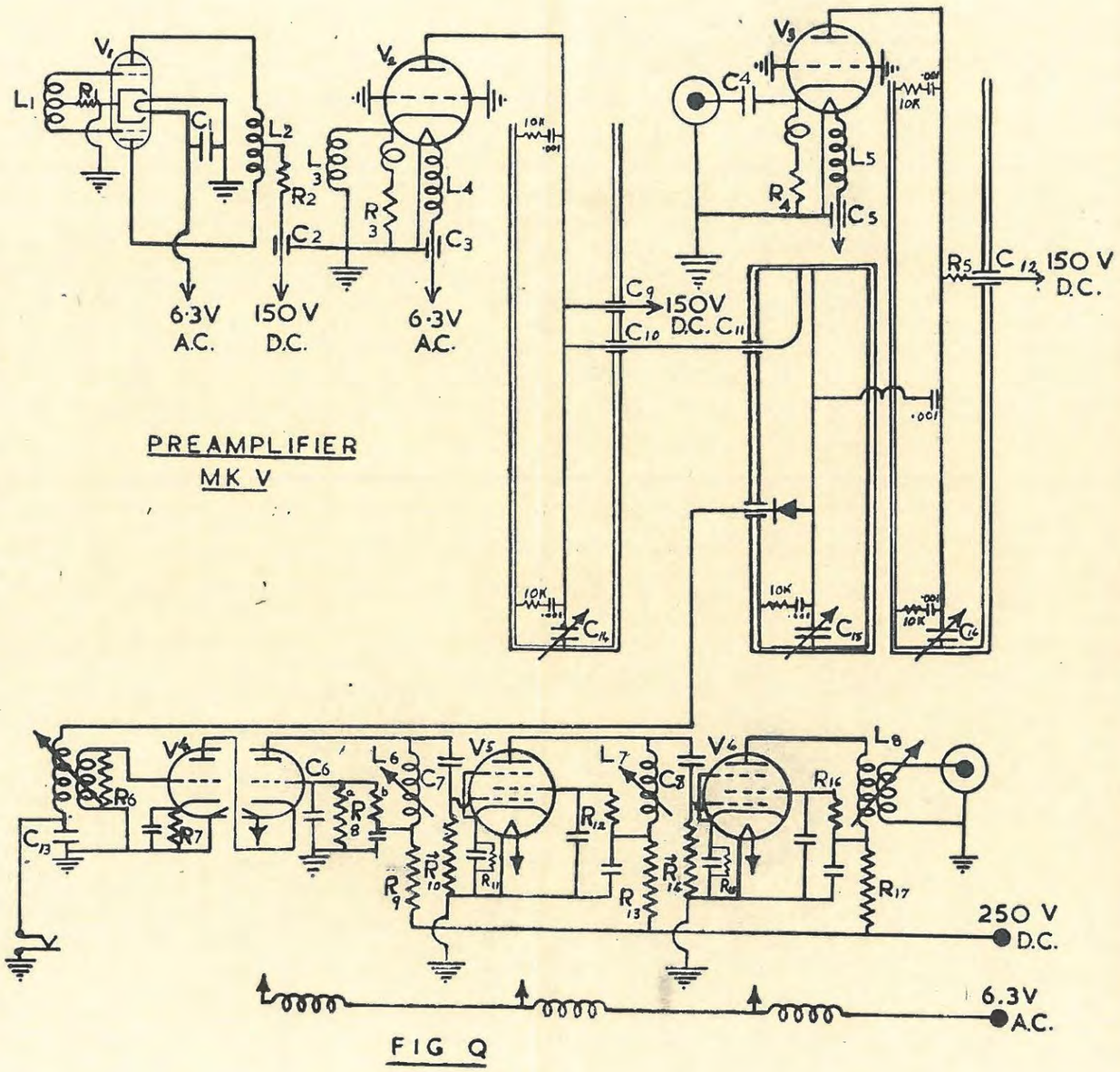

PREAMPLIFIER
MK V

FIG Q

The value of B_t for m triples is given by

$$B_t = \frac{1}{1.06\sqrt[6]{m}} \times B. \qquad (P21)$$

where B = bandwidth of one triple.

For each individual triple the required value of B is used with the curves given by Volley & Wallman to determine the other characteristics of the triple. These curves are plots of two variables α and d against a function δ given by

$$\delta = \frac{B}{f_o} \qquad (P22)$$

where f_o = central frequency of the band.

"Stagger factor" - α determines the amount by which the staggered stages must be detuned from the band centre in order to obtain the required bandwidth.

"Dissipation factor" - d determines the individual bandwidth of each stage.

For a predetermined value of δ (from P22), the values of α and d may be found from the curves; the tuned frequencies of the 3 stages are then given by f_o/α , f_o, $f_o \alpha$. The respective bandwidths corresponding to these are $f_o d/\alpha$, B, $f_o \alpha d$.

The bandwidth of each stage is determined theoretically by the value of the damping resistance in the plate circuit given by

$$R = \frac{1}{2\pi C B_s} \qquad (P23)$$

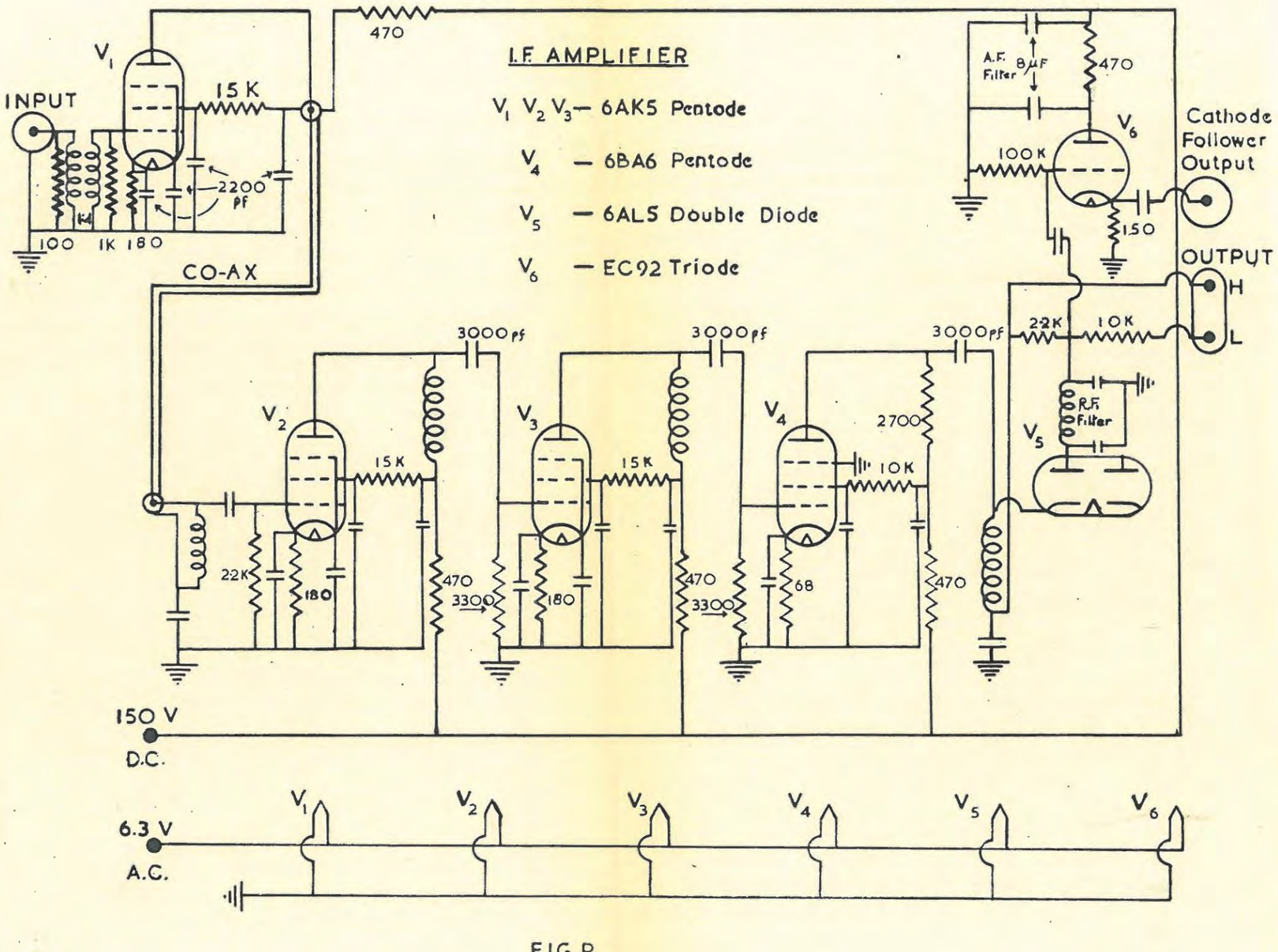
I.F. AMPLIFIER
V1 V2 V3 — 6AK5 Pentode
V4 — 6BA6 Pentode
V5 — 6AL5 Double Diode
V6 — EC92 Triode
INPUT
CO-AX
470
15K
2200 pf
100
1K
180
3000pf
22K
180
470
3300
68
2700
10K
A.F. Filter 8μF
100K
150
Cathode Follower Output
OUTPUT
H
L
22K
10K
R.F. Filter
150 V
D.C.
6.3 V
A.C.

FIG R

where B_s = required bandwidths of stage concerned.

It was originally intended to operate the I.F. stages with an overall bandwidth of 5 Mc/s. From P21 this gives a value of B = 6 Mc/s for each triple, corresponding to a value of δ = .2. From the Volley and Wallman graphs the stages had to be tuned to 27.8, 30, 32.4 Mc/s with bandwidths 2.78, 6, 3.24 Mc/s respectively.

The stages were tuned using $\frac{1}{4}$" coil formers with fine slug adjustment. All coils were wound to tune at the bandcentre with $\frac{1}{2}$ slug penetration; the staggered frequencies were then obtained by adjustments of slug positions. Empirically it was found that 16 turns on the $\frac{1}{4}$" core gave resonance at 30 Mc/s. The values of R are given by theory as 3817 ohms, 1768 ohms, and 3273 ohms; The final values actually used, however, were 3300 ohms for the staggered stages and 2700 ohms for the central stage.

Several modifications to this amplifier as described had to be made before its final instalment. In practice it was found that the value of C (See P20) was inherently large due to the construction of the amplifier, so that in order to achieve the desired bandwidth, the gain had to be seriously dropped. The amplifier was completely rebuilt in order to correct this, and to improve stability, by connecting the tube filaments in parallel instead of series. The wiring capacitances were, however, found to be still too large, so the staggered stages were brought closer to the central frequency and the amplifier was put into operation with B = 2 Mc/s, and a gain of 50 db.

When it was found that the gain of the whole receiver was too

D.C. AMPLIFIER

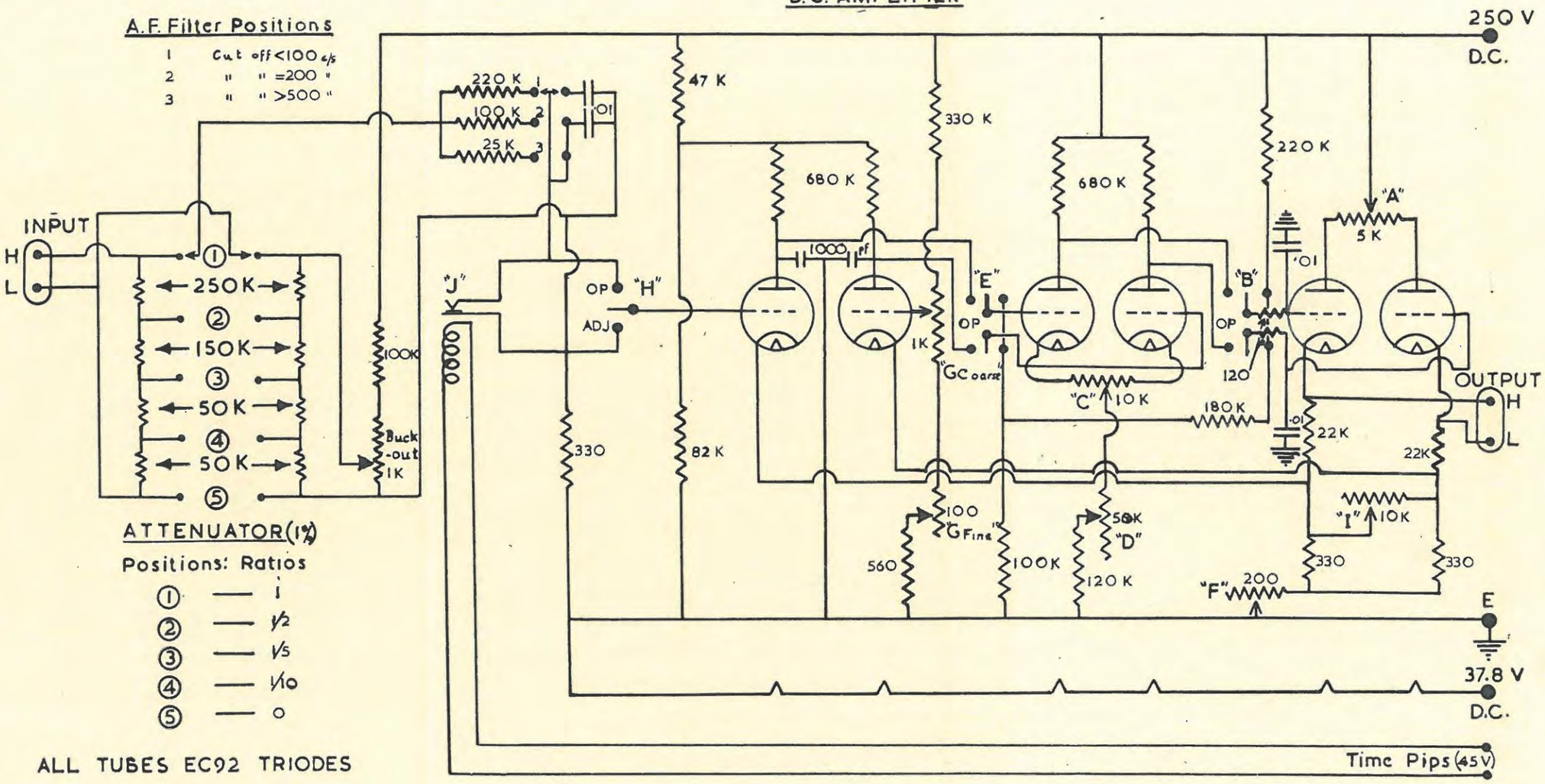

FIG 5

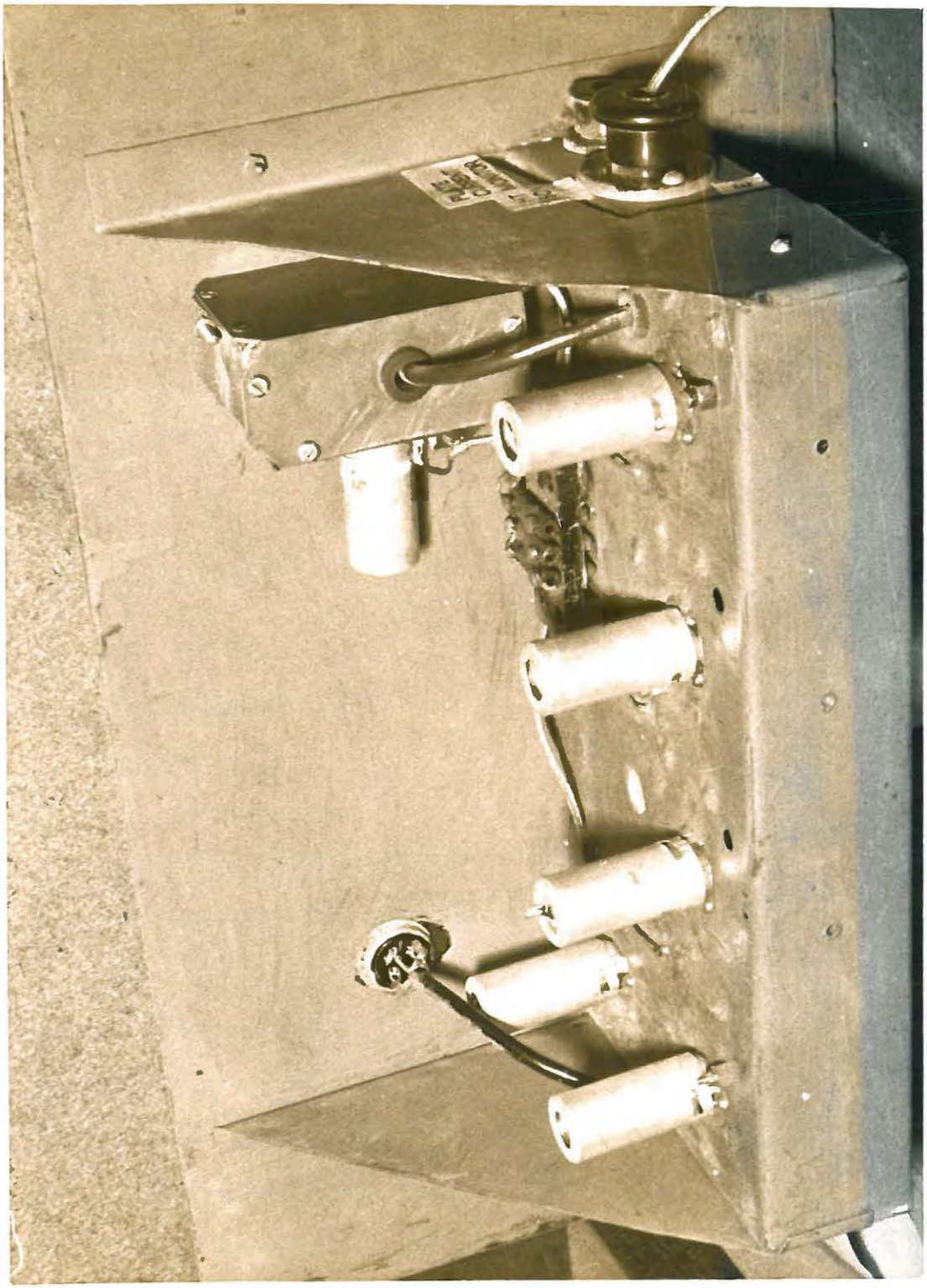

PLATE IV

low, (presumably due to dissipation in the long leads), it was decided to add a further broad-band, single 30 Mc/s stage to the I.F. line. This was done, and found to boost the gain sufficiently. The I.F. amplifier in this final form is shown in Fig.R (circuit), and Plate IV. Also included as a part of this unit was the second detector using half a twin diode (the other half was intended to be used in an A.V.C. circuit, but this did not materialize) with the output arranged to be negative, so that the small constant D.C. voltage that always appears across the detector with no input signal could be neutralized or "bucked out" by a positive voltage in the input stage of the following D.C. amplifier. Arrangement was made to monitor the output signals of the I.F. amplifier using a cathode follower stage as shown in Fig.R. Provision was also made to check the operation of the stages periodically by reading the voltage across small known resistances in the plate circuits. The I.F. amplifier as shown here had a gain of 60 db, and a bandwidth of 1.5 Mc/s.

(e) D.C. Amplifier (Plate V). The design of this amplifier, shown in Fig.S., is a slight modification of that used by the Cornell Solar Noise Observatory in the U.S.A., and is basically the same as that used for the 125 Mc/s radio telescope built at Rhodes in 1957 (Shuter (38)). Here, before the first difference stage is an attenuator giving ratios of 1, $\frac{1}{2}$, 1/5, and 1/10 of the input signal, and a low pass filter to cut out the unwanted high frequency

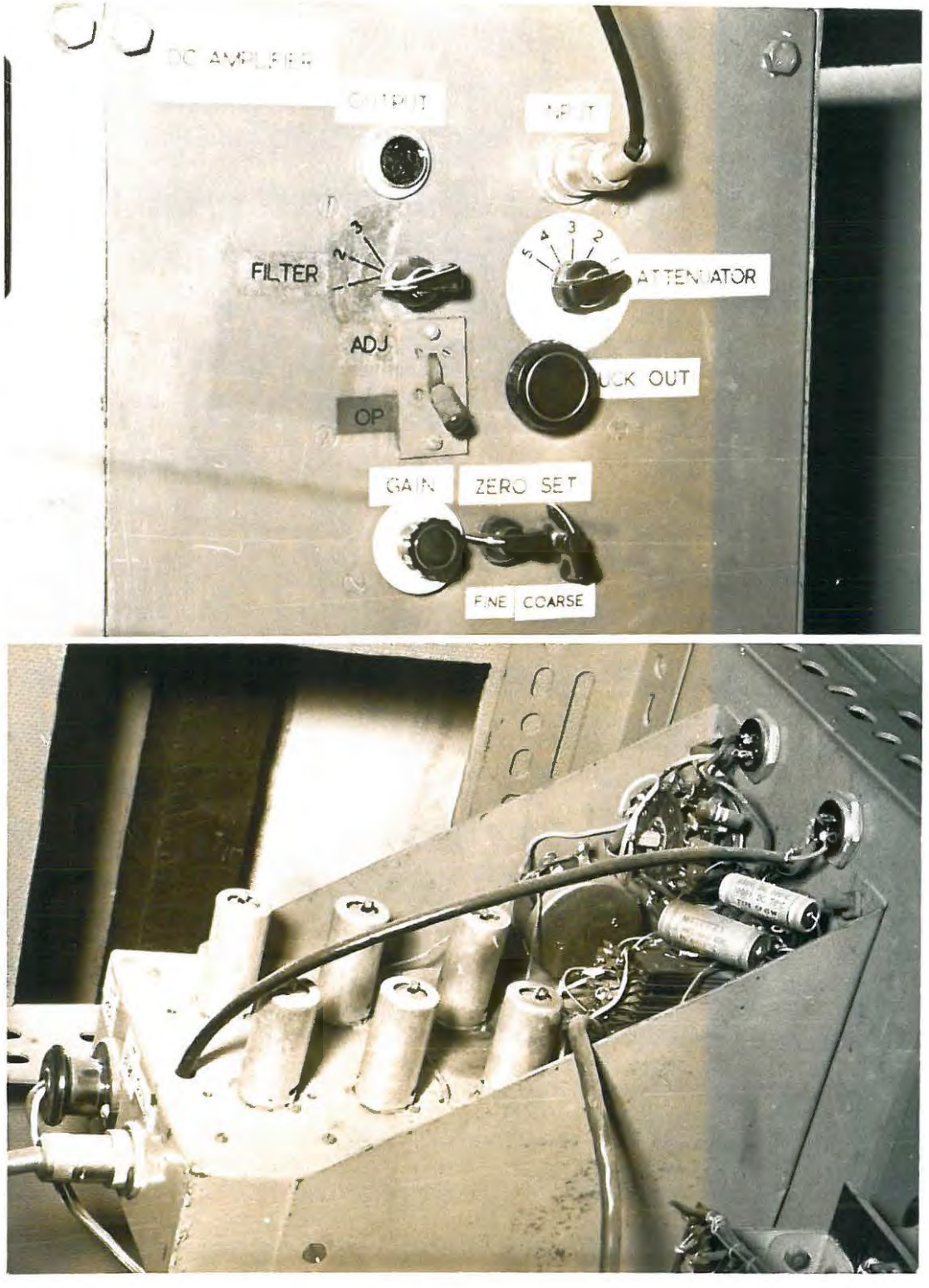

PLATE V

fluctuations which would cause the C.R.T. spot to be recorded as a blur.

With no input signal, the cathodes of the final pair should be at the same potential (or "output level"). To achieve this initial "balance", the various potentiometers controlling the balancing and the output levels of the successive pairs are adjusted as follows:

(i) Switches 'B', 'E' and 'H' are turned to "Adjust".

(ii) Potentiometer 'A' is set for balance at output.

(iii) Switch 'B' set to "Operate".

(iv) Potentiometer 'C' is set for balance at output.

(v) Output level is set approximately with potentiometer 'D'.

(vi) Switch 'E' set to "Operate".

(vii) Potentiometer 'F' used to set output level exactly.

(viii) Potentiometers 'G' are adjusted (Coarse and fine) for balance at output.

(ix) Attenuator and filter switched to desired settings.

(x) Switch 'H' set to "Operate".

(xi) "Buckout" control adjusted for final balance.

The "buckout" merely taps off a small proportion of the positive H.T. voltage, which is effectively applied across the input of the amplifier, off-setting the steady negative "noise-voltage" appearing across the I.F. detector load. The whole receiver is now balanced, bringing the C.R.T. spot into the middle of the screen. An incoming signal causes the spot to move upwards, so that in order to

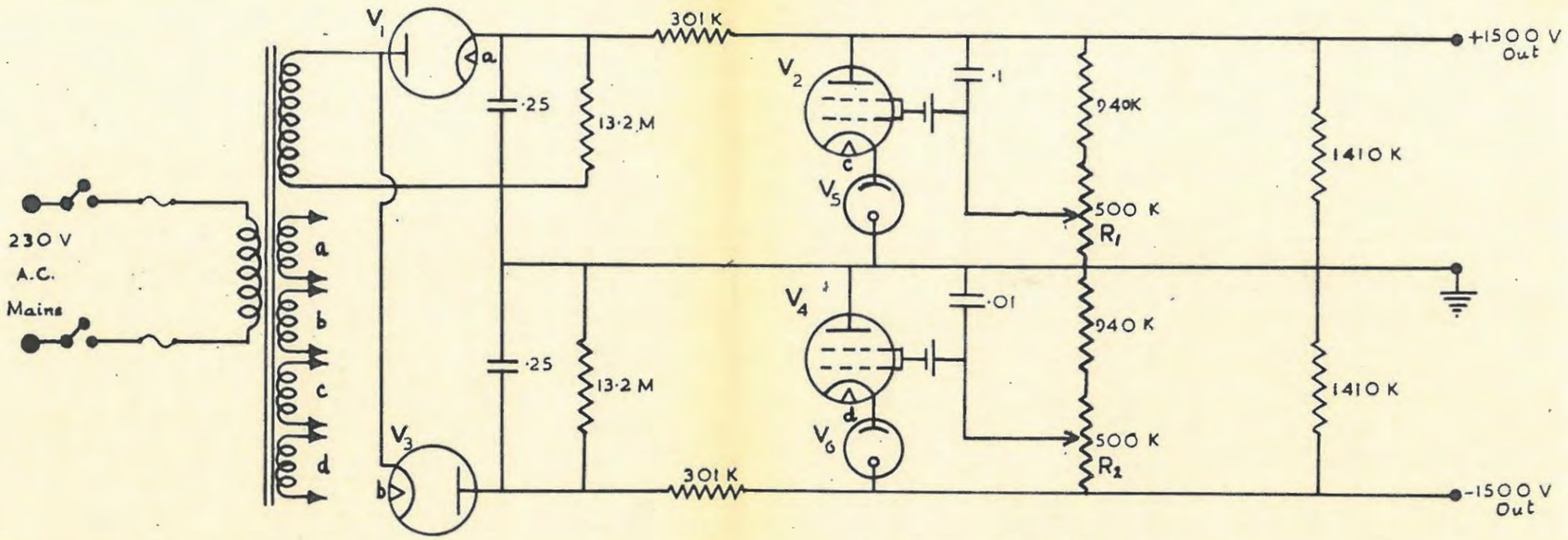

V_1 & V_3	2X2
V_2 & V_4	807
V_5 & V_6	90C1
V_7	5ADP11CRT.

Legend

C. R. T.

&

E. H. T.

SUPPLY

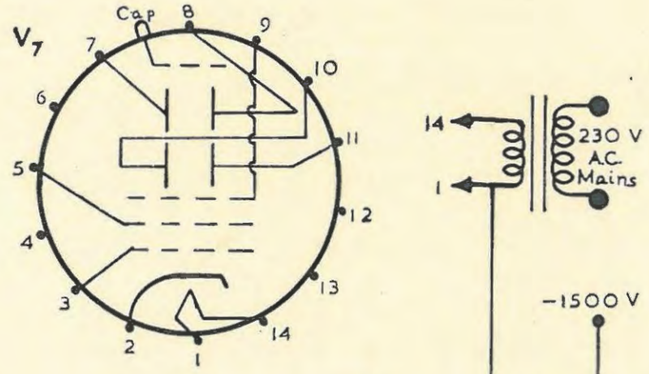

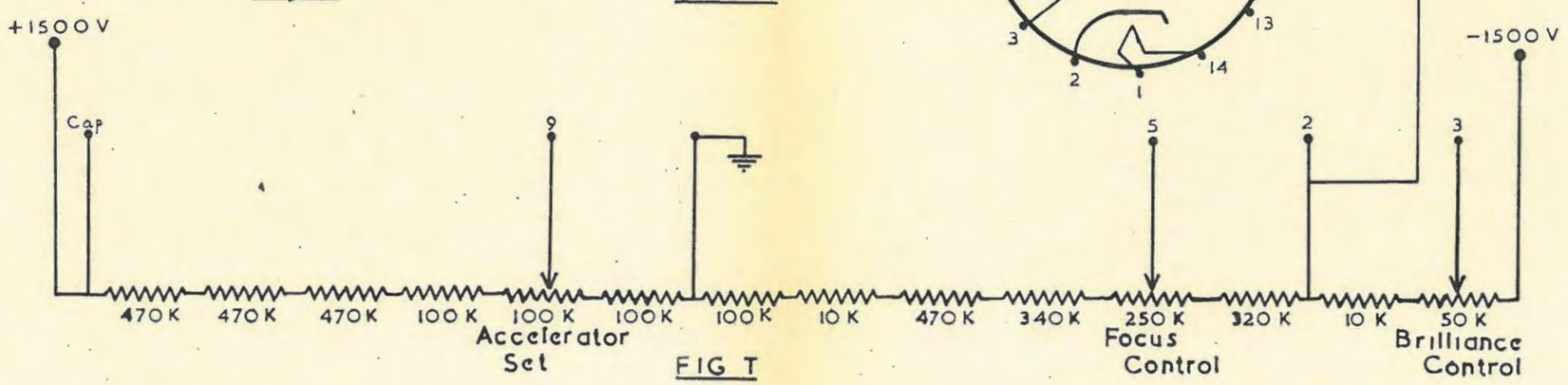

FIG T

utilize the whole screen height, it is obviously better to set the amplifier initially out of balance, giving the zero-signal position of the spot near the bottom of the screen. This done by simply readjusting potentiometers 'G'. For operation, the spot is displaced slightly from this position with the buckout control so that shorting the D.C. amplifier input at 'J' will cause the spot to drop to the base-level momentarily, giving the "time-pips" on the film record (Explained later in Section g). Any readjustment of the attenuator or filter settings, or of the gain control 'I', necessitates repeating the balancing operations after step (vii). This amplifier always worked reliably, and stably for voltage gains up to about 45 db operating with the final cathodes at about 140 volts. At the maximum setting of 60 db it tended to be unpredictable in its behaviour.

(f) C.R.T. Display. The output of the D.C. amplifier was connected across the Y plates of the C.R.T. which is shown with its regulated E.H.T. supply in Fig.T, R_1 and R_2 are adjusted to balance the 140 v. from the D.C. amplifier. The power supply was adapted from existing equipment. The X plates were connected together so that variations in the D.C. output caused the spot to move in the Y direction only.

(g) Photographic Recording Equipment. The C.R.T. screen is photographed on 35 mm positive film moving continuously in the X direction at the rate of about $\frac{3}{4}$" per minute, with the camera set up as shown in Plate VI. The record obtained thus is a straight line, upon which bursts of solar radiation appear as intensity-time profiles.

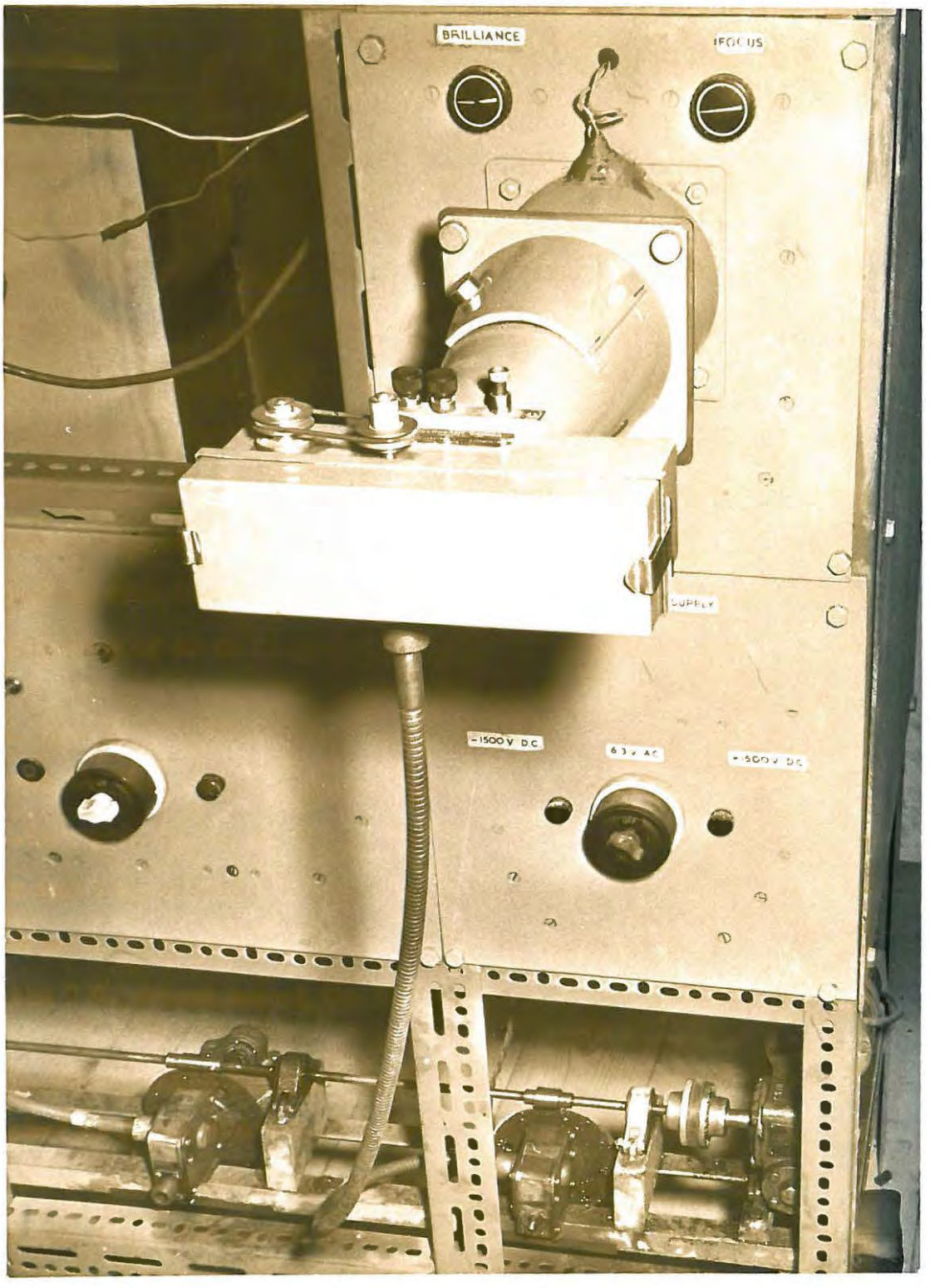

PLATE VI

Noise Storm (Type I).

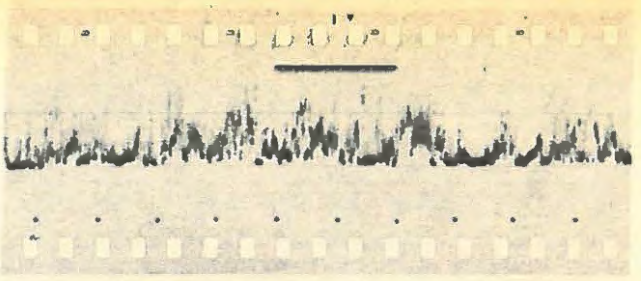

Outburst (Type II).

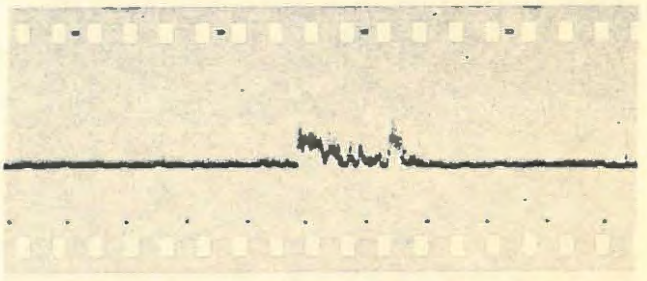

Isolated Burst (Type III).

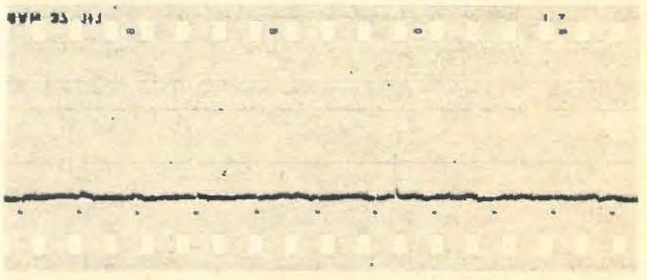

A series of type III bursts.

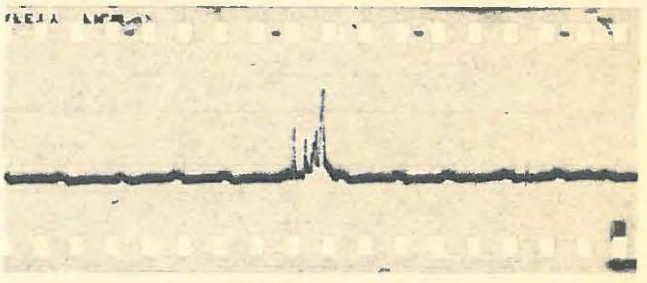

A huge outburst followed by a double-humped burst.

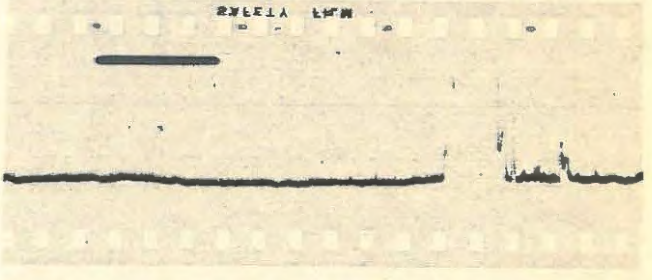

PLATE VII

Plate VII shows several burst-types as recorded by this apparatus.

In order to fix the time of any event, "time-pips" or markers were used. Pulses from the synchronome clock housed in the Physics Department were made to activate a slave clock in the shack, and the relay 'J' on the D.C. amplifier. These pulses arrived every half minute causing the spot to drop momentarily to the base level (balance level), giving a series of pips representing half minute intervals. The master clock was checked daily against time signals from station W.W.V. so that the markers were always accurate to within a fraction of a second. In addition to the half-minute pips, quarter hour markers were obtained by focusing onto the film a small 6 v. lamp which, connected through contacts in the slave clock, glowed for half a minute before and after the quarter hour mark, giving a minute long 'bar' on the record, the middle of which corresponded to the quarter hour. These markers and pips can easily be seen on the samples of record selected for Plate VII.

(h) Noise Diode Calibrations. The power generated in a noise diode can be used to measure the amplifier gain, and thus determine the flux-density of the solar radiation incident upon the antenna. This presupposes perfect matching into the receiver, but even if this condition is not fulfilled, the unit may be used to check the linearity of the response, and the constancy of the gain. The projects originally envisaged did not involve flux-density measurements as such, and no attempt at absolute calibration was made. The

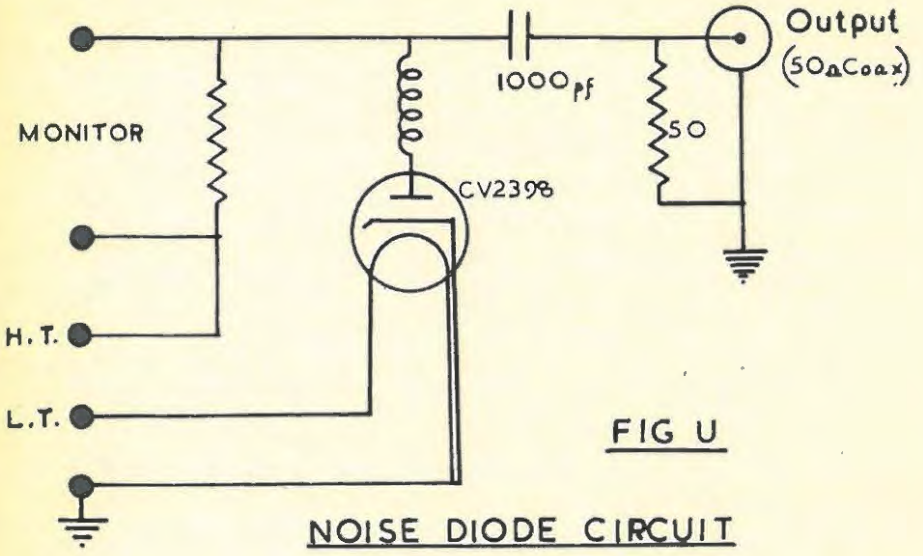

FIG U

NOISE DIODE CIRCUIT

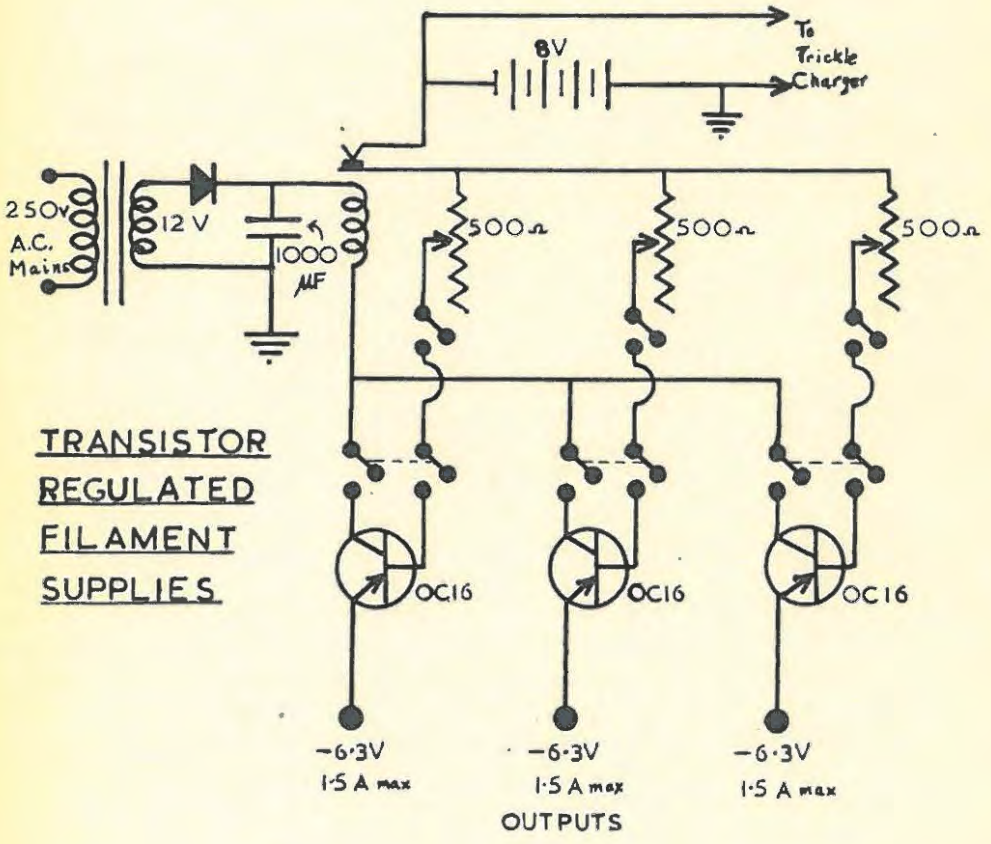

TRANSISTOR REGULATED FILAMENT SUPPLIES

FIG V

noise diode circuit built (Fig.U.) employed a CV2398 V.H.F. tube, useful for relative measurements up to 500 Mc/s, working into a 50 ohm load matching to coaxial cable, and placed in the mast housing with the preamplifier. To perform a calibration the antenna was disconnected, and the diode output plugged into the preamplifier. The filament current was adjusted from the shack, the voltage appearing across a small monitoring resistance in series with H.T. giving a measure of the plate current. Several values of diode current were used, the deflections on the screen being either measured on a meter across the D.C. output, or on the film as a series of 'bars' displaced different amounts from the zero level. If the receiver amplification is linear, the diode current should be directly proportional to the spot deflection, the constant of proportionality giving a measure of the gain. This receiver had a sufficiently linear response over the range that it was tested, but gain levels were found to vary appreciably from day to day. This did not affect the investigation into burst profiles for which these records were largely used (P.A.T. Wild).

(i) Power Supplies and Regulators. Most of the power supplies used were part of the existing 125 Mc/s receiver in the shack. All R.F. and I.F. filaments in the 300 Mc/s receiver were, however, run in parallel off transistor regulated supplies constructed for the purpose. It was found that series fed filaments, for which provision was already made tended to lead to instability due to the

formation of feedback loops.

The regulator used (Fig.V.), based on a design by Keller (74), consisted of 3 OC 16 transistors, each capable of giving 1.5 amps, supplied from a selenium rectifier connected via a transformer to the mains supply. The output was applied to the bases, and was arranged to cut out immediately if the mains supply failed, as the resultant high voltage between base and collector would damage the transistors. This device was found to give satisfactory regulation for mains variations of up to 15%.

All the other supplies and regulators for H.T. and the L.T. supply for the D.C. amplifier were already built, although some adjustments and modifications were necessary.

* * * * * * * * *

It was decided, in addition to operating the 300 Mc/s equipment described above, to convert the existing 125 Mc/s receiver to 150 Mc/s so as to obtain simultaneous records on harmonic frequencies, as this would undoubtedly have been very useful in investigating further the existing hypotheses of the origin and propagation of solar radio noise. Satisfactory operation of this equipment was, however, never achieved, although the preamplifier stage was completely rebuilt, so that this aspect of the project was eventually abandoned. The 300 Mc/s equipment was put into operation in July 1959, and more or less continuous records taken until early in December. The author carried out his investigations on these 300 Mc/s records, and upon an unrelated series of 125 Mc/s records obtained in 1958, which

had the advantage of absolute flux density calibrations, and which were kindly made available by Dr. E.F. Stack-Forsyth.

In conclusion the author wishes to state how the construction of the equipment described in this chapter was distributed between Dr. E.F. Stack-Forsyth, P.A.T. Wild, and the author.

E.F. Stack-Forsyth. Design and construction of preamplifier Mk.III, design and part construction of Mk.V. General supervision of all constructional work.

P.A.T. Wild. Design and construction of preamplifiers Mk.I and II, and H.T. and L.T. regulators (later discarded). Construction of the E.H.T. and C.R.O. circuits. Design and construction of transistor regulators and noise diode circuits. Construction of the additional I.F. stage. Part construction and wiring of mast, part testing of antenna, part calculation of time-tapes.

L.M.G. Poole. Design and construction of I.F. and D.C. amplifiers. Construction of the Mk.IV preamplifier, part construction of Mk.V. Design of antenna drive, and extension of camera drive to accommodate extra camera. Design and construction of the balun transformer. Part calculation, and manufacture of time-tapes. Addition of an extra transistor to the filament regulator. Part construction of mast, and shack wiring. Part construction and testing of antenna. Rebuilding of the 125 Mc/s amplifier.

CHAPTER FOUR.

CORONAL PROPAGATION AT 125 MC/S.

The reasons for the author's use of the 125 Mc/s records for quantitative analysis as opposed to his own 300 Mc/s records are two-fold:-

(a) The lack of absolute intensity calibrations on the author's receiver. (See Chapter 3(h)).

(b) The treatment given below applies only in the coronal regions, and even then can only be regarded as approximate, as magnetic field and coronal assymetry are neglected. The base of the corona, given by $\rho = 1$ in the Baumbach-Allen formula corresponds to a plasma frequency of only 175 Mc/s, and the extension of the succeeding consideration to the chromospheric 300 Mc/s level will be complex, and subject to even greater inaccuracies.

Briefly, the project involves the location of a burst source in the corona, and correction of the observed intensity for absorption during propagation. Comparison is then made with the flares with which the bursts are thought to be associated. Again the interest in this result is two-fold:-

(a) The possibility that there may be some linear (or other) relationship between radio intensity, and flare importance can be investigated. It would be useful to compare other factors such as area and H α intensity and/or line-width with radio intensities, but unfortunately such data over the period in question are not yet available to the author.

(b) If a definite relationship does exist, any bearing it has on the position of the source on the disc will be an indication of the way in which the intensity of the received frequency varies with the distance of the source from the plasma level of the frequency, as the received signal will arise from a higher level the greater the displacement toward the solar limb according to Smerd's equation P13. Supposing a linear plot was established in (a); then one might expect the slope to vary with source angle in a way which depended on the above variation.

The intensity of a given frequency radiated from a certain plasma level depends on the shape of the instantaneous bandwidth profile of the generated radiation. Jaeger and Westfold (43) suggested an inverse second or fourth power relationship; Shuter (38) measured anything between an inverse 7th and an inverse 20th power fall off on dynamic spectra of isolated bursts.

The position of a source in the corona can be determined by observation of the coordinates of the associated flare, and hence the corresponding ray trajectory found. The absorption integral over this path may then be found, and the effect of absorption on the received intensity quantitatively estimated.

Most of the following treatment is based on calculations on ray trajectories by Jaeger and Westfold (1950) (47) outlined previously. Four graphs labelled I, II, III and IV (obtained as described later), will be referred to:

Graph I : Polar plot of ρ (as defined in P2) vs θ (from P13) for

various values of "a" (from P9).

Graph II : Plot of τ (from P11) vs ρ for various values of "a".

Graph III : A diagram giving directly the value of θ corresponding to any set of heliographic coordinates on the sun's surface.

Graph IV : Plot of θ vs e^{τ} .

From visual records the coordinates of the associated flare on the solar disc are determined, and using Graph III, the corresponding source angle can be found. It will be assumed that the disturbance producing the burst is moving radially outwards, and that at the time of commencement of the burst the semi-angle of the cone of escape will be equal to the source angle.

From Smerd's approximate (unpublished) formula we have that the critical escape frequency f_c, and plasma frequency at the level of origin f_o and the source angle θ are related by the expression

$$f_c = f_o \sec (0.87\,\theta) \qquad \text{(See P13)}$$

At the onset of a burst f_c will be the frequency at which we are receiving the radiation, thus from P13 the value of f_o may be determined. This is used to find the height of the radio source in the corona in terms of ρ via the Tonks-Langmuir expression for natural plasma frequency (P5, giving N), and the Baumbach-Allen formula (P2) giving ρ.

We now have, for any particular burst the value of θ (from Graph III), and ρ . This enables us to plot the position of the source in the corona on Graph I, and hence to ascertain the trajectory followed by the radiation. The characteristic value of "a",

corresponding to this ray path is then used with the value of ρ (determined above) on Graph II to find the value of τ, the optical depth for any particular burst. The apparent intensity of the radiation (as received outside the corona) is then related to the generated intensity by the expression

$$I = I_o e^{-\tau} \qquad (P24)$$

where I = received intensity.

I_o = intensity without absorption.

τ = optical depth.

It was found, however, that on plotting ρ vs θ on Graph I, the points of origin of the bursts all lay along the locus of the turning points of the ray trajectories for $\theta < 80^o$, which suggested that Smerd derived P13 using this locus. It was therefore assumed that the locus represented the <u>true</u> points of burst commencement over the whole range $0 < \theta < 90^o$. This meant that for any burst when first observed (i.e. before the source had moved further out into the corona) the radiation would undergo absorption along the full length of the trajectory, so that for a particular value of "a", the value of τ would be the maximum possible on Graph II. For any "a", the magnitude of ρ at the turning point is known (ρ_a), so that a curve of ρ_a vs τ_{max} may be drawn.

We now have θ vs ρ_a; ρ_a vs τ; and it is easy to establish the relation τ vs e^{τ}, thus it is possible from the available data to draw the curve of θ vs e^{τ}. (Graph IV). From P24, the corrected

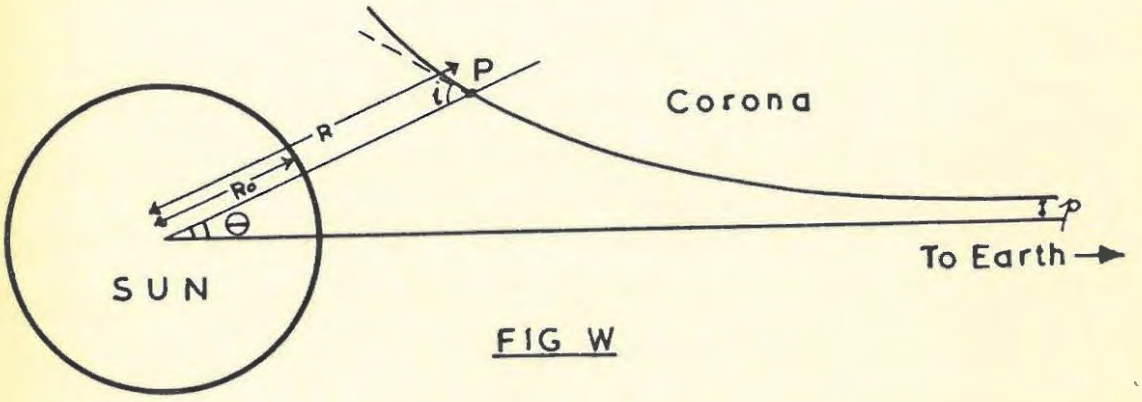

FIG W

Ray Trajectories in the Solar Corona at 125 Mc/s

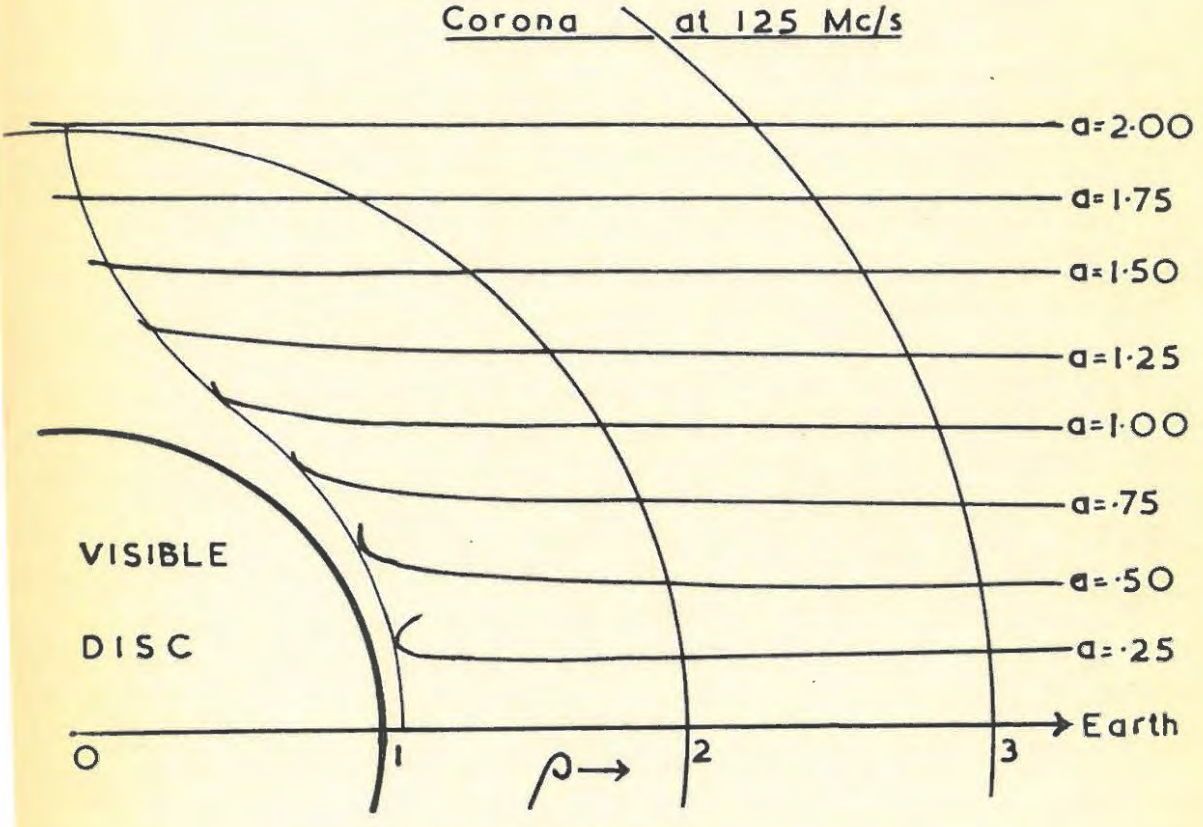

GRAPH I

intensity is given by

$$I_o = Ie^{\tau} \qquad \text{(P25)}$$

So finally for a burst with an assumed associated flare, θ is obtained from Graph III, and the observed intensity is then multiplied by the "correction factor" e^{τ} (from Graph IV), giving the generated intensity of the burst.

Derivation of Graph I, II and III.

Graph I - ρ vs θ for various values of "a".

Let μ be refractive index (without magnetic field) at a point P in Fig.W. From the application of Snell's Law to a spherically stratified corona we have the result

$$\mu \; R \sin i = \text{Constant}$$

When $R \to \infty$, then $R \sin i \to p$; and also outside the corona $\mu \to 1$.

$$\therefore \; p = \text{Constant}$$

$$\therefore \; \mu \; R \sin i = p \qquad \text{(P26)}$$

We know $R = \rho R_o$ and $p = aR_o$

whence P26 becomes $\mu\rho \sin i = a$

$$\therefore \; \operatorname{cosec}^2 i = \frac{\mu^2 \rho^2}{a^2} \qquad \text{(P27)}$$

Also we know $\operatorname{cosec}^2 i = 1 + \cot^2 i = 1 + \left\{\frac{dR}{Rd\theta}\right\}^2 = 1 + \left\{\frac{R_o d\rho}{R_o \rho \, d\theta}\right\}^2$

$$= 1 + \frac{1}{\rho^2}\left\{\frac{d\rho}{d\theta}\right\}^2 \qquad \text{(P28)}$$

Comparing P27 and P28.

$$\frac{\mu^2\rho^2}{a^2} = 1 + \frac{1}{\rho^2}\left\{\frac{d\rho}{d\theta}\right\}^2$$

$$\therefore \quad d\theta = \frac{a}{\rho} \times \frac{d\rho}{\sqrt{\mu^2\rho^2 - a^2}} \qquad \text{(P29)}$$

Integrating from P to ∞ .

$$\theta = a\int_{\rho}^{\infty} \frac{d\rho}{\rho\sqrt{\mu^2\rho^2 - a^2}} \qquad \text{(P30)}$$

For convenience in calculation we introduce a new variable $\chi = \frac{1}{\rho}$

then $d\chi = -\frac{1}{\rho^2}\, d\rho$

Equation P30 then becomes $\theta = a\int_{0}^{\frac{1}{\rho}} \frac{d\chi}{\sqrt{\mu^2 - a^2\chi^2}}$ (P31)

By the Lorenz theory the value of the variable μ is obtained from Equation P6; which for 125 mc/s gives us

$$\mu^2 = 1 - .736\chi^6(1 + 1.68\chi^{10}) \qquad \text{(P32)}$$

So that Equation P31 finally becomes

$$\theta = a\int_{0}^{\frac{1}{\rho}} \frac{d\chi}{\sqrt{1 - .736\chi^6(1 + 1.68\chi^{10}) - a^2\chi^2}} \qquad \text{(P33)}$$

For a given value of "a", the values of θ for various values of χ (i.e. ρ) may be found by numerical integration of the function in P33 from $\rho = \infty \rightarrow \rho_a$ where ρ_a and θ_a are the polar coordinates

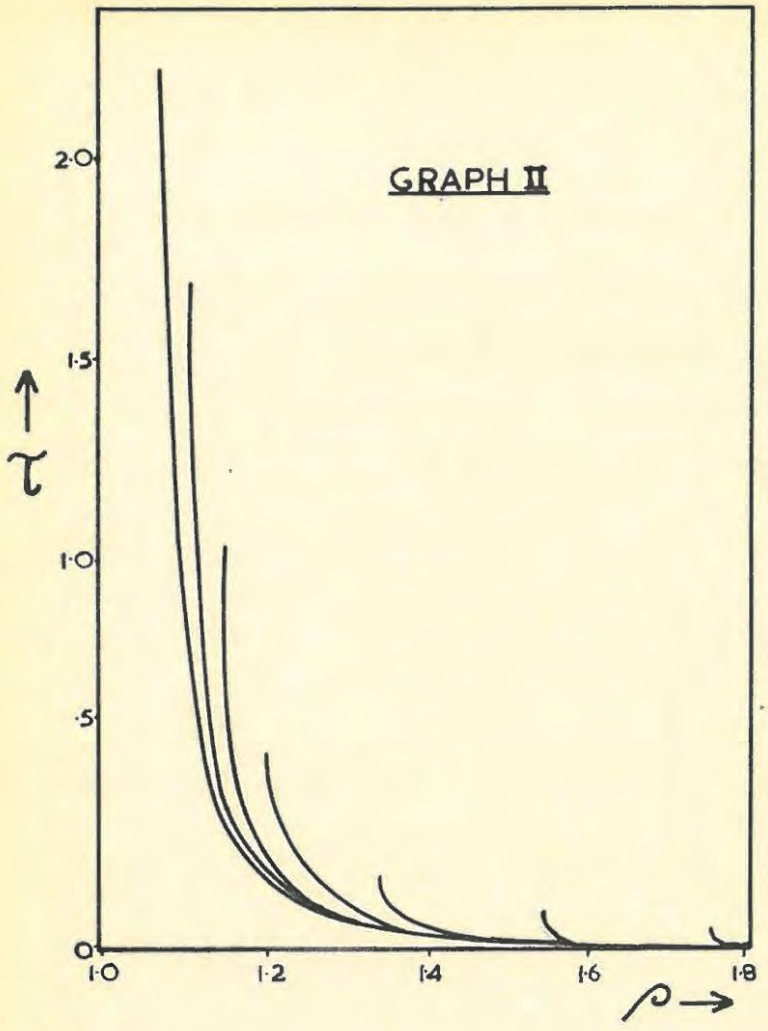
GRAPH II
2·0
1·5
τ
1·0
·5
0
1·0
1·2
1·4
1·6
1·8
ρ

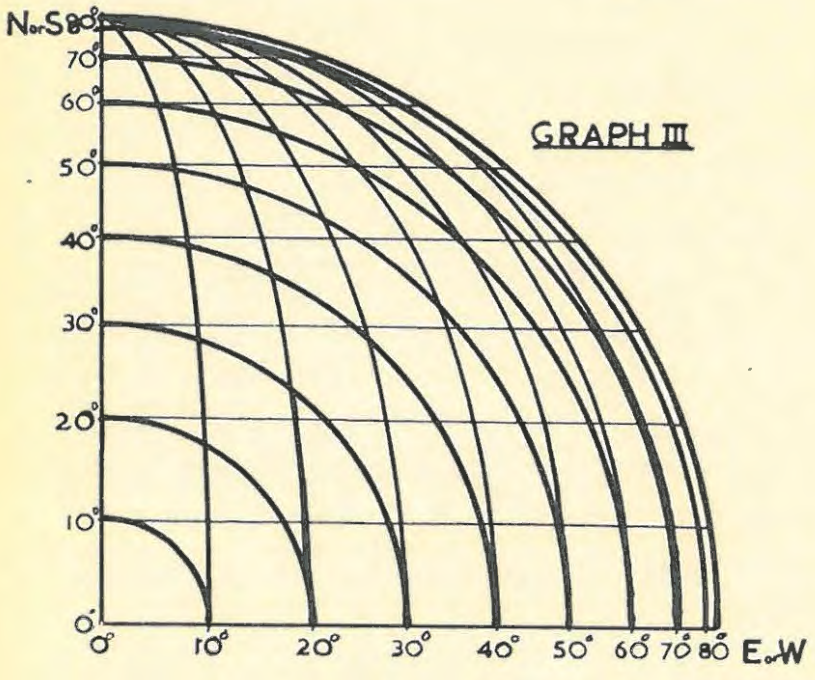
N.or S
80°
70°
60°
50°
40°
30°
20°
10°
0°
GRAPH III
0°
10°
20°
30°
40°
50°
60°
70°
80°
E.or W

of the point of nearest approach of the ray to the sun, i.e. the turning point.

ϑ is plotted against ρ on polar graph paper for various values of "a", to give a set of ray trajectories at 125 mc/s.

Graph II - τ vs ρ for various values of "a".

The absorption along a trajectory from any value of R to ∞ may be expressed in terms of the optical depth τ, defined by Eqns. P11 and P12, which after substituting for ν (collision frequency) from P4 becomes

$$\tau = \int_R^\infty \frac{42NT^{-3/2}}{C} \times \frac{1-\mu^2}{\mu} \, ds \qquad (P34)$$

where ds is an element of path length measured along the trajectory. Again we wish to express this in terms of ρ and hence χ.

We have $ds^2 = (Rd\theta)^2 + dr^2 = R_o^2 \left((\rho \, d\theta)^2 + d\rho^2 \right)$

We substitute for $d\theta$ in this expression from Eqn. P29.

$$ds^2 = R_o^2 \left(\frac{a^2}{\mu^2\rho^2 - a^2} + 1 \right) d\rho^2$$

$$= R_o^2 \, \frac{\mu^2\rho^2 \, d\rho^2}{\mu^2\rho^2 - a^2}$$

$$\therefore ds = R_o \, \frac{\mu\rho \, d\rho}{\sqrt{\mu^2\rho^2 - a^2}} \qquad \therefore \frac{ds}{\mu} = \frac{R_o \rho \, d\rho}{\sqrt{\mu^2\rho^2 - a^2}}$$

Substituting in P34

$$\tau = \int_\rho^\infty \frac{42NT^{-3/2}(1-\mu^2) \, R_o \rho \, d\rho}{C \sqrt{\mu^2\rho^2 - a^2}}$$

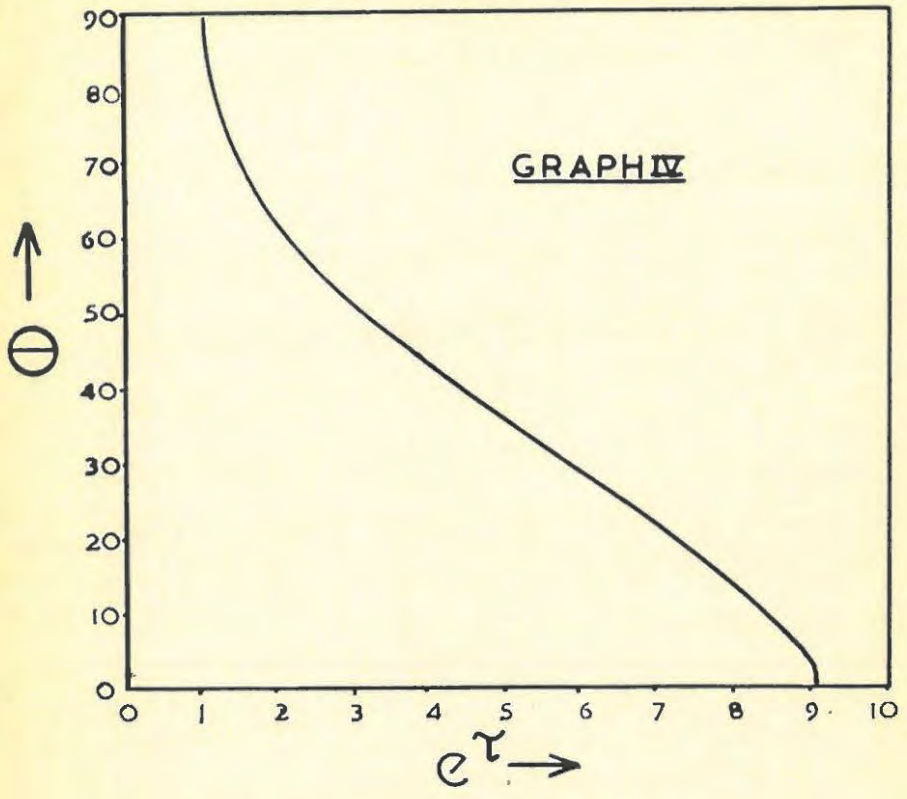
GRAPH IV
θ
90
80
70
60
50
40
30
20
10
0
0 1 2 3 4 5 6 7 8 9 10
e^τ

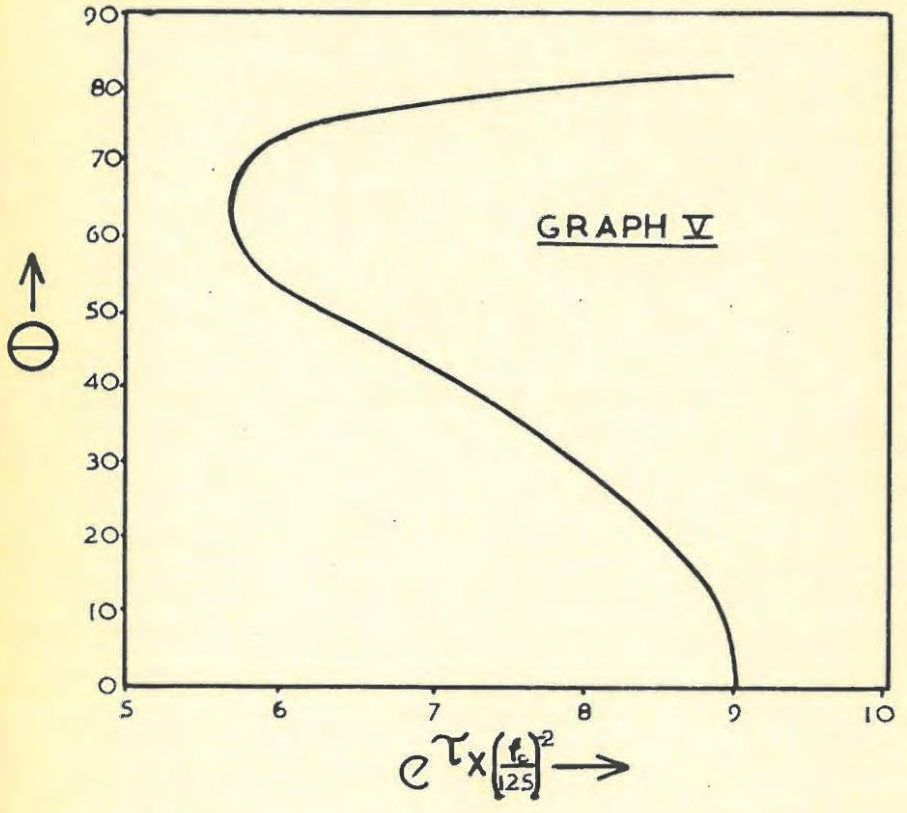
GRAPH V
θ
90
80
70
60
50
40
30
20
10
0
5 6 7 8 9 10
e^τ x (rc/125)^2

$$= \int_0^{\frac{1}{\rho}} \frac{42NT^{-3/2}}{C} \frac{(1-\mu^2)\, R_o d\chi}{\chi^2 \sqrt{\mu^2 - a^2\chi^2}}$$

If we substitute for N from P2; T from P3; μ^2 from P32; $R_o = 7.05 \times 10^{10}$ cm, and $C = 3 \times 10^{10}$ cm/sec, we then get

$$\tau = 4.954 \int_0^{\frac{1}{\rho}} \frac{\chi^{17/2}(1+1.68\chi^{10})^{7/2}\, d\chi}{(1+0.69\chi^{10})^{3/2}\sqrt{1-.736\chi^6(1+1.68\chi^{10})-a^2\chi^2}} \qquad \text{(P35)}$$

By numerical integration values of τ are plotted against ρ for various values of "a".

Graph III. The solar longitude and latitude lines are projected onto a plane at right angles to the sun-earth line, and upon this are superimposed circles corresponding to different source angles, similarly projected. From this diagram the source angle corresponding to any set of coordinates is readily determined.

CHAPTER FIVE.

RESULTS AND CONCLUSIONS.

(A) Quantitative Measurements at 125 Mc/s.

The application of the treatment described in Chapter 4 to the 125 Mc/s records was limited in its effectiveness by the shortcomings of the "importance" scale as a measure of flare magnitude. The small number of steps comprising the scale allowed at best the observation of trends, whose reliability depended on the nebulous nature of the flare categories and on the intensity calibrations, which were at times suspect.

Altogether about 150 daily records were examined, when it was found that 60 complex bursts and 23 isolated burst occurred during the lifetime of at least one or other solar flare. Often a flare had more than one accompanying burst and vice versa. The maximum generated intensity of each burst was found using Graph IV as previously described, assuming to begin with that all radio sources were situated on the same part of the solar disc as the accompanying flare. It was assumed that should any definite relationship between generated intensity and flare importance be found, a non-conforming result could be attributed to a flare coincident in time by chance, but not otherwise associated with a radio burst. For this reason too, if more than one flare accompanied a single burst, each was considered, although obviously only <u>one</u> could give the expected result. The same is of course true of a number of bursts concurrent with the same flare

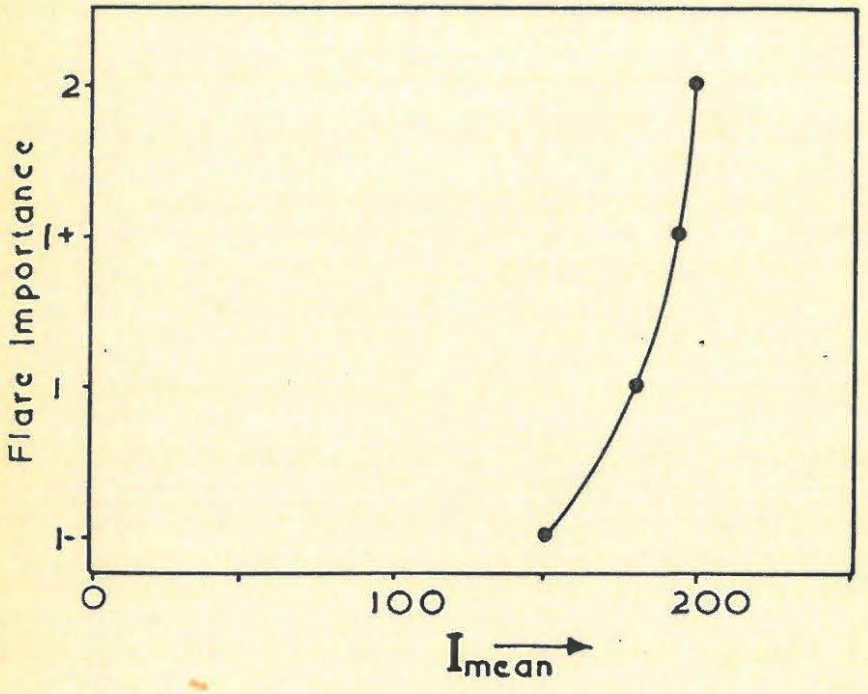
Flare Importance
2
1+
1
1-
0
100
200
Imean

FIG X

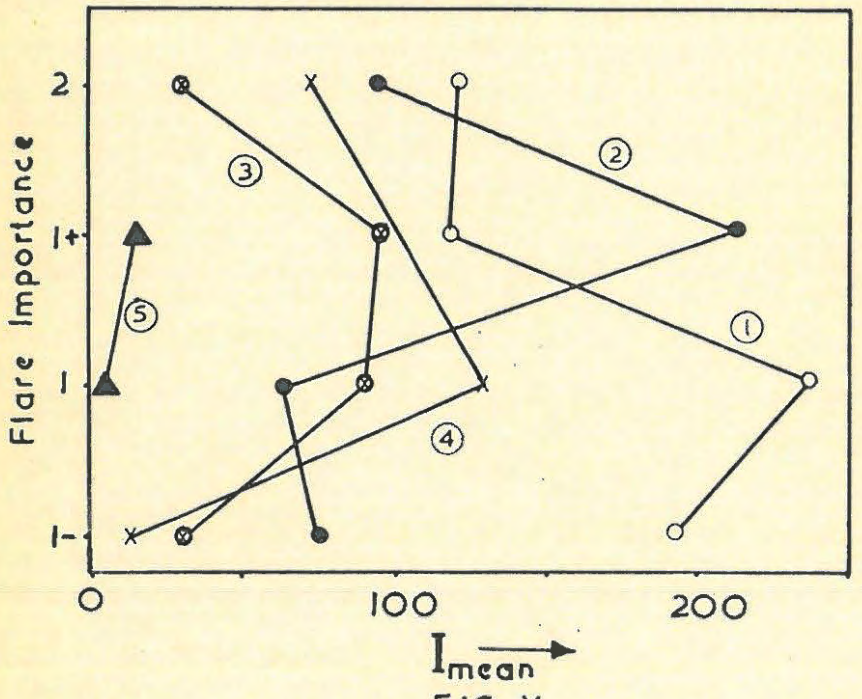
Flare Importance
2
1+
1
1-
0
100
200
Imean
1
2
3
4
5

FIG Y

although there is the possibility in this case that several successive radio events can occur as the result of a single visible disturbance. It is interesting to note at this point that according to Maxwell, Stone and Swarup (75), half the coincidence of type III bursts with flares are pure chance, so that some scatter in results is unavoidable.

As could be anticipated this preliminary investigation gave no indication of a relationship or trend of any sort as events over the entire disc were considered. For the source positions at the onset of the burst for different values of the source angle θ lie along the locus of the turning points on Graph I, so that a burst originating nearer the solar limb will be coming from a level further removed from the plasma level of the received frequency (previously discussed). Tentatively assuming that the intensity-frequency profile dropped off according to an inverse square law (Fig.D., Ref 43), the author applied a further correction to give the generated intensity of complex bursts when the source was at the received frequency plasma level and radiating radially only, (before the burst was observed). The correction was considerable at larger source angles, Graph IV becoming modified as shown in Graph V. The precise manner in which the above correction was effected will become apparent during the discussion of isolated burst profiles later (Section C). The effect of this refinement was at least to introduce some semblance of order in the previously haphazard data, shown by Fig.X. This indicated that more positive results might be expected from the

application of some other inverse power law.

To this end, according to aim (b) at the beginning of Chapter 4, the results corrected for absorption only were divided into 5 groups falling between values of source angle that divided the hemispherical solar surface into equal areas. This gave the first group which all originated from a circle in the centre of the disc, θ falling between 0° and 36°. The successive groups formed concentric rings round this centre described by $37^{\circ} < \theta < 53^{\circ}$; $54^{\circ} < \theta < 66^{\circ}$; $67^{\circ} < \theta < 78^{\circ}$; and $79^{\circ} < \theta < 90^{\circ}$ respectively. The relationship between corrected radio intensity and flare importance was studied for each of these groups separately. These results were not in themselves as consistent as those shown in Fig. X, but they nevertheless showed unmistakably the expected trends for lower flux densities for larger source angles - Fig.Y. The evident lack of relation between flare magnitude and burst intensities apparent in both Figs.X and Y would seem to indicate that the amplitude of plasma oscillation causing the radio event is not affected by the magnitude (i.e. area and /or lifetime according to Ellison (6)) of the associated flare. This is not altogether surprising. Obviously a more useful comparison could be made if reliable records of the flare H α intensities could be obtained.

However, the appreciable difference of the mean burst intensities between say the 1st, 3rd and 5th groups may be used for a semi-quantitative estimate of the mean frequency fall-off. We may conveniently tabulate our information in the following way:-

GROUP	I_b	θ	f_o
1	196	18	115
2	86	45	93
3	67	60	77
4	92	72	60
5	11	84	36

where I_b is the mean burst intensity (arbitrary units) of any group.

θ is the mean source angle of the group.

f_o is the plasma frequency of the corresponding critical escape level in Mc/s (according to Smerd's equation P13).

The means in the second column are not necessarily those expected from Fig.Y, as the bursts are not equally distributed between the importance categories.

For any group we can say that if the intensity falls off according to f^{-n}, the burst intensity I_b at 125 Mc/s is given by

$$I_b = \left\{\frac{f_o}{125}\right\}^n I \qquad \text{(P36)}$$

where I = intensity generated at the 125 Mc/s plasma level, assuming the amplitude of oscillation to be equal at the two levels.

Substituting values of I_b and f_o from groups 1 and 3 and eliminating I we get

$$\frac{196}{67} = \left\{\frac{115}{77}\right\}^n \qquad \text{whence} \quad n = 2.7$$

Similarly for groups 3 and 5 and 1 and 5 we obtain n = 2.4 and 2.5 respectively giving a mean of about 2.5 If we include group 2 in the consideration (discarding group 4 as unusable owing to the very large mean value of I_b compared to the other groups) we still obtain a mean of 2.5 for n, but with a much larger standard deviation. (Values ranging from 1.3 to 3.8). This at least indicates that the power index governing the shape of the frequency profile is probably of a low order for complex bursts (comprising mainly type II events). Any attempt at comparison with Wild's (1950 a) (48) records of out-bursts is thwarted by the complexity of the dynamic spectra. (See Fig.H.).

It is later suggested by the author that the decay constants observed are related to n and the source velocity v by an equation of the form

$$k = (An - B)v \qquad (P37)$$

This may well be consistent with the higher values of n measured by Shuter from Wild's isolated burst records (1950 b) (49). Unfortunately the determination of k for the manifold overlapping peaks of complex bursts is exceedingly difficult, although it appears that these separate elements decay more slowly than do single peak bursts at the same frequency. This is what one would expect from Equation P37, as n appears to be, and v certainly is smaller for type II bursts.

(B) Qualitative Investigations at 125 Mc/s and 300 Mc/s.

In addition to flares, sudden rises in filaments or prominences (known as "disparitions brusques" - D.B.'s) were examined in relation to 125 Mc/s bursts. It was found that of those D.B.'s which occurred during the recording period, about half were associated with at least one, and in some cases several radio bursts, which were almost invariably complex in nature. Apart from this no association between source angles and burst intensity could be established, so it seems likely that what coincidence were found occurred merely by chance. Comparison with 300 Mc/s records taken a year later was just as uninteresting.

While not directly concerned with the foregoing investigation it was decided to examine the local (Cape) records of "Sudden Ionospheric Disturbances" (S.I.D.'s) for possible correlation with 125 Mc/s and 300 Mc/s records and flares. These S.I.D.'s invariably took the form of "Sudden Enhancement of Atmospherics" (S.E.A.'s). In this case the results were slightly more positive at the higher radio frequency, outbursts in particular being liable to coincide with flares and S.E.A.'s. Neither result was of any great significance.

However, flare - burst comparisons at 300 Mc/s did provide a useful addition to the already existing data. Again it was found that outbursts and storms rather than isolated bursts were likely to be associated with flares, which were usually of a high magnitude. This prompted the author to investigate all the flares of importance 2 or more over the period when the 300 Mc/s receiver was known to be

functioning properly. 70% of such flares were accompanied by some form of activity at 300 Mc/s, the radio event often occurring soon after the onset of a flare, which according to Maxwell et al (75) is indicative of genuine association. These results are particularly noteworthy as there was not a profusion of activity on these records.

A similar procedure on the 125 Mc/s records did not yield such gratifying results. Of the large flares that occurred during the operation of this receiver, only 25% were accompanied by radio noise of any sort, although a few very good correlations were found.

This shows, as is to be expected, that the conditions of burst origin in the chromosphere (at 300 Mc/s) are probably quite different to the comparatively familiar coronal conditions (at 125 Mc/s). It seems likely that chromospheric flares could excite radio disturbances in this region, without ejecting ionized matter of the kind which would induce coronal oscillation. This notion is supported by the fact that flare associated radiation at 300 Mc/s was practically all of the complex type I and II sort, rather than the simple bursts consistent with the outward moving agency concept.

The one positive result that was obtained by the concurrent operation of the 300 Mc/s and the ill-fated 150 Mc/s receiver is interesting in the light of the foregoing suggestion. The maxima of two large outbursts near 07.15 U.T. on 17/8/59 on 300 Mc/s coincided exactly in time with two smaller bursts on 150 Mc/s, while a short-lived flare was observed by various stations to start at 07.10 and end at 07.40. Several interpretations are possible. Assuming

the disturbance to have been localized at the 300 Mc/s level, it is conceivable that the generation of sub-harmonics might account for this weak 150 Mc/s signal. However, no mechanism whereby this could occur is known to the author. In any case sub-harmonic radiation would probably not be able to escape, except possibly via a different mode of propagation described by Denisse (1960) (76), analogous to the so-called "whistler mode" in the ionosphere which requires a magnetic field which gives a gyro-frequency much higher than that of the propagated wave. As there is very little physical separation between the 150 and 300 Mc/s levels, the former, and other levels near the base of the corona (which is at about the 175 Mc/s level) could be excited by shock waves without the actual ejection of corpuscular streams, or by storm particles prevented by the solar magnetic field from moving too high into the corona (Denisse (76)). The time delay that one would expect between the two frequencies could well be too small to have been detected by the equipment in this case in view of the complex nature of the profiles. On this model then, one would expect to get a great deal of flare associated radio noise (outbursts) at chromospheric frequencies, and at high coronal frequencies. Only by obtaining a third result at an appreciably lower frequency could this point be decided (See Section D).

The qualitative results in the foregoing pages are useful in that they confirm the conclusions of previous workers about higher correlation at higher radio frequencies. In particular the results at 300 Mc/s confirm Rabben's (1960) (32) report that radio

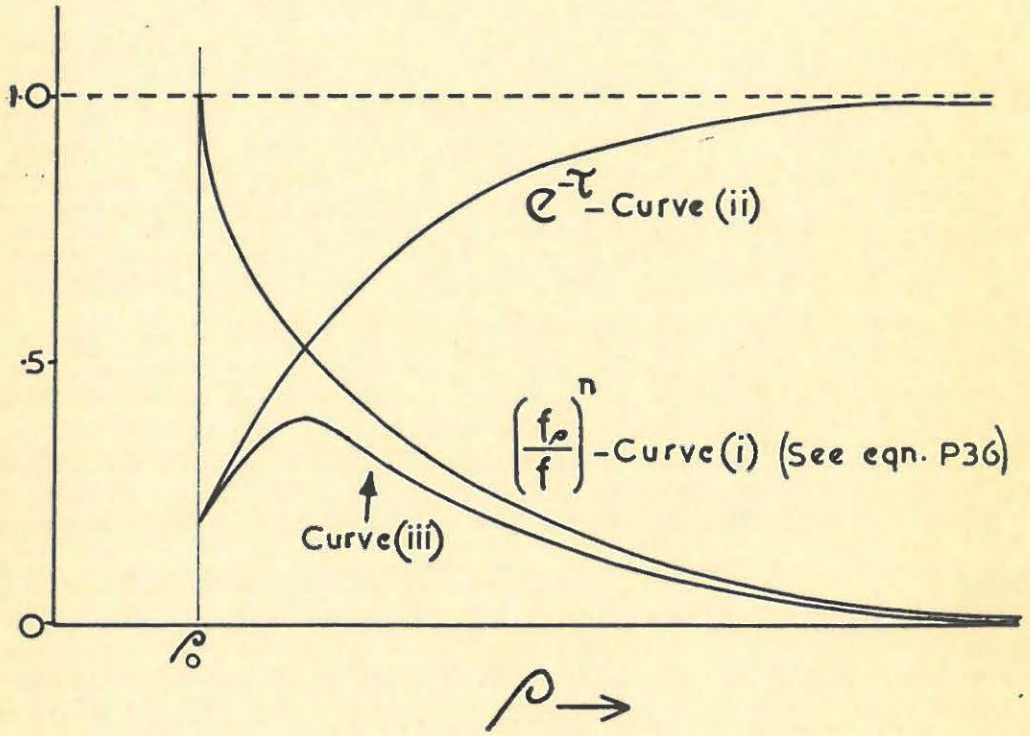

FIG 2

f_ρ plasma frequency at height ρ.

events are especially associated with the larger flares.

The quantitative results based on the absorption calculations in the foregoing chapter give us no reason to change the hitherto accepted view (with the possible exception of that of Edelson, McCullough, Santini and Coates (33)) that flare importance has no bearing on the magnitude of any associated radio events. These calculations have, however, an important theoretical application which was developed incidentally to the main project. This is discussed in the following section.

(C) The Effect of Absorption on Isolated Burst Profiles.

The variation of the generated intensity of the received frequency (f say) with ρ for a given source assuming an inverse n^{th} power fall off as the source moves away from the f-plasma level, may be represented as in Fig.2. by curve (i). The fractional transmission from the successive levels is given by the corresponding values of the $e^{-\tau}$, is represented by curve (ii). The actual received intensity, will thus vary with time (assuming a constant source velocity, that the decay of oscillations at successive levels is very rapid, and neglecting the slight delaying effect of extra equivalent path on the earlier portions of the burst) according to the product of the two curves, - curve (iii). The shape of this resultant curve should thus be a faithful representation of a typical single-frequency intensity-time record. The author has plotted a number of these curves for various values of n from 2 to 10, for various source angles, at frequencies of 60,100 and 125 Mc/s

(using Jaeger and Westfold's (47) absorption curves for the first two.) It was found that in every case a plot of log I vs ρ gave a linear decay portion sometimes varying about the mean in a way similar to that found by Shuter ((38) opp. page 51) and P.A.T. Wild (opp. page 56) in their burst analyses.

Taking an average value of source velocity of 10^5 km/sec (after Wild, Sheridan and Neylan (1959) (29) the author calculated values of k for various cases. The values which appear in the following table are for radial propagation ($\theta = 0^\circ$).

k calculated from Fig.2.

Frequency mc/s	n = 2	n = 4	n = 10.
125	.61	1.2	4.1
100	.60	1.2	-
60	.58	1.1	-
* 20	.3	-	-
* 175	1.9	-	-

The last two marked * are approximations based on the trends shown by the accurately known data. The results for other source angles are substantially the same as those shown here. It can readily be seen that for n = 2 and 4, the values of k are of the order expected from results of various workers. In the case of n = 10 we can obtain a better result if we assume a source velocity of about 2×10^4 km/sec. This is entirely consistent with Shuter's

(38) measurements on isolated bursts - viz.$7.5 < n < 19.5$ (opp. page 61) and source velocities derived from double-humped burst time delays at 125 Mc/s (page 54) in the range $0.6 - 4.1 \times 10^4$ km/sec.

The curves which the author obtained also predict (a) that the rise times are shorter for larger source angles, and for lower frequencies, and (b) that the maximum intensities at frequencies 20, 60, 100, 125, 175 Mc/s are approximately in the ratio of 8.2 : 5.6 : 4.2 : 3.1 : 2.9 respectively, for $n = 2$; while for $n = 4$, the 60, 100 and 125 Mc/s maxima are in the ratio 5.2 : 3.1 : 1.9. (N.B. the values for 20 Mc/s and 175 Mc/s are again very rough).

It can be seen from this model that k depends upon two unknowns; n, and source velocity v, which can, however, both vary to give a constant value of k. The model as it stands is thus of little more than academic interest. The result, however, becomes useful when applied to the case of a single burst observed on two well spaced frequencies. If the decay constant is measured at each frequency, and sets of absorption integral curves are available for both frequencies, then the following set of equations derived by the author (See Appendix II) may be used to find n and v. The treatment presupposes both quantities to be constant over the frequency range considered.

Consider measurements taken at two frequencies f_1 and f_2, then the subscripts 1 and 2 to the quantities in equation P38 below pertain to those respective frequencies.

$$n = \frac{k_2 \Delta\tau_1 - k_1 \Delta\tau_2}{2.3\left(k_2 \Delta \log_{10} f_{o_1} - k_1 \Delta \log_{10} f_{o_2}\right)} \qquad (P38)$$

where $\Delta\tau$ in each case is determined by finding the value of τ at a certain value of ρ $(=\rho_x)$, and at $\rho = \rho_y$ and subtracting the two. The criteria for ρ_x and ρ_y are that they should correspond to points on the curve (iii) in Fig.Z. which both lie in the apparently exponential region (i.e. where the log I vs ρ graph is linear) for all values of n. If we assume that ρ_x is the smaller of the two, then it is found that ρ_x can conveniently be given by $\rho_o + .1$, where ρ_o is the plasma level of frequency concerned; unless, as for larger source angles, the value of ρ at the critical escape level, ρ_c is $> \rho_o + .1$, in which case we take $\rho_x = \rho_c$. ρ_y is in both cases given simply by $\rho_x + .1$. If the corresponding values of τ are τ_x and τ_y, then $\Delta\tau = \tau_x - \tau_y$. In a similar way $\Delta \log_{10} f_o$ is given by the difference of the logs of the plasma frequencies at the two levels ρ_x and ρ_y. It is convenient to have a plot of ρ vs f_o on hand to facilitate the finding of f_o for various ρ, thus avoiding laborious calculations involving P2 and P5 every time.

The value of n thus obtained may then be substituted into P39 below to give v in km/sec.

$$v = \frac{7 \times 10^4 k_m}{2.3n \Delta \log_{10} f_{o_m} - \Delta\tau_m} \text{ km/sec.} \qquad (P39)$$

where m can be either 1 or 2.

In practice it was found that the answer depends very

critically on the small differences in the numerator and denominator of P38, so that the values of k, τ and f_o must be accurately known. The simplifications introduced at the beginning of this section seem still to be of little import as far as the present calculation is concerned. The decay time of the oscillations at any level, according to $e^{-\nu t}$ only becomes comparable to the lifetimes of isolated bursts below 60 Mc/s, so that this method should be used only above this frequency. The delay due to the different times of travel from different coronal levels is completely negligible except possibly for very large source angles ($> 80^{o}$) and high frequencies. It will, if anything, have the effect of slightly increasing the value of k.

As a final corollary to the foregoing treatment - if the values of n and v are already known for a particular burst, then the decay constant at any particular frequency may be predicted from P39.

The substitution of average values of k at 100 Mc/s and 60 Mc/s as determined by various workers gave unsatisfactory results, but this is only to be expected in view of the requirements. Dynamic spectrum records also proved to be unusuable. It is clear that particular care will have to be taken in the measurement of k for <u>individual bursts</u> at the two frequencies, and a method devised for accurately interpolating the values of τ from the absorption curves for intermediate values of "a", before significant results can be obtained. It may be found that the simple equations P38

and P39 need further refinement to allow for the errors previously mentioned, although it seems likely that irregularities of electron distribution and other complicating factors would make such a procedure unwarranted.

(D) Suggestions for Further Research.

The natural implication of the preceding section is that this investigation could profitably be carried further. This would necessitate the construction of two specially sensitive narrow band, single frequency receivers with logarithmic response upon which k could be measured to two significant figures. This project in itself would hardly justify such a construction, but if the receivers were, for instance, tuned to harmonic frequencies further useful general work could be carried out. The two frequencies would have to lie within the coronal range, but if a third receiver could be made to operate at twice the highest of these, at a chromospheric frequency, a further line of investigation of the comparison between chromospheric and coronal oscillations is opened, and in particular the question raised in Section B about sub-harmonics and the effect of chromospheric disturbances on the lower corona might be resolved. This would most easily be realized by running the present 300 Mc/s receiver (where k is not accurately required) concurrently with two log response receivers at 150 Mc/s and 75 Mc/s respectively.

In the field of correlations between radio events and

flares, it is clear that useful application of the author's treatment can only be realized when we have available other flare data such as H α intensities, or if in some way the extent of ionization of the group of particles forming a travelling source can be determined. Again radio readings taken with the three receivers suggested above would prove an invaluable aid in assessing the significance of the results.

****

APPENDIX I.

From the treatment of absorption in the ionosphere given by Ratcliffe (77), one would expect a value of τ which is only half that obtained here. The factor of 2 arises from the different definitions of κ in terms of

(a) wavefield strength (κ_E) by Ratcliffe, and

(b) intensities, (κ_I), used by the author where $\kappa_I = 2\kappa_E$.

Jaeger and Westfold (47) actually calculate what they call "the absorption integral" (F) which uses κ_E. To get the true optical depth, this value is doubled. The author, however, used κ_I directly for his calculations at 125 Mc/s.

APPENDIX II.

Derivation of P38 and P39.

From curve (iii) in Fig.2. we see that the negative slope of the line obtained by plotting the natural log of the resultant intensity vs ρ will be given by

$$\text{Slope} = -\frac{\Delta \ln I}{\Delta \rho}$$

where $\Delta\rho\ (=\rho_y - \rho_x)$ and Δ ln I are obtained as described in the text.

I is the product of two terms, $\left\{\frac{f_o}{f}\right\}^n$ from curve (i), and $e^{-\tau}$ from curve (ii).

$$\therefore \ln I = \ln\left\{\frac{f_o}{f}\right\}^n - \tau$$

$$= 2.3n \log_{10} f_o - \tau - 2.3n \log_{10} f$$

$$\therefore \Delta \ln I = 2.3n \Delta \log f_o - \Delta\tau$$

$$\text{Slope} = -\left(\frac{2.3\ n\ \Delta \log f_o - \Delta\tau}{\Delta\rho}\right)$$

We want now to express the denominator in terms of R (See P2) rather than ρ, so that we have $\Delta R = \Delta\rho\ R_o$ where $R_o = 7 \times 10^5$ km. For convenience we put $\Delta\rho = .1$, and the expression becomes

$$\text{Slope} = -\left(\frac{2.3\ n\ \Delta \log f_o - \Delta\tau}{7 \times 10^4}\right) \text{km}^{-1}$$

The value of k as usually defined is then directly given by

$$k = \frac{2.3\ n\ \Delta\ \log f_o - \Delta\tau}{\frac{7 \times 10^4}{v}} \quad \text{sec}^{-1}$$

where v is the source velocity in km/sec; the denominator now giving the time taken by the source to traverse the distance. Thus at two different frequencies f_1 and f_2 we have

$$k_1 = \frac{2.3\ n\ \Delta\ \log f_{o_1} - \Delta\tau_1}{7 \times 10^4} \times v$$

$$\text{and } k_2 = \frac{2.3\ n\ \Delta\ \log f_{o_2} - \Delta\tau_2}{7 \times 10^4} \times v$$

which gives us upon eliminating v, and solving for n:-

$$n = \frac{k_2 \Delta\tau_1 - k_1 \Delta\tau_2}{2.3 \left\{ k_2 \Delta \log_{10} f_{o_1} - k_1 \Delta \log_{10} f_{o_2} \right\}}$$

By substituting this value of n in the above expressions for k_1 and k_2 we can obtain v.

REFERENCES.

(1)	GILLIE G.G. MENZEL D.H.	1935	Harvard College Observatory Circular 410.
(2)	ALLEN C.W.	1947	Mon. Not. Roy. Astr. Soc. 107. 426.
(3)	SMERD S.F.	1950	Proc. Inst. Elect. Engrs. 97. 447.
(4)	ALVEN H.	1941	Arkiv. för Matematik, Astronomi och Fysik 27A. No.25.
(5)	SMERD S.F. WESTFOLD K.C.	1949	Phil. Mag. 40. 831.
(6)	ELLISON M.A.	1949	Mon. Not. Roy. Astr. Soc. 109. 3.
(7)	GIOVANELLI R.G.	1939	Astrophys. J. 89. 555.
(8)	SMERD S.F.	1950	Aust. J. Sci. Res. 3. 34.
(9)	KOMESAROFF M.	1958	Aust. J. Phys. 2. 201.
(10)	AVIGNON Y. PICK-GUTMANN M.	1959	C. R. Acad. Sci. 248. 368.
(11)	AVIGNON Y. PICK-GUTMANN M.	1959	C. R. Acad. Sci. 249. 2276.
(12)	KUNDU M.R. HADDOCK F.T.	1960	Nature 186. No.4725. 610.
(13)	McLEAN D.J.	1959	Aust. J. Phys. 12. 404.
(14)	NEYLAN A.A.	1959	Aust. J. Phys. 12. 399.
(15)	MAXWELL A. SWARUP G.	1953	Nature 181. No.4601. 36.
(16)	ROBERTS J.A.	1958	Aust. J. Phys. 2. 215.
(17)	RYLE M. VONBERG D.D.	1948	Proc. Roy. Soc. A. 193. 98.
(18)	HEY J.S. PARSONS S.J. PHILLIPS J.W.	1948	Mon. Not. Roy. Astr. Soc. 103. 354.
(19)	WILD J.P. McREADY L.L.	1950	Aust. J. Sci. Res. A. 3. 387.
(20)	PAYNE-SCOTT R. LITTLE A.G.	1952	Aust. J. Sci. Res. A. 5. 32.

(21) DODSON H.W. HEDEMAN E.R. OWREN L. 1953 Astrophys. J. 113. 169.

(22) DODSON H.W. HEDEMAN E.R. CHAMBERLAIN J. 1953 Astrophys. J. 117. 66.

(23) MENZEL D.H. 1954 Proc. Nat. Academ. Sci. 40. 973.

(24) DODSON H.W. HEDEMAN E.R. SOTTINGTON A.E. 1954 Astrophys. J. 119. 541.

(25) DODSON H.W. HEDEMAN E.A. McMATH R.R. 1956 Astrophys. J. Supplement No.20 II. 241.

(26) LOUGHHEAD R.E. ROBERTS J.A. McCABE M.K. 1957 Aust. J. Phys. 10. 483.

(27) GIOVANELLI R.G. 1958 Aust. J. Phys. 2. 350.

(28) GIOVANELLI R.G. ROBERTS J.A. 1958 Aust. J. Phys. 2. 353.

(29) WILD J.P. SHERIDAN K.V. NEYLAN A.A. 1959 Aust. J. Phys. 12. 369.

(30) HAGHENBURG O. KRUGER A. 1959 J.A.T.P. Nos.1/2. 17. 20.

(31) THOMPSON A.R. MAXWELL A. 1960 Nature 185. No.4706. 89.

(32) RABBEN H.H. 1960 Zietscrift Astroph. 49. -2 95.

(33) EDELSON S. McCULLOUGH T. SANTINI N. COATES R.J. 1960 13th General Assembly of U.R.S.I. London.

(34) MARTYN D.F. 1948 Proc. Roy. Soc. A. 193. 44.

(35) RYLE M. 1948 Proc. Roy. Soc. A. 195. 82.

(36) WILLIAMS S.E. 1948 Nature 162. 103.

(37) PAYNE-SCOTT R. 1949 Aust. J. Sci. Res. A. 2. 214.

(38) SHUTER W.L.H. 1958 M.Sc. Thesis, Rhodes University.

(39) TONKS L. 1929 Phys. Rev. 33. 195.
LANGMUIR I.

(40) RYLE M. 1949 Proc. Phys. Soc. A. 62. 483.

(41) WESTFOLD K.C. 1949 Aust. J. Sci. Res. 2. 169.

(42) APPLETON E.V. 1932 J. Inst. E. E. 71. 642.

(43) JAEGER J.C. 1949 Aust. J. Sci. Res. A. 2. 322.
WESTFOLD K.C.

(44) BOHM D. 1949a Phys. Rev. 75. 1851.
GROSS E.P.

(45) BOHM D. 1949b Phys. Rev. 75. 1864.
GROSS E.P.

(46) BOHM D. 1950 Phys. Rev. 79. 992.
GROSS E.P.

(47) JAEGER J.C. 1950 Aust. J. Sci. Res. A. 3. 376.
WESTFOLD K.C.

(48) WILD J.P. 1950a Aust. J. Sci. Res. A. 3. 399.

(49) WILD J.P. 1950b Aust. J. Sci. Res. A. 3. 541.

(50) WILD J.P. 1951 Aust. J. Sci. Res. A. 4. 36.

(51) BAILEY V.A. 1951 Phys. Rev. 83. 439.

(52) TWISS P.Q. 1951 Phys. Rev. 84. 448.

(53) CHRISTIANSEN W.N. 1951 Aust. J. Sci. Res. A. 4. 51.
HINDMAN J.V.
LITTLE A.G.
PAYNE-SCOTT R.
YABSLEY D.E.
ALLEN C.W.

(54) PIDDINGTON J.H. 1951 Aust. J. Sci. Res. A. 4. 131.
MINNETT H.C.

(55) PAYNE-SCOTT R. 1951 Aust. J. Sci. Res. A. 4. 508.

(56) WILD J.P. 1953 Nature 172. 533.
MURRAY J.D.
ROWE W.C.

(57) WILD J.P. 1954 Aust. J. Phys. 7. 439.
MURRAY J.D.
ROWE W.C.

(58)	WILD J.P. ROBERTS J.A. MURRAY J.D.	1954	Nature 173. 532.
(59)	SMERD S.F.	1955	Letter in Nature 175. 297.
(60)	KRUSE U.E. MARSHALL L. PLATT J.R.	1956	Astrophys J. 124. 601.
(61)	SCHWINGER J.	1949	Phys. Rev. 75. 1912.
(62)	PAWSEY J.L.. BRACEWELL R.N.	1955	"Radio Astronomy" (Clarendon:Oxford)
(63)	WESTFOLD K.C.	1957	Phil. Mag. 2. 1287.
(64)	CHRISTIANSEN W.N. WARBURTON J.A. DAVIES R.D.	1957	Aust. J. Phys. 10. No.4. 491.
(65)	SWARUP G. PARTHASARATHY R.	1958	Aust. J. Phys. 11. 338.
(66)	WILD J.P. SHERIDAN K.V.	1958	Proc. Inst. Rad. Engrs. 46. 160.
(67)	WILD J.P.	1957	I.A.U. Symposium No.4. - Radio Astronomy. 321.
(68)	ROBERTS J.A.	1959	Aust. J. Phys. 12. 327.
(69)	SHANE C.A. HIGGINS C.S.	1959	Aust. J. Phys. 12. 357.
(70)	BOISHOT A. LEE R.H. WARWICK J.W.	1960	Astrophys. J. 131. No.1. 61.
(71)	ROBERTS W.K.	1957	Proc. I.R.E. 45. 1628.
(72)	GODFRAY H.	1894	"A Treatise on Astronomy" - Macmillan.
(73)	VOLLEY WALLMAN		"Vacuum Tube Amplifiers" - p.190.
(74)	KELLER J.W.	1956	Electronics Nov. 168.
(75)	MAXWELL A. STONE SWARUP G.	1960	Astrophys. J. 131. 725.
(76)	DENISSE J.F.	1960	13th General Assembly of U.R.S.I. London.
(77)	RATCLIFFE J.A.		"Magneto-Ionic Theory and its application to the Ionosphere". p.113.